UM-HSRI-80-73-2

# FUTURE CONFIGURATION OF TANK VEHICLES HAULING FLAMMABLE LIQUIDS IN MICHIGAN

R. D. Ervin
C. Mallikarjunarao
T. D. Gillespie

APPENDICES
DECEMBER 1980

THE UNIVERSITY OF MICHIGAN
HIGHWAY SAFETY RESEARCH INSTITUTE

**Technical Report Documentation Page**

| 1. Report No. | 2. Government Accession No. | 3. Recipient's Catalog No. |
|---|---|---|
| UM-HSRI-80-73-2 | | |

| 4. Title and Subtitle | 5. Report Date |
|---|---|
| FUTURE CONFIGURATION OF TANK VEHICLES HAULING FLAMMABLE LIQUIDS IN MICHIGAN<br>Vol. II - Appendices | 12/80 |
| | 6. Performing Organization Code<br>384237 |
| 7. Author(s)<br>R. D. Ervin, C. Mallikarjunarao, T. D. Gillespie | 8. Performing Organization Report No.<br>UM-HSRI-80-73 |
| 9. Performing Organization Name and Address<br>Highway Safety Research Institute<br>The University of Michigan<br>Huron Parkway & Baxter Rd.<br>Ann Arbor, Michigan 48109 | 10. Work Unit No. |
| | 11. Contract or Grant No.<br>Agree. #78-2230 |
| 12. Sponsoring Agency Name and Address<br>State of Michigan<br>Dept. of State Highways & Transportation<br>State Highways Building<br>P.O. Box 30050<br>Lansing, Michigan 48909 | 13. Type of Report and Period Covered<br>Final .<br>3/6/79-11/1/80 |
| | 14. Sponsoring Agency Code |

15. Supplementary Notes

16. Abstract


The special safety hazard posed by highway tank vehicles hauling flammable liquids has been addressed through accident data analysis and engineering evaluations related to tank vehicle configuration. The study, which was mandated directly by an Act of the Michigan State Legislature, has produced a recommendation for new legislation pertaining to the configuration of tank vehicles having fluid capacities in excess of 9,000 gal. A set of four vehicle configurations are recommended, all constituting tractor-semitrailers. The specification for each vehicle covers constraints on tank capacity, tank height above the ground, rollover stability, the use of so-called "lift-axles," and the ability of manhole covers to contain the fluid load in the event of a rollover.

Analysis of accident risks has indicated that any of the four recommended vehicle configurations would yield approximately one-half of the incidence of rollover, with its potential for fire, that Michigan can expect from the use of conventional tankers having tank capacities around 9,000 gal. Further, the recommended vehicles, because of their higher carrying capacities, offer large advantages to the economy and energy efficiency of flammable fluids transportation.


| 17. Key Words | 18. Distribution Statement |
|---|---|
| tanker, flammable liquids, rollover, fire, traffic safety, vehicle dynamics, accidents | UNLIMITED |

| 19. Security Classif. (of this report) | 20. Security Classif. (of this page) | 21. No. of Pages | 22. Price |
|---|---|---|---|
| NONE | NONE | | |

TABLE OF CONTENTS

# Appendix A

## State Fire Marshall Data

This appendix contains information extracted from the "Hazardous Materials Accident Reports" which are maintained by the Michigan State Fire Marshall's Office. Accident data for the years 1978 and 1979 are tabulated in tables A-1 through A-4. The data for each year are classified into overturning and non-overturning accidents in these tables.

The following symbols are used to identify the product carried by the vehicles at the time of the accident:

G - Gasoline

F - Fuel oil

LPG - Liquid petroleum gas

The vehicle configurations are classified into three categories:

SB - Tractor-semitrailer combination (Single Bottom)

DB - Double tankers with a tractor, semitrailer and a full trailer (Double Bottom)

DT - Delivery trucks

The following symbols are used to define the roadway on which the accident occured:

RF - Rural Freeway

RH - Rural Highway

RR - Rural Road

UF - Urban Freeway

UH - Urban Highway

UR - Urban Road

Table A-1

## MICHIGAN NON-OVERTURNING ACCIDENTS - 1978

| PRODUCT | SINGLE VEHICLE | | | COLLISION | | | | VEHICLE TYPE | AREA & ROAD | TANK CAPACITY (gal) | LOAD (gal) | QUANTITY RELEASED (gal) | FIRE | CAUSE OF SPILL | INJURIES | COMMENTS |
|---|---|---|---|---|---|---|---|---|---|---|---|---|---|---|---|---|
| | RAN OFF ROAD | JACKNIFE | OTHER | FRONT | REAR | SIDE | OTHER | | | | | | | | | |
| Empty | | X | | | | | | SB | RF | Unknown | Unknown | | | | | |
| LPG | | | | | | X | | DT | RR | 3000 | 2300 | | | | | |
| G | | | | | | | X | DB | UF | 14000 | Unknown | | | | 2 injuries | Others |
| Empty | | | | | | X | | DT | UF | 2000 | Empty | | | | 1 Fatal (driver) | Accident involved another heavy vehicle |
| F | | X | | | | | | SB | RR | 11500 | 11000 | 2000 | | Punctured by tractor | | |
| F | | | | X | | | | DT | UR | 2000 | 1700 | | | | 1 injury | Other |
| Empty | | | | | | | Unknown | DB | RH | 16750 | Empty | | | | | |
| G | | | | X | | | | DB | RF | 17200 | Unknown | | | | | |
| G | | | 5th wheel | | | | | SB | RF | 6100 | 6100 | 30 | | Vents | | |
| F | | | | | X | | | DB | RF | 15400 | 14000 | | | | | |
| Naptha | | | | | | | Sideswipe | SB | UR | Unknown | Unknown | | | | | |
| Empty | | X | | | | | | SB | RF | 8000 | Empty | | | | 1 Fatal (driver) | |
| Propane | X | | | | | | | SB | RH | 11378 | 9700 | | | | | |
| Empty | | | | | | | Unknown | SB | UF | Unknown | Unknown | | | | | |
| G | | | | | X | | | SB | UF | 15000 | 15000 | | | | 4 injuries | Others |
| Empty | X | | | | | | | DT | RF | 1500 | Unknown | | | | | |
| Propane Empty | | | | X | | | | SB | RH | 15500 | Empty | | | | 2 Fatal | Others |
| G | | | 5th wheel | | | | | SB | UR | Unknown | Unknown | 1 | | | | |
| LPG | | | 5th wheel | | | | | SB | RH | 10000 | 10000 | | | | | |
| Animal feed | | | | | | | Railroad | SB | RR | Unknown | Unknown | 5000 | | Rupture | 1 injury (driver) | |
| F | X | | | | | | | DT | RR | 1500 | 1000 | | | | | |
| G Empty | | | | | | X | | DB | RH | Unknown | Empty | | | | 1 injury | Other |
| LPG Empty | | | | | | X | | SB | RF | 12500 | Empty | | | | | |
| LPG Empty | | | | X | | | | SB | UF | Unknown | Empty | | | | 2 injuries | 1 Driver & 1 Other |
| G Empty | | | | | | | Head on | SB | RH | 9400 | Empty | | | | 1 Fatal | Other |

Table A-2

MICHIGAN OVERTURNING ACCIDENTS - 1978

| PRODUCT | SINGLE VEHICLE: RAN OFF ROAD | SINGLE VEHICLE: INSTA-BILITY | SINGLE VEHICLE: TOO FAST TURN | SINGLE VEHICLE: OTHER | COLLISION: SIDE | COLLISION: FRONT | COLLISION: OTHER | VEHICLE TYPE | AREA & ROAD | TANK CAPACITY (gal) | LOAD (gal) | QUANTITY RELEASED (gal) | FIRE | CAUSE OF SPILL | INJURIES | COMMENTS |
|---|---|---|---|---|---|---|---|---|---|---|---|---|---|---|---|---|
| F | | | | Avoidance maneuver | | | | DB | RH | 7000 | 7000 | 7000 | | Rupture of pup | | Pup dragged 971' in roadway |
| F | X | Whipping | | | | | | DB | RH | 14000 | 14000 | 14000 | | Dome covers | 1 injury | All 4 dome covers failed. Ran off road |
| F | | | | Icy | | | | DT | RR | Unknown | Unknown | 20 | | Dome covers | | On roadway |
| F | | | | Icy | | | | DT | UR | | 800 | | | | 1 injury | |
| Alcohol | | | | Avoidance maneuver | | | | SB | RF | Unknown | Unknown | 3600 | | Dome covers & rupture | 1 injury | Rolled over on roadway |
| G | | | X | | | | | DB | RH | 6250 | 2050 | 2050 | X | Pup rupture | | Rolled over on roadway |
| F | | | | Avoidance maneuver | | | | DT | UR | Unknown | Unknown | | | | Driver - 1 injury | |
| Propane | X | | | | | | | SB | RR | 12000 | 12000 | | | | 1 slight injury | |
| G | | | X | | | | | SB | UF | 9000 | 9000 | 200 | | Unknown | | Possibly ran off roadway |
| Tolvene | | | | Icy & 5th Wheel failure | | | | SB | UF | 6500 | 6500 | 25 | | Dome cover | | |
| F | X | | | Steering defect | | | | DT | RR | 1830 | 1830 | 1800 | | Unknown | 1 slight | |
| Empty | | | | | Icy - Hit two vehicles | | & guard rail | SB | RF | | | | | | | |
| F | | | | Avoidance | | | | DB | RH | 11000 | 11000 | 10000 | | Rupture pup & semi | | |
| F | X | | | Avoidance | | | | DT | RH | 2000 | 1400 | 15 | | | | |
| F | | | | Wheel came off | | | | DT | RH | 1000 | 900 | 2 | | | 1 slight | |
| F | | | | | | not head on | | SB | RH | 14000 | 12500 | 9500 | | Rupture | 2-pass. car 2 bus drivers | 3 schools buses & 2 passenger cars involved |
| Refined crude | | | | | | not head on | | SB | UF | 16170 | 12600 | 3000 | X | Rupture | 1 fatal other 1 inj driver | Front right side of tank ruptured |
| LPG | | | | | ⊥ to tank | | | DT | RR | Unknown | 1550 | 1000 | | Valve | | |
| LPG | | | | | | side of car | | SB | UF | 14500 | 10500 | | | | 1 minor | |
| Benzene | X | | | Tire blowout | | | | DB | RH | 13800 | 12000 | Unknown | | Dome lid came off | | |
| F | X | | | | | | | DT | RR | 1500 | 1100 | | | | | |
| F | X | | | Avoidance | | | | DB | RH | 9100 | 9000 | 400 | | Dome gasket | | Semi alone rolled over |
| Empty | X | | | | | | | DT | RR | 2000 | | | | | | |
| F | X | | | | | | | DT | RF | 3500 | 2900 | 1000 | | Dome cover | | |
| G | X | | | | | | | DB | RR | 9300 | 9100 | 30 | | Dome gaskets | | Pup alone rolled over |
| Empty | X | | | Avoidance | | | | SB | RF | 10000 | | | | | 1 driver | |
| F | | | | | ⊥ rear side | | | DT | RH | 1600 | 1600 | 30 | | Dome cover | 1 other | |

Table A-2

MICHIGAN OVERTURNING ACCIDENTS - 1978 (cont)

| PRODUCT | SINGLE VEHICLE | | | | COLLISION | | | VEHICLE TYPE | AREA & ROAD | TANK CAPACITY (gal) | LOAD (gal) | QUANTITY RELEASED (gal) | FIRE | CAUSE OF SPILL | INJURIES | COMMENTS |
|---|---|---|---|---|---|---|---|---|---|---|---|---|---|---|---|---|
| | RAN OFF ROAD | INSTA-BILITY | TOO FAST TURN | OTHER | SIDE | FRONT | OTHER | | | | | | | | | |
| G | | | (Ramp) X | | | | | SB | UF | 9300 | 9000 | 9000 | | Uprighting operation | 1 driver | |
| G | X | | | Avoidance | | | | SB | RR | 15250 | 7000 | 100 | | Dome gasket | | 20 mph |
| G | | X | | | | | | DB | RR | 7700 | 7700 | 17000 | X | Pup skin rupture | | 45 mph Pup alone overturned dragged 273' |
| G | | X | | | | | | DB | RF | 6250 | 2100 | 4500 | X | Unknown | | Pup alone overturned dragged 300' |
| G | X | | | Avoidance | | | | DB | RH | 6025 | 2900 | 20 | | — | | |
| G | | | | | Sideswipe | | | DB | RH | 10600 | 10600 | 5500 | | Pup shell rupture | 4 others 1 driver | |
| LPG | | | | | | Head on | | SB | RH | 13500 | 11400 | — | | | 1 fatal 1 other | |
| G | X | | | | | | | DT | RH | 1500 | 1500 | 5 | | | 1 fatal (driver) | Coronary problem |
| G | | | | Avoidance | | | | DB | RH | 7500 | 7500 | 11600 | X | Pup shell 6" rupture | | Pup alone overturned Total load = 16600 gal |
| G | | | | | ⊥ | | | DT | RR | 1800 | 580 | 30 | | Dome covers | 2 others 1 driver | |
| Alcohol | X | | | | | | | SB | RF | 7500 | Unknown | Unknown | | Unknown | 1 driver (fatal) 1 passenger | |
| G | | | X | | | | | SB | RR | 7150 | Unknown | 1000 | | Vents | | |
| G | X | | | | | | Rearended | DB | RH | 16800 | 13100 | 4000 | | Unknown | 1 driver | |
| G | X | | | | | | | DT | RR | 1500 | Unknown | 213 | | Dome covers | | |
| LPG | X | | | | | | | DT | RH | 2600 | 700 | — | | | 1 driver | |
| Methanol | X | | | | | ⊥ | | DT | RR | 2000 | 1200 | 20 | | | | Landed on top |
| G | X | | | | | | | DT | RH | 2000 | 2000 | 90 | | Dome cover | | |
| Asphalt | X | | | | | | | DB | RF | Unknown | Unknown | 5000 | | | | Tractor & semi alone overturned |
| LPG (Empty) | X | | | Avoidance | | | | SB | RH | 12500 | 60 | — | | | | |
| G | | | | | | | Rearended | SB | RH | 14000 | 13000 | 13000 | X | Unknown (dome cover) | 1 fatal (driver) | Aluminum tank |
| LPG | X | | | | | | | SB | RF | 7200 | 7200 | — | | | | |
| Propane | X | | | | | | | DT | RR | 2200 | Unknown | — | | | | |
| Propane | X | | | Icy | | | | DT | RR | 2400 | 1300 | 4 | | | | |
| G | X | | | Icy | | | | DT | RR | 1800 | 1575 | 300 | | Dome covers | | |
| F | X | | | Icy | | | | DT | RH | 2000 | 2000 | 800 | | Manhole cover | 1 passenger | |
| G | X | | | Icy | | | | DB | RF | 14100 | 13500 | 1000 | | Lids & vents | | |
| G | | X | | Icy | | | | DB | RF | 16400 | Unknown | Unknown | X | Unknown | | |

Table A-3

## MICHIGAN NON-OVERTURNING ACCIDENTS — 1979

| PRODUCT | SINGLE VEHICLE | | | COLLISION | | | | VEHICLE TYPE | AREA & ROAD | TANK CAPACITY (gal) | LOAD (gal) | QUANTITY RELEASED (gal) | FIRE | CAUSE OF SPILL | INJURIES | COMMENTS |
|---|---|---|---|---|---|---|---|---|---|---|---|---|---|---|---|---|
| | RAN OFF ROAD | JACKNIFE | OTHER | FRONT | REAR | SIDE | OTHER | | | | | | | | | |
| F | | | | | | X | | DT | RH | 2500 | 1200 | 3 | | Pipe leak | | |
| F | | | | | | X | | DT | RR | 2000 | 2000 | | | | Other driver } 1 | |
| G | | | | | X | | | DT | UF | 4400 | 4400 | 1 | | | | |
| LPG | | | | X | | | | SB | RF | Unknown | Unknown | | | | Other car } 3 | |
| F | | X | | | | | | SB | RF | 7000 | Empty | 50 | | Hole in sadde tank | | |
| G | | | 5th wheel | | | | | SB | UH | 8300 | 8300 | | | | | |
| Empty | | X | | | | | | SB | RH | 11200 | Empty | | | | | |
| G | | | | | | | Sideswipe | SB | UF | Unknown | Unknown | 1000 | | Punctured shell | | |
| F | | | Pedestrian | | | | | DT | RR | 2000 | Unknown | | | | 1 Injury | 1 Fatality |
| F | | | | | | | Railroad | DT | RR | 2000 | 150 | | | | | |
| G | X | | | | | | | DB | RH | 17 300 | 8100 | | | | | |
| G | | | | | | | Railroad | DT | RR | 2000 | 2000 | 1200 | | Dome covers | Driver - 1 | |
| G | | | | X | | | | SB | RH | 9000 | 9000 | | | | | |
| G | | | | | | | Unknown | SB | RF | 15000 | 9000 | | | | Other driver 1 | |
| Propylene | | X | | | | | | SB | UF | 14000 | 4700 | | | | | |
| Ammonia | | | | | | | Head on | SB | RF | Unknown | Unknown | | | | Other driver 1 | |
| LPG | | | | | X | | | DT | UH | Unknown | 2400 | Unknown | X | | | |
| G | | | Power pole | | | | | DB | RR | Unknown | Unknown | | | | | |
| LPG | | X | | | | | | SB | UH | 13454 | Empty | | | | | |
| G | | | Tractor fire | | | | | DB | UF | Unknown | Unknown | | X | | | |
| Empty | | | | | | X | | DB | UR | Unknown | Unknown | | | | | |

Table A-4

## MICHIGAN OVERTURNING ACCIDENTS - 1979

| PRODUCT | SINGLE VEHICLE: RAN OFF ROAD | SINGLE VEHICLE: INSTA-BILITY | SINGLE VEHICLE: TOO FAST TURN | SINGLE VEHICLE: OTHER | COLLISION: SIDE | COLLISION: FRONT | COLLISION: OTHER | VEHICLE TYPE | AREA & ROAD | TANK CAPACITY (gal) | LOAD (gal) | QUANTITY RELEASED (gal) | FIRE | CAUSE OF SPILL | INJURIES | COMMENTS |
|---|---|---|---|---|---|---|---|---|---|---|---|---|---|---|---|---|
| G | X | | | | | | | SB | RR | 6000 | 2800 | 337 | | DOME | | |
| G | | | | 5th Wheel | | | | SB | UR | 9000 | 8200 | 2555 | | After rollover thru hatches | | |
| F | | | | | ⊥ to tanker X | | | DB | RH | 6700 | 6700 | 2000 | | Dome | | |
| F | | Climb on icy road | | | | | | DB | RH | 16400 | 16400 | 150 | | Unknown | | |
| F | | Braking | | | | | | DB | RH | 6700 | 5500 | 500 | | Vents & dome cover | | |
| F | Stationary roll off | | | | | | | SB | RR | 9300 | 9300 | — | | — | | |
| G | | | | | | X | | SB | RH | 12000 | 11500 | 8000 | | Rupture | 1 - Driver<br>1 - Other car | Spilled on roadway and shoulder |
| G | X | | | | | | | SB | RF | 10000 | 10000 | 5 | | — | | |
| Jet Fuel | | | | Icy | | | | DT | Airport | 2100 | 1500 | 100 | | Dome cover | Driver | |
| Empty | | | | Icy | | | | DB | RF | 16725 | — | — | | — | Driver | |
| F | X | | | Icy | | | | DT | RH | 2500 | 2500 | 700 | | Tree struck during roll | Driver | |
| G | | | | Icy | | | | DB | RF | 7300 | 7300 | 5800 | | Dome | | |
| Ammonia | X | | | Driveway | | | | SB | RR | Unknown | — | — | | — | | |
| G | X | | | Driveway | | | | SB | UR | 9000 | 9000 | 50 | | Unknown | | |
| G | X | | | | | | | DB | RH | 13700 | 13700 | 100 | | Dome | | |
| G | X | | | | | | | DT | RR | 2500 | 2500 | 184 | | Unknown | | |
| Propane | X | | | Collided w/ bridge | | | | SB | UF | Unknown | — | — | | — | Driver | |
| Cutting oil | | | | | Sideswiped ran off road | | | SB | RH | 8000 | 8000 | 500 | | Unknown | | |
| Ammonia | X | | | | | | | SB | RF | 9000 | Unknown | — | | — | | |
| G | | | Ramp | | | | | SB | UF | 8000 | 8000 | 8000 | X | Unknown | | |

Table A-4

MICHIGAN OVERTURNING ACCIDENTS - 1979 (cont)

| PRODUCT | SINGLE VEHICLE | | | | COLLISION | | | VEHICLE TYPE | AREA & ROAD | TANK CAPACITY (gal) | LOAD (gal) | QUANTITY RELEASED (gal) | FIRE | CAUSE OF SPILL | INJURIES | COMMENTS |
|---|---|---|---|---|---|---|---|---|---|---|---|---|---|---|---|---|
| | RAN OFF ROAD | INSTA-BILITY | TOO FAST TURN | OTHER | SIDE | FRONT | OTHER | | | | | | | | | |
| G | | | Ramp | | | | | SB | UH | 9000 | 9000 | 800 | | Unknown | | |
| Fuel oil | X | | Curve | | | | | DB | RR | 16100 | 16100 | 5800 | | Dome | Driver | |
| G | X | | | | | | | DB | RF | 7400 | 7400 | 13300 | X | Rupture & dome | | |
| Alcohol | | | Ramp | 5th Wheel | | | | SB | UH | 9000 | 9000 | 2 | | Dome | | |
| LPG | X | | | | | | | SB | RF | | | | | | | |
| G | | | | | ⊥ to tanker | | | SB | UH | 8200 | 8200 | 8200 | X | Unknown | Driver 1 other | |
| G | X | | Curve | | | | | SB | UR | 8600 | 8600 | Unknown | | Dome | | |
| LPG | X | | | | | | | SB | RH | | | | | | Driver-fatal | |
| LPG | | | | Ice | | | | SB | RH | | | | | | | |
| F | | | | Retro Hitch | | | | DB | RH | Unknown | 11500 | 1325 | | | | |

## APPENDIX B

## STATIC ROLL MODEL

This appendix deals with the roll plane model which was developed for the purpose of estimating the rollover thresholds of the candidate tank vehicles. The essential features of the model and the assumptions made in deriving the equations are included in Section 4.1.3. In this appendix, the method adopted for computing the rollover threshold is first described; following which, the set of 10 static equilibrium equations which are needed to solve for the roll equilibrium of the vehicle are derived. Then, the parameters needed to describe the candidate vehicle configurations are listed. A computer program which can be used for computing the steady turning rollover thresholds of multiaxled vehicles is listed at the end of the appendix.

### B.1 Method of Solution

The calculations begin with the vehicle in the upright position. Initially, the lateral acceleration, the sprung mass roll angle, and the axle roll angles are all set to zero. The sprung mass roll angle is then increased in small increments. For each increment of the sprung mass roll angle, a set of 10 linear static equilibrium equations are solved to determine the changes in the roll angles of the axles, the vertical distance of the axles above the ground level, and the vertical distance between the sprung mass and each of the three axles.

The equations are of the form:

$$[A]\ \{\Delta x\} \ = \ \{b\}\Delta\phi_s \qquad (1)$$

where the elements of [A] (a 10 x 10 matrix) and {b} (a vector of size 10) are functions of the vehicle parameters, and

$$\{\Delta x\} = [\Delta a_y, \Delta\phi_{u_1}, \Delta\phi_{u_2}, \Delta\phi_{u_3}, \Delta z_1, \Delta z_2, \Delta z_3, \Delta z_{T_1}, \Delta z_{T_2}, \Delta z_{T_3}]^T$$

In the computer program, Equation (1) is solved for each small increment of the sprung mass roll angle, $\Delta\phi_s$. As the calculations proceed through a series of equilibrium positions, the matrices [A] and {b} are continuously updated to reflect changes in the roll properties of the vehicle, due to nonlinearities in the suspension system, and due to loss of contact at the tire-road interfaces.

The calculations are terminated when the sprung mass roll angle reaches a level at which the tires on one side of the tractor rear axle as well as those on one side of the trailer axle are completely lifted off the ground. The highest lateral acceleration level achieved in this computation is termed as the rollover threshold.

## B.2 Static Equilibrium Equations

There are a total of 10 static equilibrium equations needed to define the roll equilibrium of the vehicle at any given lateral acceleration. The equations are derived below. The symbols used in the equations are defined in Table B.1.

B.2.1 Rolling Moment Equation for the Sprung Mass. Taking moments of all the external forces acting on the sprung mass (see Fig. 4.13 in Section 4.1.3) we get

$$\sum_{i=1}^{3} (F_{i1}-F_{i2})s_i \cos(\phi_s-\phi_{u_i}) - \sum_{i=1}^{3} F_{R_i} z_{R_i} \cos(\phi_s-\phi_{u_i})$$

$$+ \sum_{i=1}^{3} (F_{i1}+F_{i2}) z_{R_i} \sin(\phi_s-\phi_{u_i}) = 0 \qquad (2)$$

Applying the small roll angle assumptions

$$\sin(\phi_s-\phi_{u_i}) = (\phi_s-\phi_{u_i})$$

and $\cos(\phi_s-\phi_{u_i}) = 1.0$ in (2)

we get

Table B.1. Definition of Symbols

| | |
|---|---|
| $W_s$ | Weight of the sprung mass (lb) |
| $W_{u_i}$ | Weight of the $i^{th}$ unsprung mass (lb) |
| $WAXL_i$ | Load carried by the axle i (lb) |
| $F_{y_i}$ | The total lateral force reacted at the tire-road interface of axle i (lb) |
| $F_{R_i}$ | The lateral force acting through the roll center, $R_i$ (lb) |
| $F_{ij}$ | The vertical load carried by the $j^{th}$ suspension spring on axle i (lb) |
| $F_{T_{ij}}$ | The vertical load carried by the $j^{th}$ tire on axle i (lb) |
| $r_i$ | Radius of the tires on axle i (in) |
| $z_i$ | Vertical distance from the axle c.g. to the roll center, $R_i$ (in) |
| $z_{T_i}$ | Vertical distance from the ground plane to the c.g. of the axle (in) |
| $z_{R_i}$ | Vertical distance from the sprung mass c.g. to the roll center, $R_i$ (in) |
| $H_s$ | Height of the sprung mass c.g. above ground level (in) |
| $HR_i$ | Height of roll center, $R_i$, above the ground plane (in) |
| $s_i$ | Half spring spacing at axle i (in) |
| $T_i$ | Half the track width of the inner tires on axle i (in) |
| $*A_i$ | Lateral distance between the dual tires on axle i (in) |
| $a_y$ | Lateral acceleration of the steady turn (g's) |
| $\phi_s$ | Sprung mass roll angle (rad) |
| $\phi_{u_i}$ | Roll angle of the $i^{th}$ unsprung mass (rad) |
| $K_{T_{ij}}$ | Vertical rate of the $j^{th}$ tire on the composite axle i (lb/in) |
| $**K_{ij}$ | Vertical rate of the $j^{th}$ suspension spring on axle i (lb/in) |

Table B.1. (Cont.)

Notes:

*In the case of single tires, $A_i$ is set to zero and a vertical tire spring rate value ($K_{T_{ij}}$), which is half the value for the single tire, is used.

**$K_{ij}$ is not an input parameter. The computer program calculates the local spring rate at any given deflection, based on the tabular input of spring data.

$$\sum_{i=1}^{3}(F_{i1} - F_{i2})s_i - \sum_{i=1}^{3} F_{R_i} Z_{R_i} + \sum_{i=1}^{3}(F_{i1} + F_{i2})z_{R_i}(\phi_s - \phi_{u_i}) = 0 \tag{3}$$

The effect of a small increment of the sprung mass roll angle, from a given equilibrium condition, can be studied by writing the above equation in the form:

$$\sum_{i=1}^{3}(\Delta F_{i1} - \Delta F_{i2})s_i - \sum_{i=1}^{3} \Delta F_{R_i} z_{R_i} + \sum_{i=1}^{3}(\Delta F_{i1} + \Delta F_{i2})z_{R_i}(\phi_s - \phi_{u_i})$$
$$+ \sum_{i=1}^{3} (F_{i1} + F_{i2})z_{R_i}(\Delta\phi_s - \Delta\phi_{u_i}) = 0 \tag{4}$$

The changes, $\Delta F_{ij}$, in the suspension spring forces can be related to the deflection, $\Delta\phi_s$, $\Delta\phi_{u_i}$, and $\Delta z_i$, by the equation

$$\Delta F_{ij} = \frac{\partial F_{ij}}{\partial z_i} \Delta z_i + \frac{\partial F_{ij}}{\partial \phi_s} \Delta\phi_s + \frac{\partial F_{ij}}{\partial \phi_{u_i}} \Delta\phi_{u_i} \tag{5}$$

Equation (5) can be expanded and written for the left- and right-hand side suspension springs. If the local spring rate is $K_{ij}$ for the spring ij, we get

$$\Delta F_{i1} = K_{i1} \Delta z_i - K_{i1} s_i \Delta\phi_s + K_{i1} s_i \Delta\phi_{u_i} \tag{6}$$

and

$$\Delta F_{i2} = K_{i2} \Delta z_i + K_{i2} s_i \Delta\phi_s - K_{i2} s_i \Delta\phi_{u_i} \tag{7}$$

The increment in the lateral force, $F_{R_i}$, is given by the equation

$$\Delta F_{R_i} = (WAXL_i - W_{u_i})\Delta a_y - (WAXL_i - W_{u_i})\Delta\phi_{u_i} \tag{8}$$

Upon substituting (5), (7), and (8) into (4), we get the sprung mass roll equation for a small increment in the roll angle, from a given equilibrium condition:

$$\left[- \sum_{i=1}^{3} (K_{i1}+K_{i2})s_i^2 + \sum_{i=1}^{3} (F_{i1}+F_{i2})z_{R_i} - \sum_{i=1}^{3} (K_{i1}-K_{i2})s_i z_{R_i}(\phi_s-\phi_{u_i})\right]\Delta\phi_s$$

$$+ \left[\sum_{i=1}^{3}\left((K_{i1}+K_{i2})s_i^2 + (WAXL_i-W_{u_i})z_{R_i} + (K_{i1}-K_{i2})s_i z_{R_i}(\phi_s-\phi_{u_i}) - (F_{i1}+F_{i2})z_{R_i}\right)\Delta\phi_{u_i}\right]$$

$$+ \left[\sum_{i=1}^{3}\left((K_{i1}-K_{i2})s_i + (K_{i1}+K_{i2})z_{R_i}(\phi_s-\phi_{u_i})\right)\Delta z_i\right]$$

$$- \sum_{i=1}^{3} (WAXL_i-W_{u_i})z_{R_i}\Delta a_y = 0.0 \qquad (9)$$

B.2.2 Rolling Moment Equations for the Unsprung Masses. Taking moments of all the forces acting on axle i, about the mass center of the axle, we get

$$- F_{i1}s_i + F_{i2}s_i + (F_{T_{i1}}-F_{T_{i4}})(T_i+A_i)\cos\phi_{u_i} + (F_{T_{i2}}-F_{T_{i3}})T_i\cos\phi_{u_i}$$

$$+ F_{R_i}z_i + F_{y_i}z_{T_i} + (F_{T_{i1}}+F_{T_{i2}}+F_{T_{i3}}+F_{T_{i4}})\, r_i \sin\phi_{u_i} = 0.0 \qquad (10)$$

Applying the small angle assumption to (10) we get

$$(- F_{i1}+F_{i2})s_i + (F_{T_{i1}}-F_{T_{i4}})(T_i+A_i) + (F_{T_{i2}}-F_{T_{i3}})T_i + F_{R_i}z_i + F_{y_i}z_{T_i}$$

$$+ (F_{T_{i1}}+F_{T_{i2}}+F_{T_{i3}}+F_{T_{i4}})r_i\phi_{u_i} = 0.0 \qquad (11)$$

For a small increment in the sprung mass roll angle, Equation (11) can be rewritten as

$$(- \Delta F_{i1}+\Delta F_{i2})s_i + (\Delta F_{T_{i1}}+\Delta F_{T_{i2}})(T_i+A_i) + (\Delta F_{T_{i2}}-\Delta F_{T_{i3}})T_i + F_{R_i}\Delta z_i$$

$$+ \Delta F_{R_i}z_i + \Delta F_{y_i}z_{T_i} + (\Delta F_{T_{i1}}+\Delta F_{T_{i2}}+\Delta F_{T_{i3}}+\Delta F_{T_{i4}})r_i\phi_{u_i} + F_{y_i}\Delta z_{T_i}$$

$$+ (F_{T_{i1}}+F_{T_{i2}}+F_{T_{i3}}+F_{T_{i4}})r_i\Delta\phi_{u_i} = 0.0 \qquad (12)$$

The changes in the tire loads, $F_{T_{ij}}$, can be related to the deflections, $\Delta\phi_{u_i}$ and $\Delta z_{T_i}$. The equations are of the form:

$$\Delta F_{T_{i1}} = - K_{T_{i1}}(T_i+A_i)\Delta\phi_{u_i} + K_{T_{i1}}\Delta z_{T_i} \tag{13}$$

$$\Delta F_{T_{i2}} = - K_{T_{i2}}T_i \,\Delta\phi_{u_i} + K_{T_{i2}}\Delta z_{T_i} \tag{14}$$

$$\Delta F_{T_{i3}} = K_{T_{i3}}T_i \,\Delta\phi_{u_i} + K_{T_{i3}}\Delta z_{T_i} \tag{15}$$

$$\Delta F_{T_{i4}} = K_{T_{i4}}(T_i+A_i)\Delta\phi_{u_i} + K_{T_{i4}}\Delta z_{T_{i4}} \tag{16}$$

Upon substituting (6), (7), (8), (13), (14), (15), and (16) into (12), we get the unsprung mass roll equations, for a small increment in the roll angle of the sprung mass:

$$\begin{aligned}
&(K_{i1}+K_{i2})s_i^2\Delta\phi_s - [(K_{i1}+K_{i2})s_i^2 - WAXL_i r_i - (WAXL_i-W_{u_i})z_i + (K_{T_{i1}}+K_{T_{i4}})(T_i+A_i)^2 \\
&+ (K_{T_{i2}}+K_{T_{i3}})T_i^2]\Delta\phi_{u_i} + [-(K_{i1}-K_{i2})s_i + (WAXL_i-W_{u_i}) \cdot (a_y-\phi_{u_i})]\Delta z_i \\
&+ [(K_{T_{i1}}-K_{T_{i4}})(T_i+A_i) + (K_{T_{i2}}-K_{T_{i3}})T_i + WAXL_i \cdot a_y]\Delta z_{T_i} \\
&- [(WAXL_i-W_{u_i}) \cdot HR_i + W_{u_i}z_{T_i}]\Delta a_y = 0.0
\end{aligned} \tag{17}$$

B.2.3 <u>Equations for the Bounce of the Sprung Mass with Respect to the Axles</u>. If the sprung mass is to maintain an equilibrium along the $\vec{k}_{u_i}$ axis, it has to satisfy three equations which are of the form:

$$F_{i1} + F_{i2} = (WAXL_i-W_{u_i})\cos\phi_{u_i} + (WAXL_i-W_{u_i})a_y \cdot \sin\phi_{u_i} \tag{18}$$

Applying the small angle assumption to (18) we get:

$$F_{i1} + F_{i2} = (WAXL_i-W_{u_i}) + (WAXL_i-W_{u_i})a_y\phi_{u_i} \tag{19}$$

For a small increment of the sprung mass roll angle, Equation (19) can be written as

$$\Delta F_{i1} + \Delta F_{i2} = (WAXL_i - W_{u_i})\Delta a_y \cdot \phi_{u_i} + (WAXL_i - W_{u_i})a_y \cdot \Delta\phi_{u_i} \tag{20}$$

Substituting (6) and (7) into (20), we get

$$(K_{i1}+K_{i2})\Delta z_i - (K_{i1}-K_{i2})s_i\Delta\phi_s + (K_{i1}-K_{i2})s_i\Delta\phi_{u_i}$$

$$= (WAXL_i - W_{u_i})\phi_{u_i} \cdot \Delta a_y + (WAXL_i - W_{u_i})a_y \cdot \Delta\phi_{u_i} \tag{21}$$

B.2.4 Equations for the Vertical Displacement of the Unsprung Masses with Respect to the Ground Plane. The vertical load carried by each axle is assumed to remain constant during a rollover. Therefore, if equilibrium is to be maintained, in the vertical direction, each axle has to satisfy the equation:

$$(F_{T_{i1}} + F_{T_{i2}} + F_{T_{i3}} + F_{T_{i4}}) = WAXL_i \tag{22}$$

For small increments in the sprung mass roll angle, (22) can be rewritten as

$$\Delta F_{T_{i1}} + \Delta F_{T_{i2}} + \Delta F_{T_{i3}} + \Delta F_{T_{i4}} = 0.0 \tag{23}$$

Upon substituting (13)-(15) into (23) we get

$$[-K_{T_{i1}}(T_i+A_i) - K_{T_{i2}}T_i + K_{T_{i3}}T_i + K_{T_{i4}}(T_i+A_i)]\Delta\phi_{u_i}$$

$$+ (K_{T_{i1}}+K_{T_{i2}}+K_{T_{i3}}+K_{T_{i4}})\Delta z_{T_i} = 0.0 \tag{24}$$

The set of 10 linear equations which define the roll behavior of the vehicle, for small increments of the sprung mass roll angle away from equilibrium conditions, can now be formed. They are the sprung mass roll equilibrium Equation ( 9) and three equations each of (17), (21), and (24), respectively.

### B.3 Parameters for Candidate Vehicle Configurations

The parameters which were used to define the candidate vehicle configurations are listed in Tables B.2 and B.3. The parameters are for vehicle combinations that have 96-inch wide tractors and 102-inch wide trailers. The symbols used in Tables B.2 and B.3 are defined in Table B.1. The spring characteristics of the suspension springs on the tractor front axle, tractor rear axle, and the trailer axles are shown in Figures B.1, B.2, and B.3, respectively.

### B.4 Computer Programs for Calculating Rollover Thresholds

A computer program which was used for calculating the rollover threshold of the candidate vehicles is listed at the end of this appendix. The roll equilibrium equations—Equations (9), (17), (21), and (24)—are utilized in the computer program. The program is coded in the FORTRAN language. The symbols used for the vehicle parameters are the same as those listed in Table B.1.

In the program, the parameter "DELPH" defines the increment of sprung mass roll, $\Delta\phi_s$, for which the static equilibrium equations are solved. A roll angle increment of 0.02 degree was found to be sufficient for producing accurate results. The parameter XPRINT defines the interval, in the sprung mass roll, for which the roll response of the vehicle is printed out.

Table B.2. Roll Plane Parameters for Candidate Tractor-Semitrailer Configurations.

| | 1 | 2a | 2b | 3a | 3b | 4a | 4b | 5a | 5b | 6 | 7 |
|---|---|---|---|---|---|---|---|---|---|---|---|
| $W_s$ | 69300 | 74800 | 89800 | 86300 | 91300 | 97800 | 102800 | 109300 | 114300 | 120800 | 132300 |
| $W_{u_1}$ | 1200 | | | | | | | | | | |
| $W_{u_2}$ | 4500 | | | | | | | | | | |
| $W_{u_3}$ | 3000 | 4500 | 4500 | 6000 | 6000 | 7500 | 7500 | 9000 | 9000 | 10500 | 12000 |
| $WAXL_1$ | 14000 | 14000 | 14000 | 14000 | 14000 | 14000 | 14000 | 14000 | 14000 | 14000 | 14000 |
| $WAXL_2$ | 32000 | 32000 | 32000 | 32000 | 32000 | 32000 | 32000 | 32000 | 32000 | 32000 | 32000 |
| $WAXL_3$ | 32000 | 39000 | 54000 | 52000 | 57000 | 65000 | 70000 | 78000 | 83000 | 91000 | 104000 |
| $HR_1$ | 22.0 | | | | | | | | | | |
| $HR_2$ | 29.0 | | | | | | | | | | |
| $HR_3$ | 29.0 | | | | | | | | | | |
| $H_s$ | 71.1 | 72.1 | 76.1 | 73.8 | 75.6 | 77.0 | 78.9 | 80.4 | 82.3 | 83.8 | 87.4 |
| $r_1, r_2, r_3$ | 20.0 | | | | | | | | | | |
| $T_1$ | 40.3 | | | | | | | | | | |
| $T_2$ | 29.0 | | | | | | | | | | |
| $T_3$ | 32.0 | | | | | | | | | | |
| $A_1$ | 0.0 | | | | | | | | | | |
| $A_2$ | 13.0 | | | | | | | | | | |
| $A_3$ | 13.0 | | | | | | | | | | |
| $s_1$ | 16.0 | | | | | | | | | | |
| $s_2$ | 19.0 | | | | | | | | | | |
| $s_3$ | 22.0 | | | | | | | | | | |
| $K_{T_{1j}}$ | 2500 | | | | | | | | | | |
| $K_{T_{2j}}$ | 10000 | | | | | | | | | | |
| $K_{T_{3j}}$ | 10000 | 15000 | 15000 | 20000 | 20000 | 25000 | 25000 | 30000 | 30000 | 35000 | 40000 |

When left blank, parameter value is same as the value listed for configuration #1.

Table B.3. Roll Plane Parameters for Candidate Tractor/Semitrailer/Semitrailer Configurations.

| | I | IIa | IIb | III | IVa | IVb | V | VI | VII |
|---|---|---|---|---|---|---|---|---|---|
| $W_s$ | 90800 | 102300 | 109300 | 113800 | 102300 | 109300 | 113800 | 120800 | 132300 |
| $W_{u_1}$ | 1200 | | | | | | | | |
| $W_{u_2}$ | 4500 | | | | | | | | |
| $W_{u_3}$ | 7500 | 9000 | 9000 | 10500 | 9000 | 9000 | 10500 | 10500 | 12000 |
| $WAXL_1$ | 12000 | 12000 | 14000 | 12000 | 12000 | 14000 | 12000 | 14000 | 14000 |
| $WAXL_2$ | 27000 | 27000 | 32000 | 27000 | 27000 | 32000 | 27000 | 32000 | 32000 |
| $WAXL_3$ | 65000 | 78000 | 78000 | 91000 | 78000 | 78000 | 91000 | 91000 | 104000 |
| $HR_1$ | 22.0 | | | | | | | | |
| $HR_2$ | 29.0 | | | | | | | | |
| $HR_3$ | 29.0 | | | | | | | | |
| $H_s$ | 73.9 | 77.5 | 79.5 | 80.5 | 74.6 | 76.2 | 77.1 | 79.3 | 82.1 |
| $r_1,r_2,r_3$ | 20.0 | | | | | | | | |
| $T_1$ | 40.3 | | | | | | | | |
| $T_2$ | 29.0 | | | | | | | | |
| $T_3$ | 32.0 | | | | | | | | |
| $A_1$ | 0.0 | | | | | | | | |
| $A_2$ | 13.0 | | | | | | | | |
| $A_3$ | 13.0 | | | | | | | | |
| $s_1$ | 16.0 | | | | | | | | |
| $s_2$ | 19.0 | | | | | | | | |
| $s_3$ | 22.0 | | | | | | | | |
| $K_{T_{1j}}$ | 2500 | | | | | | | | |
| $K_{T_{2j}}$ | 10000 | | | | | | | | |
| $K_{T_{3j}}$ | 25000 | 30000 | 30000 | 35000 | 30000 | 30000 | 35000 | 35000 | 40000 |

When left blank, parameter value is same as the value listed for configuration #I.

SPRING #1

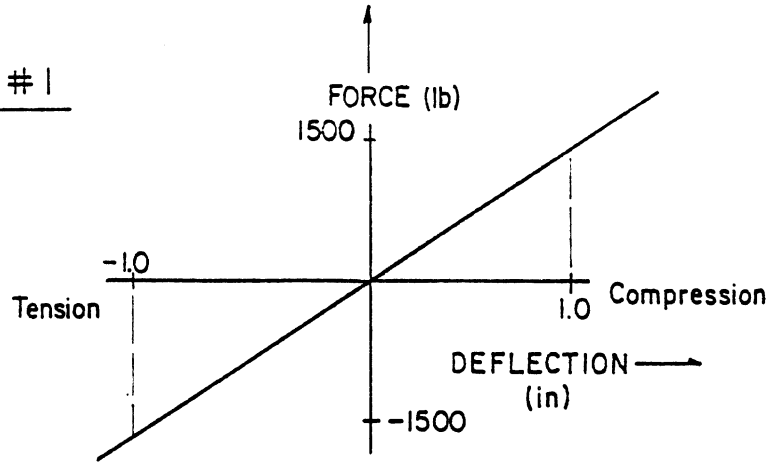


Figure B.1. Tractor front suspension spring.

SPRING #2

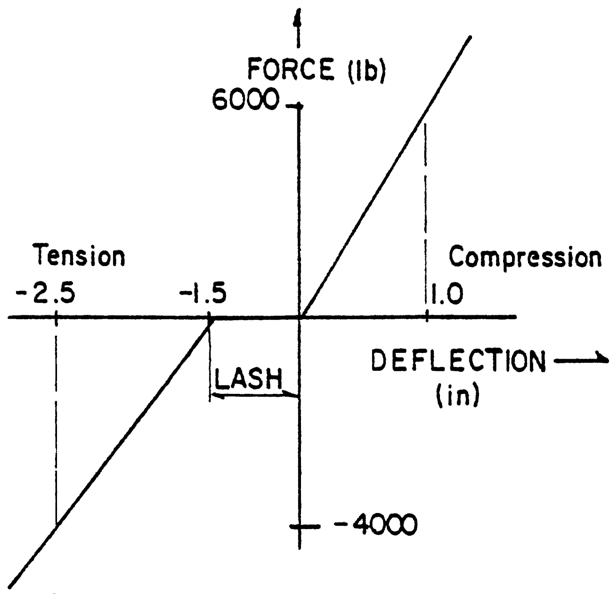


Figure B.2. Tractor rear suspension spring.

SPRING #3

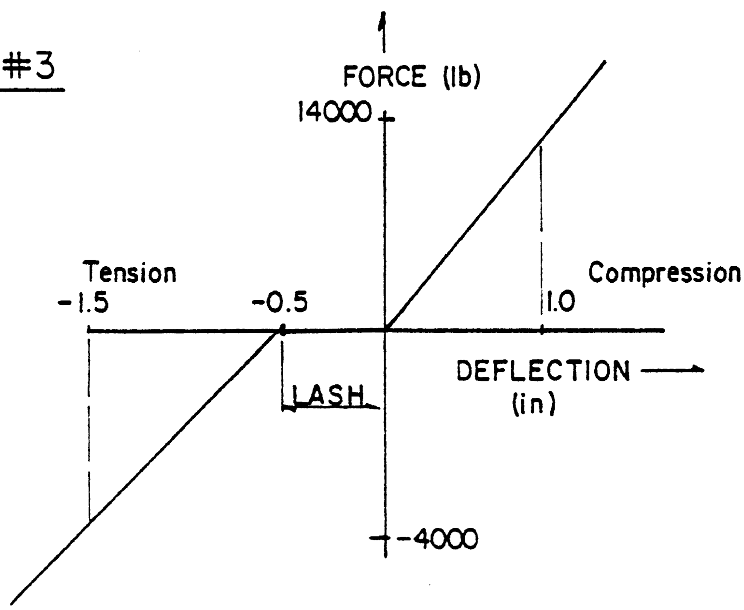


Figure B.3. Trailer suspension spring.

COMPUTER PROGRAM FOR CALCULATING ROLLOVER THRESHOLDS

```
C
C PROGRAM FOR COMPUTING RCLLANGLE-LATERAL ACC'N RELATIONSHIP
C FOR A 3AXLE VEHICLE
C
C
      COMMON FORC(3,10), DEL(3,10), NUM(3)
      DIMENSION AA(10,10), F(10), HEAD(20)
      REAL*4 KT11, KT12, KT13, KT14, KT21, KT22, KT23, KT24, K11, K12,
     1       K21, K22, KT31, KT32, KT33, KT34, K31, K32
      XNEG = -9999.0
      READ (5,70) HEAD
      WRITE (6,80) HEAD
      READ (5,90) WU1, WU2, WU3, WAXL1, WAXL2, WAXL3, T1, A1, T2, A2,
     1T3, A3, S1, S2, S3
      READ (5,90) ZR1, ZR2, ZR3, Z1, Z2, Z3, HR1, HR2, HR3
      READ (5,90) KT11, KT21, KT31
      READ (5,90) DELPH, XPRINT
C
C     INITIALIZATIONS
C
      R1 = HR1 - Z1
      R2 = HR2 - Z2
      R3 = HR3 - Z3
      KT12 = KT11
      KT13 = KT11
      KT14 = KT11
      KT22 = KT21
      KT23 = KT21
      KT24 = KT21
      KT32 = KT31
      KT33 = KT31
      KT34 = KT31
      TEMP = 0.0
      TICK = 0.0
      AY = 0.0
      DELPH1 = DELPH
      DELPH = DELPH / 57.2958
      PHIS = 0.0
      PHIU1 = 0.0
      PHIU2 = 0.0
      PHIU3 = 0.0
C
      WSIN1 = (WAXL1 - WU1) / 2.0
      CALL SPRING(1, WSIN1, DELS11)
      DELS12 = DELS11
      ZU1 = DELS11
C
      WSIN2 = (WAXL2 - WU2) / 2.0
      CALL SPRING(2, WSIN2, DELS21)
      DELS22 = DELS21
      ZU2 = DELS21
C
      WSIN3 = (WAXL3 - WU3) / 2.0
      CALL SPRING(3, WSIN3, DELS31)
      DELS32 = DELS31
      ZU3 = DELS31
C
      WTIN1 = WAXL1 / 4.0
      DELT11 = WTIN1 / KT11
      DELT12 = DELT11
      DELT13 = DELT11
      DELT14 = DELT11
      ZT1 = DELT11
C
      WTIN2 = WAXL2 / 4.00
      DELT21 = WTIN2 / KT21
      DELT22 = DELT21
      DELT23 = DELT21
      DELT24 = DELT21
      ZT2 = DELT21
```

```
C
      WTIN3 = WAXL3 / 4.00
      DELT31 = WTIN3 / KT31
      DELT32 = DELT31
      DELT33 = DELT31
      DELT34 = DELT31
      ZT3 = DELT31
C
C
C
   10 CONTINUE
      CALL STIFF(1, DELS11, K11, F11)
      CALL STIFF(1, DELS12, K12, F12)
      CALL STIFF(2, DELS21, K21, F21)
      CALL STIFF(2, DELS22, K22, F22)
      CALL STIFF(3, DELS31, K31, F31)
      CALL STIFF(3, DELS32, K32, F32)
      IF (DELT11 .LE. 0.0) KT11 = 0.0
      IF (DELT12 .LE. 0.0) KT12 = 0.0
      IF (DELT21 .LE. 0.0) KT21 = 0.0
      IF (DELT22 .LE. 0.0) KT22 = 0.0
      IF (DELT31 .LE. 0.0) KT31 = 0.0
      IF (DELT32 .LE. 0.0) KT32 = 0.0
      IF ((KT21 + KT22 + KT31 + KT32) .EQ. 0.0) GO TO 60
      IF ((KT21 + KT22) .EQ. 0.0) GO TO 20
      IF ((KT31 + KT32) .EQ. 0.0) GO TO 20
      GO TO 30
   20 CONTINUE
      IF (TICK .EQ. 0.0) WRITE (6,100) AY, SPMASS, USPM1, USPM2, USPM3,
     1DELT21, DELT22, DELT23, DELT24, DELT31, DELT32, DELT33, DELT34,
     2ZU1, ZU2, ZU3, ZT1, ZT2, ZT3
      TICK = 1.0
   30 CONTINUE
C
C
      DO 40 J = 1, 10
        F(J) = 0.0
C
        DO 40 I = 1, 10
   40 AA(I,J) = 0.0
C
      AA(1,1) = -((WAXL1 - WU1)*ZR1 + (WAXL2 - WU2)*ZR2 + (WAXL3 - WU3)*
     1ZR3)
      AA(1,2) = (K11 + K12) * S1 * S1 + (WAXL1 - WU1) * ZR1 * (1 + AY*(
     1PHIS - PHIU1)) - (F11 + F12) * ZR1
      AA(1,3) = (K21 + K22) * S2 * S2 + (WAXL2 - WU2) * ZR2 * (1 + AY*(
     1PHIS - PHIU2)) - (F21 + F22) * ZR2
      AA(1,4) = (K31 + K32) * S3 * S3 + (WAXL3 - WU3) * ZR3 * (1 + AY*(
     1PHIS - PHIU3)) - (F31 + F32) * ZR3
      AA(1,5) = (K11 - K12) * S1
      AA(1,6) = (K21 - K22) * S2
      AA(1,7) = (K31 - K32) * S3
C
      AA(2,1) = -(WAXL1 - WU1) * HR1 - WU1 * (HR1 - Z1)
      AA(2,2) = -(K11 + K12) * S1 * S1 + WAXL1 * R1 + (WAXL1 - WU1) *
     1Z1 - (KT11 + KT14) * ((T1 + A1)**2) - (KT12 + KT13) * T1 * T1
      AA(2,5) = -(K11 - K12) * S1 + (WAXL1 - WU1) * (AY - PHIU1)
      AA(2,8) = (KT11 - KT14) * (T1 + A1) + (KT12 - KT13) * T1 + WAXL1 *
     1 AY
C
      AA(3,1) = -(WAXL2 - WU2) * HR2 - WU2 * (HR2 - Z2)
      AA(3,3) = -(K21 + K22) * S2 * S2 + WAXL2 * R2 + (WAXL2 - WU2) *
     1Z2 - (KT21 + KT24) * (T2 + A2) * (T2 + A2) - (KT22 + KT23) * T2 *
     2T2
      AA(3,6) = -(K21 - K22) * S2 + (WAXL2 - WU2) * (AY - PHIU2)
      AA(3,9) = (KT21 - KT24) * (T2 + A2) + (KT22 - KT23) * T2 + WAXL2 *
     1 AY
C
      AA(4,1) = -(WAXL3 - WU3) * HR3 - WU3 * (HR3 - Z3)
      AA(4,4) = -(K31 + K32) * S3 * S3 + WAXL3 * R3 + (WAXL3 - WU3) *
```

```
     1Z3 - (KT31 + KT34) * (T3 + A3) * (T3 + A3) - (KT32 + KT33) * T3 *
     2T3
      AA(4,7) = -(K31 - K32) * S3 + (WAXL3 - WU3) * (AY - PHIU3)
      AA(4,10) = (KT31 - KT34) * (T3 + A3) + (KT32 - KT33) * T3 + WAXL3
     1* AY
C
      AA(5,1) = -(WAXL1 - WU1) * PHIU1
      AA(5,2) = K11 * S1 - K12 * S1 - (WAXL1 - WU1) * AY
      AA(5,5) = K11 + K12
C
      AA(6,1) = -(WAXL2 - WU2) * PHIU2
      AA(6,3) = K21 * S2 - K22 * S2 - (WAXL2 - WU2) * AY
      AA(6,6) = K21 + K22
C
      AA(7,1) = -(WAXL3 - WU3) * PHIU3
      AA(7,4) = K31 * S3 - K32 * S3 - (WAXL3 - WU3) * AY
      AA(7,7) = K31 + K32
C
      AA(8,2) = (-KT11 + KT14) * (T1 + A1) - (KT12 - KT13) * T1
      AA(8,8) = KT11 + KT12 + KT13 + KT14
C
      AA(9,3) = (-KT21 + KT24) * (T2 + A2) - (KT22 - KT23) * T2
      AA(9,9) = KT21 + KT22 + KT23 + KT24
C
      AA(10,4) = (-KT31 + KT34) * (T3 + A3) - (KT32 - KT33) * T3
      AA(10,10) = KT31 + KT32 + KT33 + KT34
C
      F(1) = -(-(K11 + K12)*S1*S1 - (K21 + K22)*S2*S2 + ((F11 + F12)*
     1ZR1 + (F21 + F22)*ZR2 + (F31 + F32)*ZR3) - (K31 + K32)*S3*S3) *
     2DELPH
      F(2) = -(K11 + K12) * S1 * S1 * DELPH
      F(3) = -(K21 + K22) * S2 * S2 * DELPH
      F(4) = -(K31 + K32) * S3 * S3 * DELPH
      F(5) = -(-K11*S1 + K12*S1) * DELPH
      F(6) = -(-K21*S2 + K22*S2) * DELPH
      F(7) = -(-K31*S3 + K32*S3) * DELPH
   50 CALL SIMQ(AA, F, 10, IER)
C
      AY = AY + F(1)
      PHIU1 = PHIU1 + F(2)
      PHIU2 = PHIU2 + F(3)
      PHIU3 = PHIU3 + F(4)
      Z1 = Z1 - F(5)
      Z2 = Z2 - F(6)
      Z3 = Z3 - F(7)
      HR1 = HR1 - F(5) - F(8)
      HR2 = HR2 - F(6) - F(9)
      HR3 = HR3 - F(7) - F(10)
      ZU1 = ZU1 + F(5)
      ZU2 = ZU2 + F(6)
      ZU3 = ZU3 + F(7)
      ZT1 = ZT1 + F(8)
      ZT2 = ZT2 + F(9)
      ZT3 = ZT3 + F(10)
      PHIS = PHIS + DELPH
      TEMP = TEMP + DELPH1
      SPMASS = PHIS * 57.2958
      USPM1 = PHIU1 * 57.2958
      USPM2 = PHIU2 * 57.2958
      USPM3 = PHIU3 * 57.2958
C
      DELS11 = ZU1 - S1 * (PHIS - PHIU1)
      DELS12 = ZU1 + S1 * (PHIS - PHIU1)
      DELS21 = ZU2 - S2 * (PHIS - PHIU2)
      DELS22 = ZU2 + S2 * (PHIS - PHIU2)
      DELS31 = ZU3 - S3 * (PHIS - PHIU3)
      DELS32 = ZU3 + S3 * (PHIS - PHIU3)
      DELT11 = -(T1 + A1) * PHIU1 + ZT1
      DELT12 = -T1 * PHIU1 + ZT1
      DELT13 = T1 * PHIU1 + ZT1
```

```
      DELT14 = (T1 + A1) * PHIU1 + ZT1
      DELT21 = -(T2 + A2) * PHIU2 + ZT2
      DELT22 = -T2 * PHIU2 + ZT2
      DELT23 = T2 * PHIU2 + ZT2
      DELT24 = (T2 + A2) * PHIU2 + ZT2
      DELT31 = -(T3 + A3) * PHIU3 + ZT3
      DELT32 = -T3 * PHIU3 + ZT3
      DELT33 = T3 * PHIU3 + ZT3
      DELT34 = (T3 + A3) * PHIU3 + ZT3
      IF (ABS(TEMP) .GE. ABS(XPRINT)) WRITE (6,100) AY, SPMASS, USPM1,
     1USPM2, USPM3, DELT21, DELT22, DELT23, DELT24, DELT31, DELT32,
     2DELT33, DELT34, ZU1, ZU2, ZU3, ZT1, ZT2, ZT3
      IF (ABS(TEMP) .GE. ABS(XPRINT)) TEMP = 0.0
C
      GO TO 10
   60 CONTINUE
      WRITE (6,100) AY, SPMASS, USPM1, USPM2, USPM3, DELT21, DELT22,
     1DELT23, DELT24, DELT31, DELT32, DELT33, DELT34, ZU1, ZU2, ZU3,
     2ZT1, ZT2, ZT3
      WRITE (6,100) XNEG
      STOP
   70 FORMAT (20A4)
   80 FORMAT (T1, 'DATA FROM:  ', 20A4)
   90 FORMAT (16F10.2)
  100 FORMAT (T1, 20F10.3)
      END
C
C   SUBROUTINE SPRING
C   ********** ******
C                        CALLED BY MAIN FOR COMPUTING THE STATIC
C   DEFLECTIONS OF THE SUSPENSION SPRINGS.
C
      SUBROUTINE SPRING(N, W, DELS)
      COMMON FORC(3,10), DEL(3,10), NUM(3)
      READ (5,40) NUMBER
      NUM(N) = NUMBER
C
      DO 10 I = 1, NUMBER
   10 READ (5,50) FORC(N,I), DEL(N,I)
C
      DO 20 J = 1, NUMBER
        IF (W .LT. FORC(N,J)) GO TO 30
   20 CONTINUE
C
   30 DELS = DEL(N,J - 1) + ((W - FORC(N,J - 1))*(DEL(N,J) - DEL(N,J -
     11))/(FORC(N,J) - FORC(N,J - 1)))
      RETURN
   40 FORMAT (I2)
   50 FORMAT (2F10.3)
      END
C
C
C SUBROUTINE STIFF
C ********** *****
C                    CALLED BY MAIN FOR COMPUTING THE LOCAL STIFFNESS
C          OF THE SUSPENSION SPRINGS AT ANY GIVEN DEFLECTION.
C
      SUBROUTINE STIFF(N, DELS, XK, XF)
      COMMON FORC(3,10), DEL(3,10), NUM(3)
      NUMBER = NUM(N)
C
      DO 10 I = 1, NUMBER
        IF (DELS .LT. DEL(N,I)) GO TO 20
   10 CONTINUE
C
   20 XK = (FORC(N,I) - FORC(N,I - 1)) / (DEL(N,I) - DEL(N,I - 1))
      XF = FORC(N,I - 1) + ((DELS - DEL(N,I - 1))*(FORC(N,I) - FORC(N,I
     1- 1))/(DEL(N,I) - DEL(N,I - 1)))
      RETURN
      END
```

# APPENDIX C

## EQUATIONS OF MOTION FOR THE YAW/ROLL MODEL

The differential equations which govern the yaw and roll motions of a multiple articulated vehicle will be derived in this appendix. In the model, each sprung mass is treated as a rigid body with five degrees of freedom, namely: lateral, vertical, yaw, roll, and pitch. Since the forward velocity of the lead unit (or the tractor) is assumed to be constant, no longitudinal degree of freedom is incorporated in the equation of motion for the sprung masses. The unsprung mass degrees of freedom are the roll and bounce of each unsprung mass with respect to the sprung mass to which it is attached.

The equations are formulated such that the computer code does not place any limitations on the number of sprung and unsprung masses. The kinematic constraints between the sprung masses are treated in such a fashion that the computer code can be easily modified to accommodate any kind of constraint.

In order to simplify the equations, it is assumed that the pitch angles of the sprung masses and the relative roll angles between the sprung and unsprung masses are small. Further, the principal axes of inertia of the sprung and unsprung masses are assumed to coincide with their respective body fixed coordinate systems.

The discussion to follow is organized under the following subheadings:

1) Axis systems

2) Suspension forces

3) Equations for the sprung masses

4) Equations for the unsprung masses

5) Constraint force and moment equations

6) Tire forces

## C.1 Axis Systems

Three types of axis systems are used in the process of developing the equations of motion. They are: (1) an inertial axis system fixed in space, (2) an axis system fixed to each of the sprung masses, and (3) an axis system fixed to each of the unsprung masses. Figure C.1 shows the axis systems for a four-axle, multiple-articulated vehicle with two articulation points, $C_1$ and $C_2$, respectively.

Euler angles are used to define the orientation of the sprung and unsprung masses with respect to the inertial axis system. Since all sprung mass axis systems are defined alike, the axis transformation equations are given below for only one sprung mass. For the same reason, the transformation equations for the unsprung mass axis systems are derived for a single unsprung mass. The symbols used in the derivation of the equations are defined in Table C.1.

C.1.1 Sprung Mass Axis System. The three Euler angles of yaw ($\psi_s$), pitch ($\theta_s$), and roll ($\phi_s$) which are needed to describe the orientation of each of the sprung mass axis systems are shown in Figures C.2, C.3, and C.4, respectively.

The transformation equation between the inertial and sprung mass axis systems can be derived using the three sequential steps of rotation which are illustrated. For the yaw rotation, $\psi_s$

$$\begin{Bmatrix} \vec{i}_n \\ \vec{j}_n \\ \vec{k}_n \end{Bmatrix} = \begin{bmatrix} \cos\psi_s & -\sin\psi_s & 0 \\ \sin\psi_s & \cos\psi_s & 0 \\ 0 & 0 & 1 \end{bmatrix} \begin{Bmatrix} \vec{i}_1 \\ \vec{j}_1 \\ \vec{k}_1 \end{Bmatrix} \tag{1}$$

or

$$\{\vec{i}_n,\vec{j}_n,\vec{k}_n\}^T = [a_{ij}]\,\{\vec{i}_1,\vec{j}_1,\vec{k}_1\}^T \tag{2}$$

For the rotation, $\theta_s$, illustrated in Figure C.3

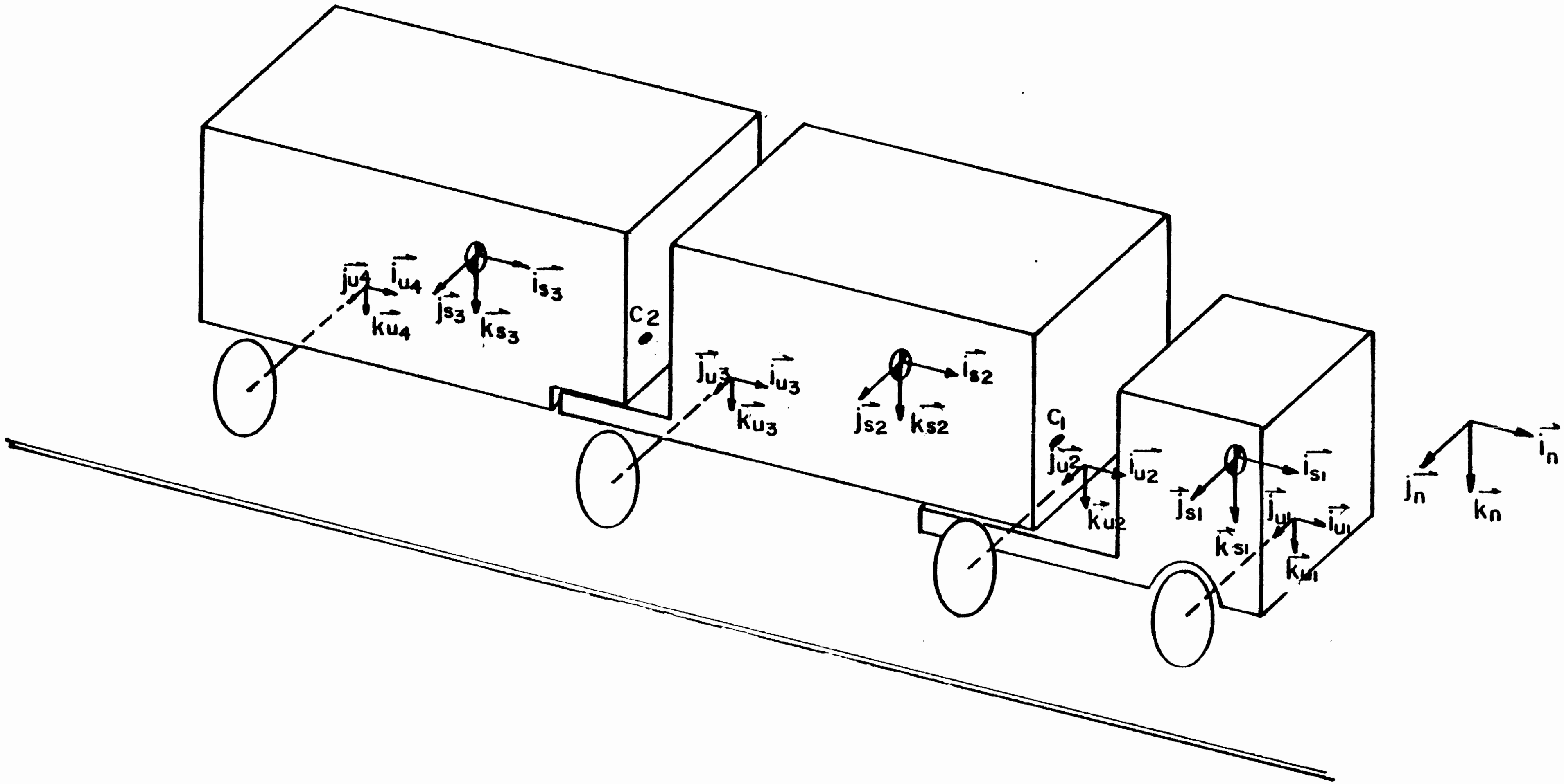


Figure C.1. Axis systems for an articulated vehicle with three sprung masses and four unsprung masses.

Table C.1. Definition of Symbols

| | |
|---|---|
| $\phi_s$ | Sprung mass roll angle (rad) |
| $\psi_s$ | Sprung mass yaw angle (rad) |
| $\theta_s$ | Sprung mass pitch angle (rad) |
| $\phi_u$ | Unsprung mass roll angle (rad) |
| $\psi_u$ | Unsprung mass yaw angle (rad) |
| $\theta_u$ | Unsprung mass pitch angle (rad) |
| $p_s$ | Roll rate of the sprung mass (rad/sec) |
| $q_s$ | Pitch rate of the sprung mass (rad/sec) |
| $r_s$ | Yaw rate of the sprung mass (rad/sec) |
| $p_u$ | Roll rate of the unsprung mass (rad/sec) |
| $q_u$ | Pitch rate of the unsprung mass (rad/sec) |
| $r_u$ | Yaw rate of the unsprung mass (rad/sec) |
| $u_s$ | Longitudinal velocity of the sprung mass c.g. (in/sec) |
| $v_s$ | Lateral velocity of the sprung mass c.g. (in/sec) |
| $w_s$ | Vertical velocity of the sprung mass c.g. (in/sec) |
| $\vec{a}_{m_s}$ | Acceleration of the sprung mass c.g. (in/sec$^2$) |
| $\vec{a}_{m_u}$ | Acceleration of the unsprung mass c.g. (in/sec$^2$) |
| $m_s$ | Mass of the sprung mass (lb-sec$^2$/in) |
| $m_u$ | Mass of the unsprung mass (lb-sec$^2$/in) |
| $(I_{xx_s}, I_{yy_s}, I_{zz_s})$ | Roll, pitch, and yaw moments of inertia of the sprung mass (lb-in-sec$^2$) |
| $(I_{xx_u}, I_{yy_u}, I_{zz_u})$ | Roll, pitch, and yaw moments of inertia of the unsprung mass (lb-in-sec$^2$) |

Table C.1 (Cont.)

| | |
|---|---|
| $S_i$ | Half of the lateral distance between suspension springs on axle i (in) |
| $T_i$ | Half of the lateral distance between the inner tires on axle i (in) |
| $GY_i$ | Dual tire spacings on axle i (in) |
| $HR_i$ | Vertical distance from the roll center $R_i$ to the ground plane (in) |
| $z_{R_i}$ | Vertical distance from the sprung mass c.g. to the roll center of axle i (in) |
| $x_{u_i}$ | Longitudinal distance from the sprung mass c.g. to axle i (in) |
| $z_{u_i}$ | Vertical distance from the roll center $R_i$ to the c.g. of axle i (in) |
| $F_{y_{ji}}$ | Lateral force produced at the tire-road interface of the $j^{th}$ tire on axle i (lb) |
| $F_{z_{ji}}$ | Vertical force acting at the tire-road interface of the $j^{th}$ tire on axle i (lb) |
| $AT_{ji}$ | Aligning torque generated at the tire-road interface of the $j^{th}$ tire on axle i (in-lb) |
| $FR_i$ | Force acting through the roll center $R_i$ in a direction parallel to the $\vec{j}_u$ axis (lb) |
| $F_{ji}$ | Compressive or tensile force reacted by the $j^{th}$ suspension spring on axle i. Compressive force is assumed to be positive (lb) |
| $KRS_i$ | Auxiliary roll stiffness of the suspension springs on axle i (in-lb/rad) |
| g | Acceleration due to gravity (386.4 in/sec$^2$) |

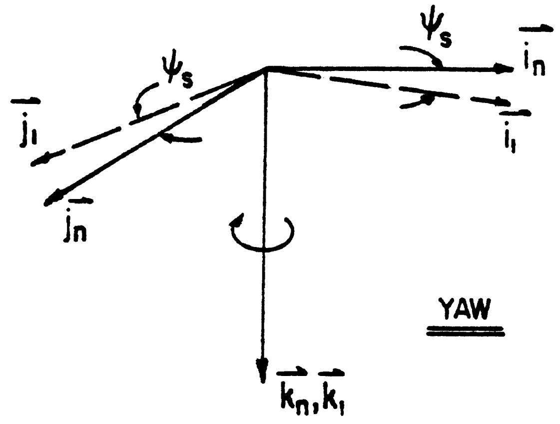


Figure C.2

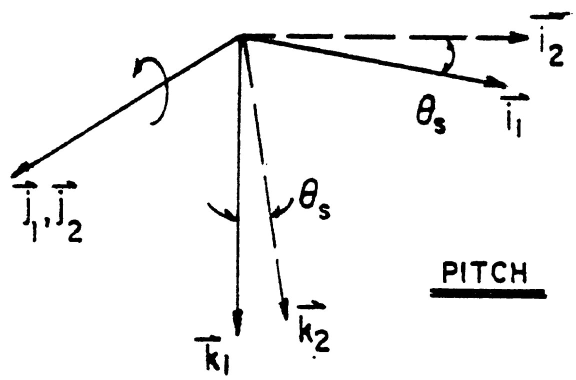


Figure C.3

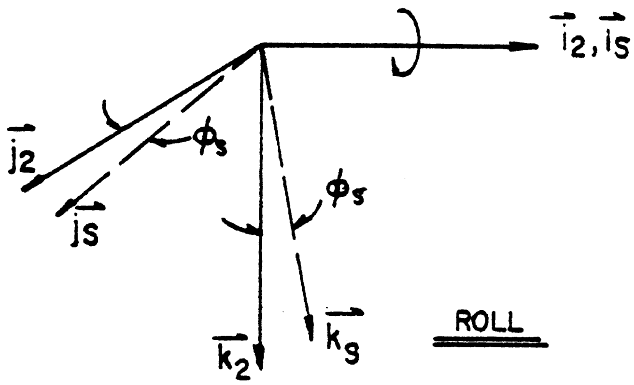


Figure C.4

Euler angles needed to define the orientation of each of the sprung mass axis systems.

$$\begin{Bmatrix} \vec{i}_1 \\ \vec{j}_1 \\ \vec{k}_1 \end{Bmatrix} = \begin{bmatrix} \cos\theta_s & 0 & \sin\theta_s \\ 0 & 1 & 0 \\ -\sin\theta_s & 0 & \cos\theta_s \end{bmatrix} \begin{Bmatrix} \vec{i}_2 \\ \vec{j}_2 \\ \vec{k}_2 \end{Bmatrix} \tag{3}$$

or

$$\{\vec{i}_1,\vec{j}_1,\vec{k}_1\}^T = [b_{ij}]\ \{\vec{i}_2,\vec{j}_2,\vec{k}_2\}^T \tag{4}$$

On similar lines, the roll rotation illustrated in Figure C.4 yields

$$\begin{Bmatrix} \vec{i}_2 \\ \vec{j}_2 \\ \vec{k}_2 \end{Bmatrix} = \begin{bmatrix} 1 & 0 & 0 \\ 0 & \cos\phi_s & -\sin\phi_s \\ 0 & \sin\phi_s & \cos\phi_s \end{bmatrix} \begin{Bmatrix} \vec{i}_s \\ \vec{j}_s \\ \vec{k}_s \end{Bmatrix} \tag{5}$$

or

$$\{\vec{i}_2,\vec{j}_2,\vec{k}_2\}^T = [c_{ij}]\ \{\vec{i}_s,\vec{j}_s,\vec{k}_s\}^T \tag{6}$$

The transformation matrix which is needed to relate the sprung mass axis system and the inertial axis system can now be obtained by combining (2), (4), and (6). Doing so, we get

$$\{\vec{i}_n,\vec{j}_n,\vec{k}_n\}^T = [A_{ij}]\ \{\vec{i}_s,\vec{j}_s,\vec{k}_s\}^T \tag{7}$$

where $$[A_{ij}] = [a_{ij}]\ [b_{ij}]\ [c_{ij}]$$

Sprung mass pitch angles are usually restricted to very small values, during directional maneuvers, hence $\sin\theta_s$ can be replaced by $\theta_s$ and $\cos\theta_s$ by 1.0 in the transformation equations. Expanding (7), we get:

$$\begin{Bmatrix} \vec{i}_n \\ \vec{j}_n \\ \vec{k}_n \end{Bmatrix} =$$

$$\begin{bmatrix} \cos\psi_s & -\sin\psi_s\cos\phi_s+\cos\psi_s\theta_s\sin\phi_s & \sin\psi_s\sin\phi_s+\cos\psi_s\theta_s\cos\phi_s \\ \sin\psi_s & \cos\psi_s\cos\phi_s+\sin\psi_s\theta_s\sin\phi_s & -\cos\psi_s\sin\phi_s+\sin\psi_s\theta_s\cos\phi_s \\ -\theta_s & \sin\phi_s & \cos\phi_s \end{bmatrix} \begin{Bmatrix} \vec{i}_s \\ \vec{j}_s \\ \vec{k}_s \end{Bmatrix} \tag{8}$$

Also

$$\begin{Bmatrix} \vec{i}_s \\ \vec{j}_s \\ \vec{k}_s \end{Bmatrix} =$$

$$\begin{bmatrix} \cos\psi_s & \sin\psi_s & -\theta_s \\ -\sin\psi_s\cos\phi_s+\cos\psi_s\theta_s\sin\phi_s & \cos\psi_s\cos\phi_s+\sin\psi_s\theta_s\sin\phi_s & \sin\phi_s \\ \sin\psi_s\sin\phi_s+\cos\psi_s\theta_s\cos\phi_s & -\cos\psi_s\sin\phi_s+\sin\psi_s\theta_s\cos\phi_s & \cos\phi_s \end{bmatrix} \begin{Bmatrix} \vec{i}_n \\ \vec{j}_n \\ \vec{k}_n \end{Bmatrix} \tag{9}$$

Sprung Mass Angular Velocities:

The equations of motion of each sprung mass are written in terms of the body-fixed angular velocities ($p_s,q_s,r_s$) and their derivatives. In order to determine the Euler angles, the Euler angular velocities ($\dot{\phi}_s,\dot{\theta}_s,\dot{\psi}_s$) have to be calculated from the body-fixed angular velocities ($p_s,q_s,r_s$) and then integrated numerically. The Euler angular velocities ($\dot{\phi}_s,\dot{\theta}_s,\dot{\psi}_s$) are defined along the ($\vec{i}_s,\vec{j}_2,\vec{k}_n$) directions. Therefore, equating the body-fixed and Euler angular velocities, we get

$$p_s\vec{i}_s + q_s\vec{j}_s + r_s\vec{k}_s = \dot{\phi}_s\vec{i}_s + \dot{\theta}_s\vec{j}_2 + \dot{\psi}_s\vec{k}_n \tag{10}$$

From (5) we note that

$$\vec{j}_2 \; = \; \cos\phi_s\vec{j}_s - \sin\phi_s\vec{k}_s \tag{11}$$

Also (8) indicates that

$$\vec{k}_n \; = -\theta_s\vec{i}_s + \sin\phi_s\vec{j}_s + \cos\phi_s\vec{k}_s \tag{12}$$

Substituting (11) and (12) into (10) we get

$$p_s\vec{i}_s = (\dot{\phi}_s - \theta_s\dot{\psi}_s)\,\vec{i}_s \tag{13}$$

$$q_s\vec{j}_s = (\dot{\theta}_s \cos\phi_s + \sin\phi_s\dot{\psi}_s)\,\vec{j}_s \tag{14}$$

$$r_s\vec{k}_s = (-\dot{\theta}_s \sin\phi_s + \dot{\psi}_s \cos\phi_s)\,\vec{k}_s \tag{15}$$

The above three equations can also be written for solving the Euler angular velocities in terms of the body-fixed angular velocities $(p_s, q_s, r_s)$. In doing so, we get:

$$\dot{\phi}_s \; = \; p_s + (q_s\sin\phi_s + r_s\cos\phi_s)\theta_s \tag{16}$$

$$\dot{\theta}_s \; = \; q_s\cos\phi_s - r_s\sin\phi_s \tag{17}$$

$$\dot{\psi}_s \; = \; q_s\sin\phi_s + r_s\cos\phi_s \tag{18}$$

Therefore, Equations (16)-(18) can be numerically integrated to obtain the Euler angles at any time t of the simulation.

C.1.2 Unsprung Mass Axis System. No pitch degree of freedom has been incorporated in the unsprung mass equations. Each unsprung mass is permitted only to roll and bounce with respect to the sprung mass to which it is attached. The orientation of the unsprung mass with respect to the inertial axis system is therefore defined by the yaw angle, $\psi_s$, and the roll angle, $\phi_u$, shown in Figure C.5 and Figure C.6, respectively. Below, we shall derive the transformation equation which relates the axis systems located in the sprung and unsprung masses, respectively.

Figure C.6 indicates that

$$\begin{Bmatrix} \vec{i}_u \\ \vec{j}_u \\ \vec{k}_u \end{Bmatrix} = \begin{bmatrix} 1 & 0 & 0 \\ 0 & \cos\phi_u & \sin\phi_u \\ 0 & -\sin\phi_u & \cos\phi_u \end{bmatrix} \begin{Bmatrix} \vec{i}_1 \\ \vec{j}_1 \\ \vec{k}_1 \end{Bmatrix} \tag{19}$$

When Equations (3) and (5) are combined, we have

$$\begin{Bmatrix} \vec{i}_1 \\ \vec{j}_1 \\ \vec{k}_1 \end{Bmatrix} = [b_{ij}]\,[c_{ij}] \begin{Bmatrix} \vec{i}_s \\ \vec{j}_s \\ \vec{k}_s \end{Bmatrix} \tag{20}$$

Therefore, combining Equations (19) and (20) and substituting for $[b_{ij}]$ and $[c_{ij}]$, we get

$$\begin{Bmatrix} \vec{i}_u \\ \vec{j}_u \\ \vec{k}_u \end{Bmatrix} = \begin{bmatrix} 1 & \theta_s \sin\phi_s & \theta_s \cos\phi_s \\ -\theta_s \sin\phi_u & \cos(\phi_s-\phi_u) & -\sin(\phi_s-\phi_u) \\ -\theta_s \cos\phi_u & \sin(\phi_s-\phi_u) & \cos(\phi_s-\phi_u) \end{bmatrix} \begin{Bmatrix} \vec{i}_s \\ \vec{j}_s \\ \vec{k}_s \end{Bmatrix} \tag{21}$$

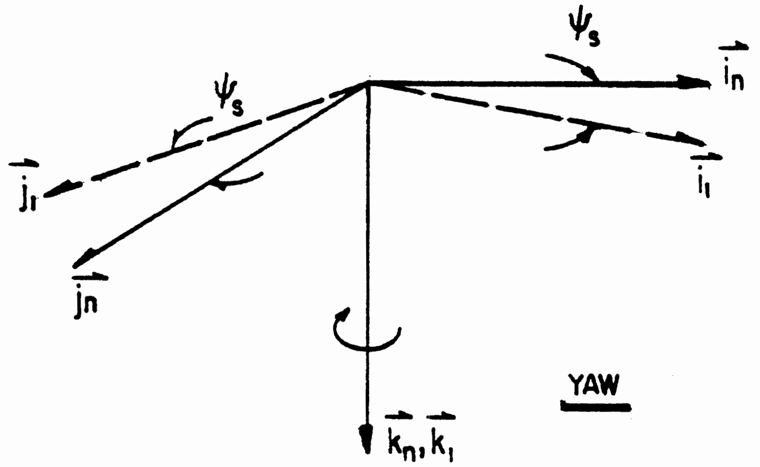


Fiqure C.5

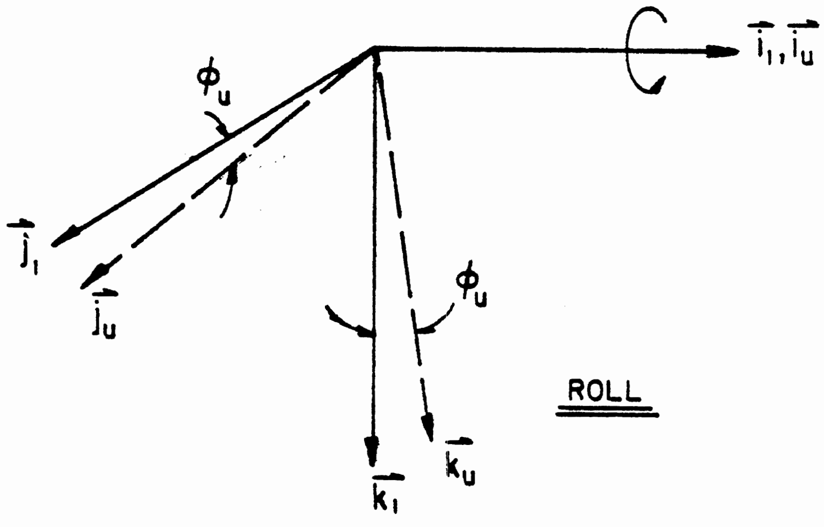


Fiqure C.6

Euler angles needed to define the orientation of each of the unsprung masses.

## C.2 Suspension Forces

Each suspension is assumed to consist of a pair of linear springs and linkages which establish a roll center, $R_i$. Figure C.7 is a schematic diagram showing that the suspension springs are assumed to remain parallel to the $\vec{k}_{u_i}$ axis of the unsprung mass, and are capable of transmitting either compressive or tensile forces only. All roll plane forces which are perpendicular to the suspension springs are assumed to act through the roll center, $R_i$. The roll center, $R_i$, is located at a fixed distance, $Z_{R_i}$, beneath the sprung mass, and is permitted to slide along the $\vec{k}_{u_i}$ axis of the unsprung mass. Figure C.7 shows that the suspension forces transmitted to the sprung mass from any given axle, i, are therefore

$$F_{susp_i} = F_{R_i}\vec{j}_{u_i} - (F_{1i}+F_{2i})\vec{k}_{u_i} \tag{22}$$

The suspension forces can be defined in the sprung mass coordinate system by applying the coordinate transformation expressed by Equation (21). Upon applying the transformation, we get

$$\begin{aligned} F_{susp_i} &= F_{R_i}[-\theta_s \sin\phi_{u_i}\vec{i}_s + \cos(\phi_s-\phi_{u_i})\vec{j}_s - \sin(\phi_s-\phi_{u_i})\vec{k}_s] \\ &\quad - [F_{1i}+F_{2i}][\theta_s \cos\phi_{u_i}\vec{i}_s + \sin(\phi_s-\phi_{u_i})\vec{j}_s + \cos(\phi_s-\phi_{u_i})\vec{k}_s] \end{aligned} \tag{23}$$

$$\begin{aligned} &= [-F_{R_i}\theta_s \sin\phi_{u_i} + (F_{1i}+F_{2i})\theta_s\cos\phi_{u_i}]\vec{i}_s + [F_{R_i}\cos(\phi_s-\phi_{u_i}) \\ &\quad - (F_{1i}+F_{2i})\sin(\phi_s-\phi_{u_i})]\vec{j}_s - [F_{R_i}\sin(\phi_s-\phi_{u_i}) + (F_{1i}+F_{2i})\cos(\phi_s-\phi_{u_i})]\vec{k}_s \end{aligned} \tag{24}$$

The force, $F_{R_i}$, acting through the roll center, $R_i$, is an internal force which can be eliminated by inspecting the dynamic equilibrium of the axle in the $\vec{j}_{u_i}$ direction. The equation for the lateral equilibrium of the axle is

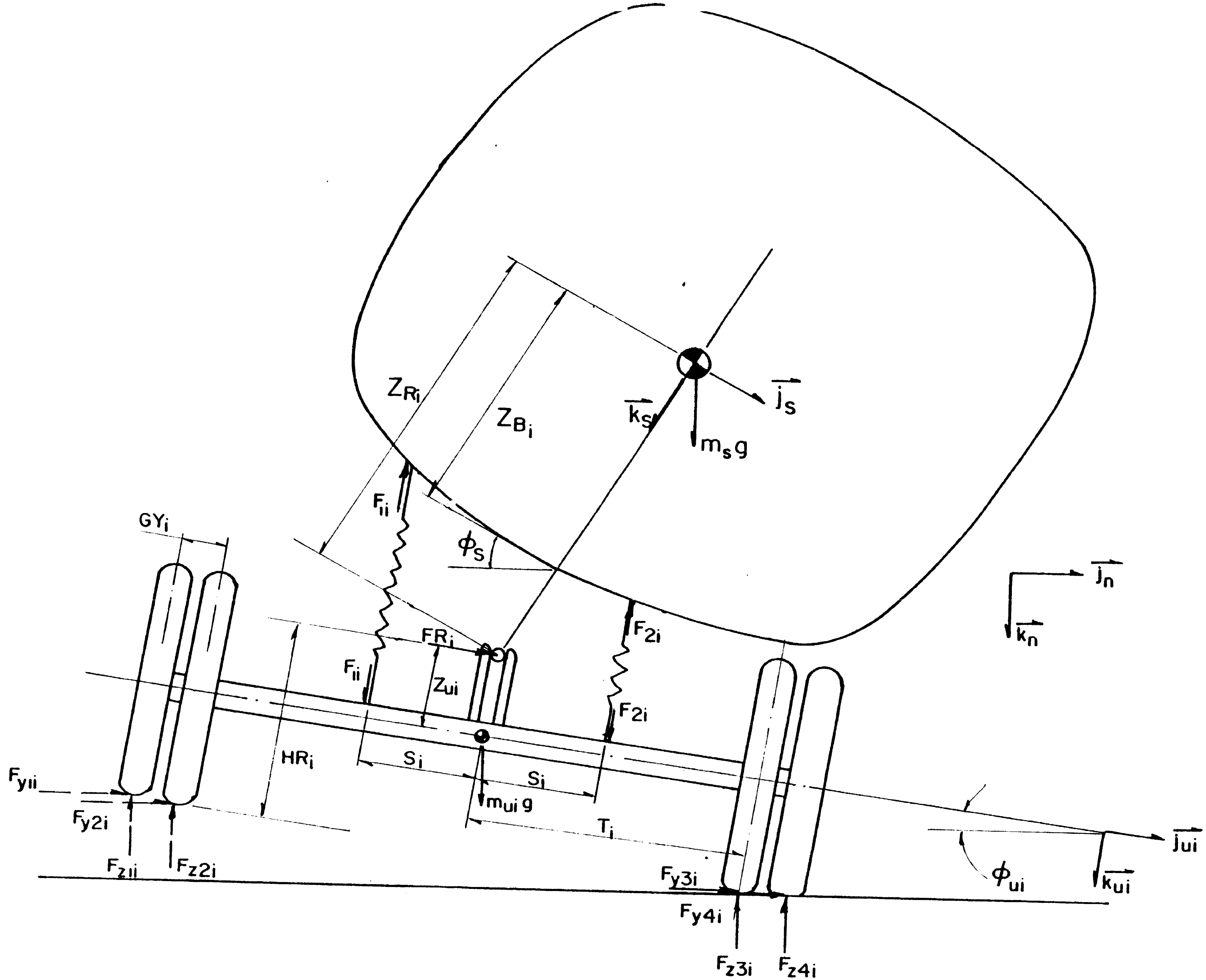


Figure C.7. Suspension and tire forces at each axle.

$$m_{u_i}[\vec{a}_{m_{u_i}} \cdot \vec{j}_{u_i}] = -F_{R_i} + \begin{pmatrix} F_{y_{1i}} + F_{y_{2i}} \\ + F_{y_{3i}} + F_{y_{4i}} \end{pmatrix} \cos \phi_{u_i}$$

$$- \begin{pmatrix} F_{z_{1i}} + F_{z_{2i}} \\ + F_{z_{3i}} + F_{z_{4i}} \end{pmatrix} \sin \phi_{u_i} + m_{u_i} g \sin \phi_{u_i} \tag{25}$$

Rearranging, we get

$$F_{R_i} = -m_{u_i}[\vec{a}_{m_{u_i}} \cdot \vec{j}_{u_i}] + \begin{pmatrix} F_{y_{1i}} + F_{y_{2i}} \\ + F_{y_{3i}} + F_{y_{4i}} \end{pmatrix} \cos \phi_{u_i}$$

$$- \begin{pmatrix} F_{z_{1i}} + F_{z_{2i}} \\ + F_{z_{3i}} + F_{z_{4i}} \end{pmatrix} \sin \phi_{u_i} + m_{u_i} g \sin \phi_{u_i} \tag{26}$$

Of the terms in the right-hand side of (26), the only unknown is the acceleration, $\vec{a}_{m_{u_i}}$ of the unsprung mass. Since the position of the unsprung mass is defined relative to the sprung mass to which it is attached, the acceleration of the unsprung mass is given by:

$$\vec{a}_{m_{u_i}} = \vec{a}_{m_s} + \vec{a}_{R_i/m_s} + \vec{a}_{m_{u_i}/R_i} \tag{27}$$

where $\vec{a}_{m_s}$ is the acceleration at the c.g. of the sprung mass

$\vec{a}_{R_{i/m_s}}$ is the relative acceleration at the roll center, $R_i$, with respect to the sprung mass c.g.

and $\vec{a}_{m_{u_i}/R_i}$ is the relative acceleration at the c.g. of the axle with respect to the roll center, $R_i$

We shall now derive expressions for each of the three terms in the right-hand side of (27).

The acceleration of the sprung mass along the body-fixed coordinates $(\vec{i}_s, \vec{j}_s, \vec{k}_s)$ is given by:

$$\vec{a}_{m_s} = (\dot{u}_s + q_s w_s - r_s v_s)\vec{i}_s + (\dot{v}_s + u_s r_s - p_s w_s)\vec{j}_s + (\dot{w}_s + p_s v_s - q_s u_s)\vec{k}_s \tag{28}$$

Since the roll center, $R_i$, is at a fixed distance from the sprung mass c.g., the acceleration of $R_i$ with respect to the sprung mass c.g. $(\vec{a}_{R_i/m_s})$ can be derived as follows:

$$\vec{r}_{R_i/m_s} = x_{R_i}\vec{i}_s + z_{R_i}\vec{k}_s \tag{29}$$

$$\vec{v}_{R_i/m_s} = \dot{\vec{r}}_{R_i/m_s} = (z_{R_i} q_s)\vec{i}_s + (-p_s z_{R_i} + x_{R_i} r_s)\vec{j}_s - x_{R_i} q_s \vec{k}_s \tag{30}$$

$$\begin{aligned}\vec{a}_{R_i/m_s} = \dot{\vec{v}}_{R_i/m_s} = {} & [\dot{q}_s z_{R_i} - x_{R_i} q_s^2 + p_s r_s z_{R_i} - x_{R_i} r_s^2]\vec{i}_s \\ & + [-\dot{p}_s z_{R_i} + x_{R_i}\dot{r}_s + z_{R_i} q_s r_s + x_{R_i} q_s p_s]\vec{j}_s \\ & + [-p_s^2 z_{R_i} + x_{R_i} r_s p_s - z_{R_i} q_s^2 - x_{R_i}\dot{q}_s]\vec{k}_s\end{aligned} \tag{31}$$

The third term in (27), $\vec{a}_{m_{u_i}/R_i}$, can be derived along the same lines as $\vec{a}_{R_i/m_s}$, viz.:

$$\vec{r}_{m_{u_i}/R_i} = z_{u_i}\vec{k}_{u_i} \tag{32}$$

$$\vec{v}_{m_{u_i}/R_i} = \dot{\vec{r}}_{m_{u_i}/R_i} = \dot{z}_{u_i}\vec{k}_{u_i} - p_{u_i} z_{u_i}\vec{j}_{u_i} \tag{33}$$

$$\vec{a}_{m_{u_i}/R_i} = \dot{\vec{v}}_{m_{u_i}/R_i} = \ddot{z}_{u_i}\vec{k}_{u_i} - (\dot{p}_{u_i} z_{u_i} + 2p_{u_i}\dot{z}_{u_i})\vec{j}_{u_i} - p_{u_i}^2 z_{u_i}\vec{k}_{u_i} + p_{u_i} r_{u_i} z_{u_i}\vec{i}_{u_i} \tag{34}$$

Hence, combining (28), (31) and (34) and transforming the acceleration defined in the sprung mass coordinate system to the unsprung mass coordinate system, we get:

$$\vec{a}_{m_{u_i}} \cdot \vec{j}_{u_i} = -(\dot{u}_s + q_s w_s - r_s v_s + \dot{q}_s z_{R_i} - x_{R_i} q_s^2 + p_s r_s z_{R_i} - x_{R_i} r_s^2)\theta_s \sin\phi_{u_i}$$
$$+ (\dot{v}_s + u_s r_s - p_s w_s - \dot{p}_s z_{R_i} + x_{R_i}\dot{r}_s + z_{R_i} q_s r_s$$
$$+ x_{R_i} q_s p_s)\cos(\phi_s - \phi_{u_i}) - [\dot{w}_s + p_s v_s - q_s u_s - p_s^2 z_{R_i}$$
$$+ x_{R_i} r_s p_s - z_{R_i} q_s^2 - x_{R_i}\dot{q}_s]\sin(\phi_s - \phi_{u_i}) - \dot{p}_{u_i} z_{u_i} - 2p_{u_i}\dot{z}_{u_i} \tag{35}$$

On substituting the right-hand side of (25) for the term $(\vec{a}_{m_{u_i}} \cdot \vec{j}_{u_i})$ in Equation (26), we get the following result for $F_{R_i}$:

$$F_{R_i} = -m_{u_i}\{-[\dot{u}_s + q_s w_s - r_s v_s + \dot{q}_s z_{R_i} - x_{R_i} q_s^2 + p_s r_s z_{R_i} + x_{R_i} r_s^2]\theta_s \sin\phi_{u_i}$$
$$+ (\dot{v}_s + u_s r_s - p_s w_s - \dot{p}_s z_{R_i} + x_{R_i}\dot{r}_s + z_{R_i} q_s r_s + x_{R_I} q_s p_s]\cos(\phi_s - \phi_{u_i})$$
$$- (\dot{w}_s + p_s v_s - q_s u_s - p_s^2 z_{R_i} + x_{R_i} r_s p_s - z_{R_i} q_s^2 - x_{R_i}\dot{q}_s]\sin(\phi_s - \phi_{u_i})$$
$$- \dot{p}_{u_i} z_{u_i} - 2p_{u_i}\dot{z}_{u_i}\} + \begin{pmatrix} F_{y_{1i}} + F_{y_{2i}} \\ + F_{y_{3i}} + F_{y_{4i}} \end{pmatrix} \cos\phi_{u_i}$$
$$- \begin{pmatrix} F_{z_{1i}} + F_{z_{2i}} \\ + F_{z_{3i}} + F_{z_{4i}} \end{pmatrix} \sin\phi_{u_i} + m_{u_i} g \sin\phi_{u_i} \tag{36}$$

## C.3 Sprung Mass Equations

The five second-order differential equations for each of the sprung masses can be written as follows.

Lateral Force Equation:

$$\begin{aligned} m_s\dot{v}_s - m_s(p_s w_s - r_s u_s) &= \sum \vec{j}_s \text{ component of constraint forces} \\ &+ \sum \vec{j}_s \text{ component of the suspension forces} \\ &+ \vec{j}_s \text{ component of gravity} \\ &= \sum \vec{j}_s \text{ component of constraint forces} \\ &+ \sum_{i=i_1}^{i_2} [F_{R_i}\cos(\phi_s - \phi_{u_i}) - (F_{1i}+F_{2i})\sin(\phi_s-\phi_{u_i})] \\ &+ m_s g \sin \phi_s \qquad (37) \end{aligned}$$

Note: For the sprung mass under consideration, the axle numbers are assumed to vary from $i_1$ to $i_2$.

Vertical Force Equation:

$$\begin{aligned} m_s\dot{w}_s - m_s(q_s u_s - p_s v_s) &= \sum \vec{k}_s \text{ component of constraint forces} \\ &+ \sum \vec{k}_s \text{ component of the suspension forces} \\ &+ \vec{k}_s \text{ component of gravity} \\ &= \sum \vec{k}_s \text{ component of constraint forces} \\ &- \sum_{i=i_1}^{i_2} [F_{R_i}\sin(\phi_s - \phi_{u_i}) + (F_{1i}+F_{2i})\cos(\phi_s-\phi_{u_i})] \\ &+ m_s g \cos \phi_s \qquad (38) \end{aligned}$$

Rolling Moment Equation:

$$I_{xx_s}\dot{p}_s - (I_{yy_s} - I_{zz_s})q_s r_s = \sum \text{roll moments from the constraints}$$
$$+ \sum \text{roll moments from the suspension}$$
$$= \sum \text{roll moments from the constraints}$$
$$- \sum_{i=i_1}^{i_2} F_{R_i}\cos(\phi_s-\phi_{u_i})z_{R_i} + \sum_{i=i_1}^{i_2} (F_{1i}+F_{2i})s_i$$
$$+ \sum_{i=i_1}^{i_2} (F_{1i}+F_{2i})\sin(\phi_s-\phi_{u_i})z_{R_i}$$
$$+ \sum_{i=i_1}^{i_2} KRS_i\,(\phi_s-\phi_{u_i}) \qquad (39)$$

Pitching Moment Equation:

$$I_{yy_s}\dot{q}_s - (I_{zz_s} - I_{xx_s})p_s r_s = \sum \text{pitching moments from the constraints}$$
$$+ \sum \text{pitching moments from the suspension}$$
$$= \sum \text{pitching moments from the constraints}$$
$$+ \sum_{i=i_1}^{i_2} [F_{R_i}\sin(\phi_s-\phi_{u_i})$$
$$+ (F_{1i}+F_{2i})\cos(\phi_s-\phi_{u_i})]x_{u_i} \qquad (40)$$

Yawing Moment Equation:

Note that the unsprung masses do not have a separate yaw degree of freedom. Consequently, the yaw moments of inertia of the unsprung masses are combined with the sprung-mass yaw moment of inertia to obtain an equation applicable to the sprung and unsprung masses in combination. Thus we write:

$$\left[\sum_{i=i_1}^{i_2} I_{zz_{u_i}} + I_{zz_s}\right]\dot{r}_s - (I_{xx_s} - I_{yy_s})p_s q_s$$

$$= \sum \text{yaw moments from the constraints}$$

$$+ \sum_{i=i_1}^{i_2} \{[F_{R_i}\cos(\phi_s-\phi_{u_i}) - (F_{1i}+F_{2i})\sin(\phi_s-\phi_{u_i}]x_{u_i}$$

$$+ \begin{pmatrix} AT_{1i} + AT_{2i} \\ + AT_{3i} + AT_{4i} \end{pmatrix} \cos\phi_s\} \qquad (41)$$

Equations (37)-(41) are the governing differential equations for the sprung masses. The equations needed to evaluate the unknown constraint forces and tire forces will be developed in subsequent sections.

## C.4 Unsprung Mass Equations

Given that the unsprung mass is assumed to yaw with the sprung mass, the remaining significant degrees of freedom for the unsprung mass are roll and bounce (or jounce/rebound). The equations for the roll and bounce degrees of freedom are given below.

Roll Moment Equation:

$$I_{xx_{u_i}}\dot{p}_{u_i} = -(F_{1i}-F_{2i})S_i - F_{R_i}z_{u_i} - \begin{pmatrix} F_{y_{1i}} + F_{y_{2i}} \\ + F_{y_{3i}} + F_{y_{4i}} \end{pmatrix}\cos\phi_{u_i}$$

$$- \begin{pmatrix} F_{z_{1i}} + F_{z_{2i}} \\ + F_{z_{3i}} + F_{z_{4i}} \end{pmatrix}\sin\phi_{u_i} \quad (HR\cos\phi_{u_i} - z_{u_i})$$

$$+ (F_{z_{2i}} - F_{z_{4i}})(T_i + a_{y_i})\cos\phi_{u_i} + (F_{z_{2i}} - F_{z_{3i}})T_i\cos\phi_{u_i}$$

$$+ KRS_i(\phi_s-\phi_{u_i}) \qquad (42)$$

Jounce/Rebound Force Equation:

$$m_{u_i}\vec{a}_{m_{u_i}} \cdot \vec{k}_{u_i} = m_{u_i} g \cos \phi_{u_i} + F_{1i} + F_{2i}$$

$$- (F_{z_{1i}} + F_{z_{2i}} + F_{z_{3i}} + F_{z_{4i}})\cos \phi_{u_i} - \begin{pmatrix} F_{y_{1i}} + F_{y_{2i}} \\ + F_{y_{3i}} + F_{y_{4i}} \end{pmatrix} \sin \phi_{u_i} \tag{43}$$

The left-hand side of Equation (43) can be evaluated in a manner similar to that shown for Equation (35). Doing so, we get:

$$\vec{a}_{m_{u_i}} \cdot \vec{k}_{u_i} = [- \dot{u}_s + q_s w_s - r_s v_s + \dot{q}_s z_{R_i} - x_{R_i} q_s^2 + p_s r_s z_{R_i} - x_{R_i} r_s^2]\theta_s \cos \phi_{u_i}$$

$$+ [\dot{v}_s + u_s r_s - p_s w_s - \dot{p}_s z_{R_i} + x_{R_i} \dot{r}_s + z_{R_i} q_s r_s + x_{R_i} q_s p_s]\sin(\phi_s - \phi_{u_i})$$

$$+ [\dot{w}_s + p_s v_s - q_s u_s - p_s^2 z_{R_i} + x_{R_i} r_s p_s - z_{R_i} q_s^2 - x_{R_i} q_s^2]\cos(\phi_s - \phi_{u_i})$$

$$+ (\ddot{z}_{u_i} - p_{u_i}^2 z_{u_i}) \tag{44}$$

## C.5 Constraint Equations

The differential equations which govern the motion of the sprung masses (Equations (37)-(41)) contain terms which are related to the constraint forces and moments. These constraint forces and moments arise at the points of connection between the various sprung masses. We shall develop a method by which these unknown constraint forces and moments can be solved for by making use of the kinematic equations which define the constraints.

The set of differential equations (37)-(43) which give the motion of the sprung and unsprung masses can be written using matrix notation. If the vehicle is composed of n sprung masses and m unsprung masses, we would get a set of k second-order differential equations, where $k = 5n + 2m$. This set of k differential equations, when written using matrix notation, is of the form:

$$M \ddot{\vec{x}} = \vec{y} + N \vec{f}_c \tag{45}$$

where

$M$ is the inertia matrix of size $k \times k$

$\dot{\vec{x}}$ is a vector of the first derivative of the motion variables of size k:

$$[(v_i, w_i, r_i, q_i, p_i)_{i=1}^{n}, (p_{u_i}, z_{u_i})_{i=1}^{m}]$$

$\vec{y}$ is a vector of size k, which is a function of $\vec{x}$, $\dot{\vec{x}}$ and the dimension of the vehicle

$\vec{f}_c$ is a vector of j unknown constraint forces and moments

N is a matrix of size $k \times j$, which is a function of vehicle dimensions and $\vec{x}$.

The kinematic constraints that exist at the various connecting points, when written as a set of acceleration constraint equations, are of the form:

$$C \ddot{\vec{x}} = \vec{d} \tag{46}$$

where

C is a matrix of size $j \times k$, which is a function of the vehicle dimensions and $\vec{x}$

$\vec{d}$ is a vector of size j, which is a function of $\vec{x}$, $\dot{\vec{x}}$, and the dimensions of the vehicle.

We shall solve for the constraint force vector, $\vec{f}_c$, using Equations (45) and (46). Firstly, if we solve (45) for $\ddot{\vec{x}}$, we obtain:

$$\ddot{\vec{x}} = M^{-1} \vec{y} + M^{-1} N \vec{f}_c \tag{47}$$

Substituting (47) in (46), we get

$$C M^{-1} \vec{y} + C M^{-1} N \vec{f}_c = \vec{d} \tag{48}$$

Upon solving (48) for the constraint forces, we obtain:

$$\vec{f}_c = [C\ M^{-1}\ N]^{-1}\ \{\vec{d} - C\ M^{-1}\ \vec{y}\} \tag{49}$$

The set of differential equations given by Equation (45) can now be solved by substituting (49) back into (45). Upon doing so, we obtain:

$$\ddot{\vec{x}} = M^{-1}\ \vec{y} + M^{-1}\ N[C\ M^{-1}\ N]^{-1}\ \{\vec{d} - C\ M^{-1}\ \vec{y}\} \tag{50}$$

Since all the terms in the right-hand side of (50) are known, Equation (50) can be integrated by any standard integration subroutine.

In its present form, the computer program permits four types of constraints to be represented. They are: (1) fifth wheel, (2) inverted fifth wheel, (3) kingpin, and (4) pintle hook. Schematic diagrams of each of the connections are shown in Figures C.8 through C.11.

The fifth wheel and the inverted fifth wheel arrangement permit the lead and the trailing units to yaw and pitch with respect to one another, but are stiff in roll. The kingpin-type connection permits only yaw motions. In the case of the pintle hook connection, the trailing unit is permitted to roll, bounce, yaw, and pitch with respect to the lead unit. The only constraint placed by a pintle hook is that of lateral motion.

The roll and pitch moments transmitted through the fifth wheel, inverted fifth wheel, and the kingpin connection can be easily evaluated in terms of the relative roll and pitch displacements between the adjacent units. Therefore, the acceleration constraint approach is not adopted for solving for the roll and pitch moments. In the discussion to follow, the acceleration constraint equations needed for determining the lateral and vertical forces at the connecting points are developed. Following which, the equation for the roll and pitch constraining moments, which are based on the roll and pitch displacements, are developed separately for the fifth wheel, inverted fifth wheel, and the kingpin connections.

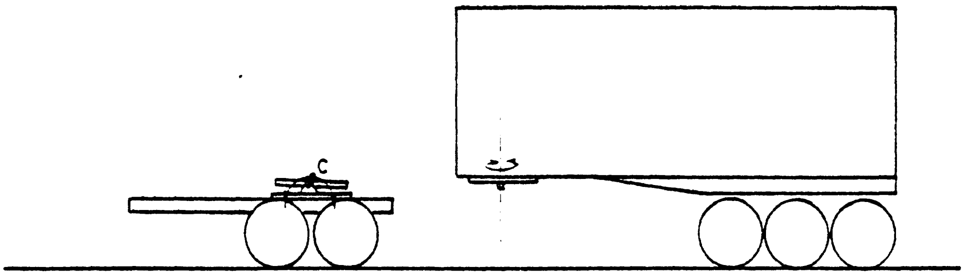


Figure C.8. Conventional fifth wheel.

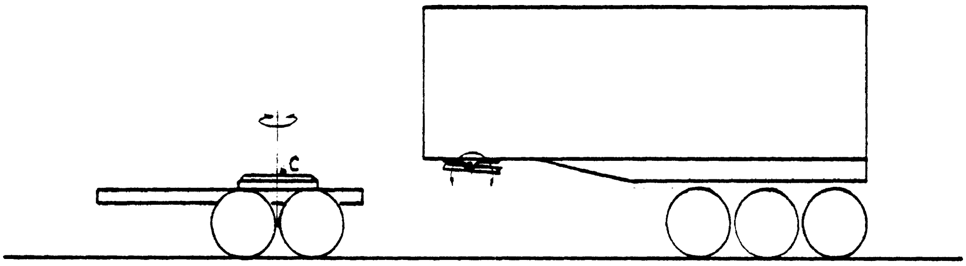


Figure C.9. Inverted fifth wheel

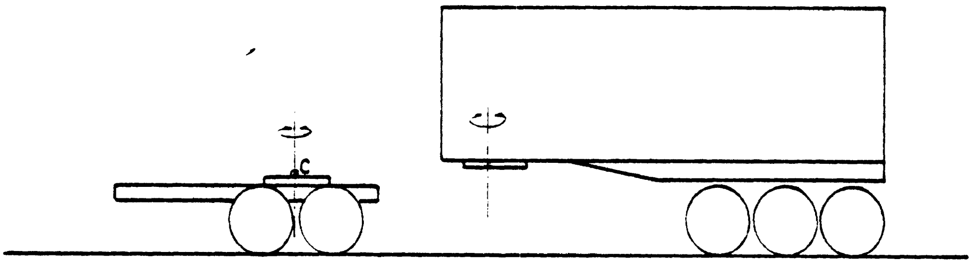


Figure C.10. Kingpin

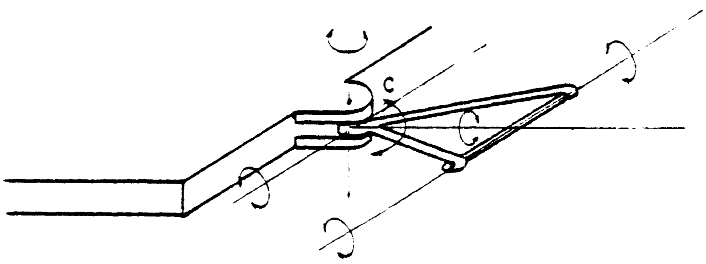


Figure C.11. Pintle hook

C.5.1 Lateral and Vertical Constraint Forces. Each of the four connections that are considered here are single point constraints. In these connections there is a point C (see Fig. C.12), which is common to both the lead and the trailing units, about which the articulation takes place. The acceleration constraint equations, which are needed for solving for the lateral and vertical forces, can therefore be formed by equating the lateral and vertical accelerations of the point C on the lead unit to the acceleration of the same point on the trailing unit.

The acceleration of the constraint point C on the lead unit is given by the expression:

$$\begin{aligned}
\vec{a}_C = {} & [\dot{u}_{s_1} + q_{s_1}w_{s_1} - r_{s_1}v_{s_1} + \dot{q}_{s_1}z_{c_1} - x_{c_1}q^2_{s_1} + p_{s_1}r_{s_1}z_{c_1} - x_{c_1}r^2_{s_1}]\vec{x}_{s_1} \\
& + [\dot{v}_{s_1} + u_{s_1}r_{s_1} - p_{s_1}w_{s_1} - \dot{p}_{s_1}z_{c_1} + x_{c_1}\dot{r}_{s_1} + z_{c_1}q_{s_1}r_{s_1} + x_{c_1}q_{s_1}r_{s_1}]\vec{y}_{s_1} \\
& + [\dot{w}_{s_1} + p_{s_1}v_{s_1} - q_{s_1}u_{s_1} - x_{c_1}\dot{q}_{s_1} - p^2_{s_1}z_{c_1} + x_{c_1}r_{s_1}p_{s_1} - z_{c_1}q^2_{s_1}]\vec{z}_{s_1} \\
= {} & a_1\vec{x}_{s_1} + b_1\vec{y}_{s_1} + c_1\vec{z}_{s_1} \qquad (51)
\end{aligned}$$

The acceleration of the same point in terms of the trailing unit motion variables is:

$$\begin{aligned}
\vec{a}_C = {} & [\dot{u}_{s_2} + q_{s_2}w_{s_2} - r_{s_2}v_{s_2} + \dot{q}_{s_2}z_{c_2} - x_{c_2}q^2_{s_2} + p_{s_2}r_{s_2}z_{c_2} - x_{c_2}r^2_{s_2}]\vec{x}_{s_2} \\
& + [\dot{v}_{s_2} + u_{s_2}r_{s_2} - p_{s_2}w_{s_2} - \dot{p}_{s_2}z_{c_2} + x_{c_2}\dot{r}_{s_2} + z_{c_2}q_{s_2}r_{s_2} + x_{c_2}q_{s_2}p_{s_2}]\vec{y}_{s_2} \\
& + [\dot{w}_{s_2} + p_{s_2}v_{s_2} - q_{s_2}u_{s_2} - x_{c_2}\dot{q}_{s_2} - p^2_{s_2}z_{c_2} + x_{c_2}r_{s_2}p_{s_2} - z_{c_2}q^2_{s_2}]\vec{z}_{s_2} \\
= {} & a_2\vec{x}_{s_2} + b_2\vec{y}_{s_2} + c_2\vec{z}_{s_2} \qquad (52)
\end{aligned}$$

Before the right-hand side of (51) can be equated with the right-hand side of (52), the lead unit coordinate system has to be transformed to the trailing unit coordinate system, or vice versa.

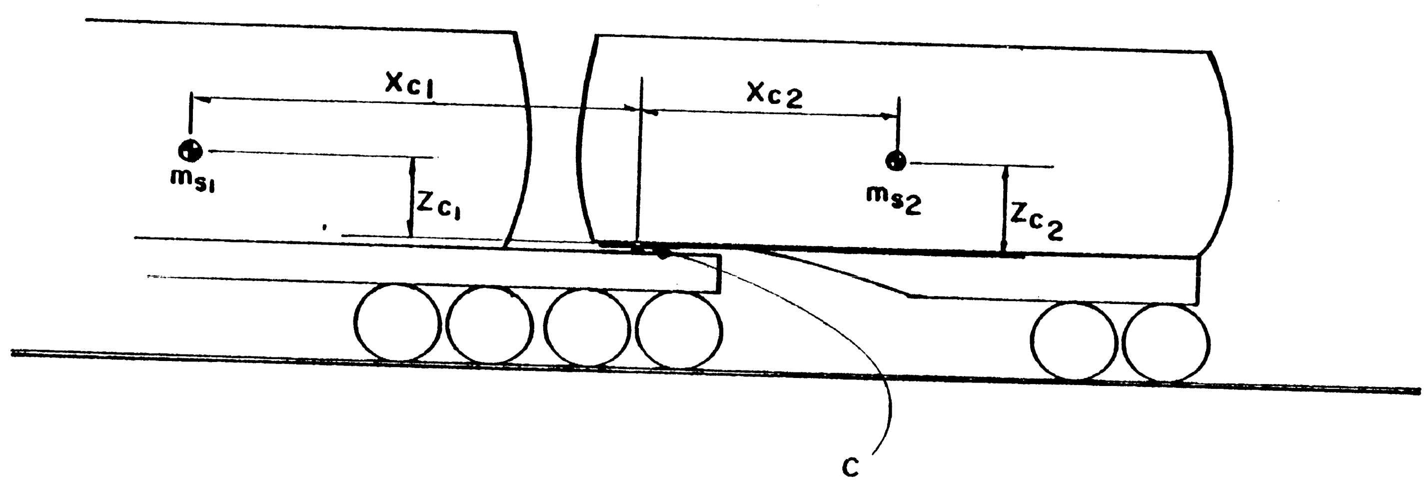


Figure C.12. A single point constraint in which the articulation takes place about point C.

Referring to Equation (7), we note that

$$\begin{Bmatrix} \vec{i}_n \\ \vec{j}_n \\ \vec{k}_n \end{Bmatrix} = [A_{ij}]_1 \{\vec{i}_{s_1}, \vec{j}_{s_1}, \vec{k}_{s_1}\}^T \tag{53}$$

But

$$\begin{Bmatrix} \vec{i}_{s_2} \\ \vec{j}_{s_2} \\ \vec{k}_{s_2} \end{Bmatrix} = [A_{ij}]_2^T \{\vec{i}_n, \vec{j}_n, \vec{k}_n\}^T \tag{54}$$

Upon eliminating the inertia vector, $\{\vec{i}_n, \vec{j}_n, \vec{k}_n\}$, from (53) and (54), we get:

$$\begin{Bmatrix} \vec{i}_{s_2} \\ \vec{j}_{s_2} \\ \vec{k}_{s_2} \end{Bmatrix} = [A_{ij}]_2^T [A_{ij}]_1 \{\vec{i}_{s_1}, \vec{j}_{s_1}, \vec{k}_{s_1}\}^T = [T_{ij}] \{\vec{i}_{s_1}, \vec{j}_{s_1}, \vec{k}_{s_1}\}^T \tag{55}$$

Elements of the matrix $[T_{ij}]$ can be determined using the transformation matrices in Equations (8) and (9). Upon doing so, we get:

$$T_{11} = \cos(\psi_{s_2} - \psi_{s_1})$$
$$T_{12} = \sin(\psi_{s_2} - \psi_{s_1})\cos\phi_{s_1} - \theta_{s_2}\sin\phi_{s_1} + \sin\phi_{s_1}\theta_{s_1}\cos(\psi_{s_2}-\psi_{s_1})$$
$$T_{13} = -\sin(\psi_{s_2}-\psi_{s_1})\sin\phi_{s_1} - \theta_{s_2}\cos\phi_{s_1} + \cos\phi_{s_1}\theta_{s_1}\cos(\psi_{s_2}-\psi_{s_1})$$

$$T_{21} = -\cos\phi_{s_2}\sin(\psi_{s_2}-\psi_{s_1}) - \theta_{s_1}\sin\phi_{s_2} + \sin\phi_{s_2}\theta_{s_2}\cos(\psi_{s_2}-\psi_{s_1})$$
$$T_{22} = \cos\phi_{s_1}\cos\phi_{s_2}\cos(\psi_{s_2}-\psi_{s_1}) + \sin\phi_{s_1}\sin\phi_{s_2}$$
$$- \sin\phi_{s_1}\theta_{s_1}\cos\phi_{s_2}\sin(\psi_{s_2}-\psi_{s_1}) + \sin\phi_{s_2}\theta_{s_2}\cos\phi_{s_1}\sin(\psi_{s_2}-\psi_{s_1})$$

(Continued)

$$T_{23} = -\sin\phi_{s_1}\cos\phi_{s_2}\cos(\psi_{s_2}-\psi_{s_1}) + \cos\phi_{s_1}\sin\phi_{s_2}$$

$$- \cos\phi_{s_1}\cos\phi_{s_2}\theta_{s_1}\sin(\psi_{s_2}-\psi_{s_1}) - \sin\phi_{s_1}\sin\phi_{s_2}\theta_{s_2}\sin(\psi_{s_2}-\psi_{s_1})$$

$$T_{31} = \sin\phi_{s_2}\sin(\psi_{s_2}-\psi_{s_1}) - \cos\phi_{s_2}\theta_{s_1} + \cos\phi_{s_2}\theta_{s_2}\cos(\psi_{s_2}-\psi_{s_1})$$

$$T_{32} = -\cos\phi_{s_1}\sin\phi_{s_2}\cos(\psi_{s_2}-\psi_{s_1}) + \cos\phi_{s_2}\sin\phi_{s_1}$$

$$+ \sin\phi_{s_1}\sin\phi_{s_2}\theta_{s_1}\sin(\psi_{s_2}-\psi_{s_1}) + \cos\phi_{s_1}\cos\phi_{s_2}\theta_{s_2}\sin(\psi_{s_2}-\psi_{s_1})$$

$$T_{33} = \sin\phi_{s_1}\sin\phi_{s_2}\cos(\psi_{s_2}-\psi_{s_1}) + \cos\phi_{s_1}\cos\phi_{s_2}$$

$$+ \cos\phi_{s_1}\sin\phi_{s_2}\theta_{s_1}\sin(\psi_{s_2}-\psi_{s_1}) - \sin\phi_{s_1}\cos\phi_{s_2}\theta_{s_2}\sin(\psi_{s_2}-\psi_{s_1})$$

(56)

Therefore, the constraint equations for lateral and vertical motions are:

$$b_2\vec{j}_{s_2} = (a_1T_{21} + b_1T_{22} + c_1T_{23})\vec{j}_{s_2} \qquad (57)$$

$$c_2\vec{k}_{s_2} = (a_1T_{31} + b_1T_{32} + c_1T_{33})\vec{k}_{s_2} \qquad (58)$$

Equations (57) and (58) are needed to evaluate the lateral and vertical constraint forces, respectively. In the case of the pintle hook connection, the lead and the trailing units are free to bounce with respect to each other. Hence, no significant constraint forces arise in the vertical direction. Therefore, the lateral acceleration constraint equation (57) alone is used in conjunction with a pintle hook connection.

C.5.2 Roll and Pitch Moments for a Conventional Fifth Wheel Connection. Figure C.13 shows the side and rear views of a conventional fifth wheel arrangement. The fifth wheel connection permits free rotational motions of the trailing unit along the pitch axis, $\vec{j}_{s_1}$, of the lead unit, and along the yaw axis, $\vec{k}_{s_2}$, of the trailing unit. When the two units are in line, the pitch axis, $\vec{j}_{s_2}$, of the trailing unit coincides with the $\vec{j}_{s_1}$ axis. Therefore, when the relative yaw angle is zero, the trailing unit is free to <u>pitch</u> with respect to the lead unit. When the relative yaw angle between the two units reaches 90 degrees, the roll axis, $\vec{i}_{s_2}$, of the trailing unit coincides with the pitch axis, $\vec{j}_{s_1}$, making the trailing unit free to <u>roll</u> with respect to the lead unit.

Any frictional couples that exist along the $\vec{j}_{s_1}$ and $\vec{k}_{s_2}$ directions are small enough that they can be neglected. The only constraining moment that can act on the lead unit is therefore a roll moment along the $\vec{i}_{s_1}$ direction. Any roll compliance that exists in the tractor and trailer structures and in the coupling device is lumped together and represented by a torsional type of stiffness, $K_{s_1}$, shown in Figure C.14. A second set of axes ($\vec{i}\,'_{s_1}$, $\vec{j}\,'_{s_1}$, $\vec{k}\,'_{s_1}$) affixed to the fifth wheel are also defined in Figure C.14. This axis system has the same yaw and pitch angles as those of the lead unit, but has a different roll angle, $\phi'_{s_1}$. The difference in the roll angle ($\phi'_{s_1}-\phi_{s_1}$) represents the structural compliance. The roll moment acting through the fifth wheel is given by the expression

$$M_{s_1} = K_{s_1}(\phi'_{s_1}-\phi_{s_1}) \tag{59}$$

The construction of the fifth wheel arrangement is such that the pitch axis, $\vec{j}\,'_{s_1}$, is always perpendicular to the yaw axis, $\vec{k}_{s_2}$. In terms of unit vectors, this condition can be written as:

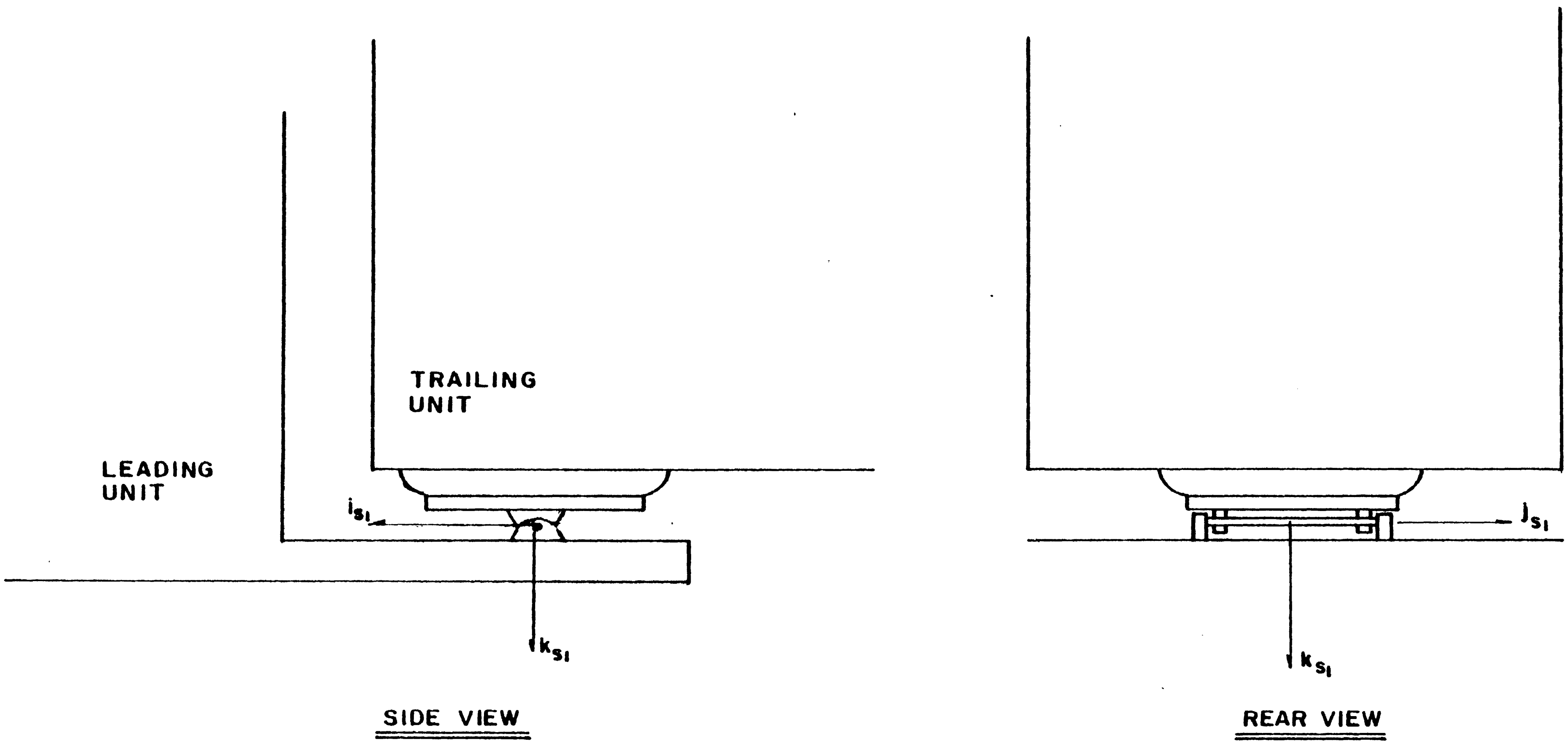


Figure C.13. Conventional fifth wheel arrangement.

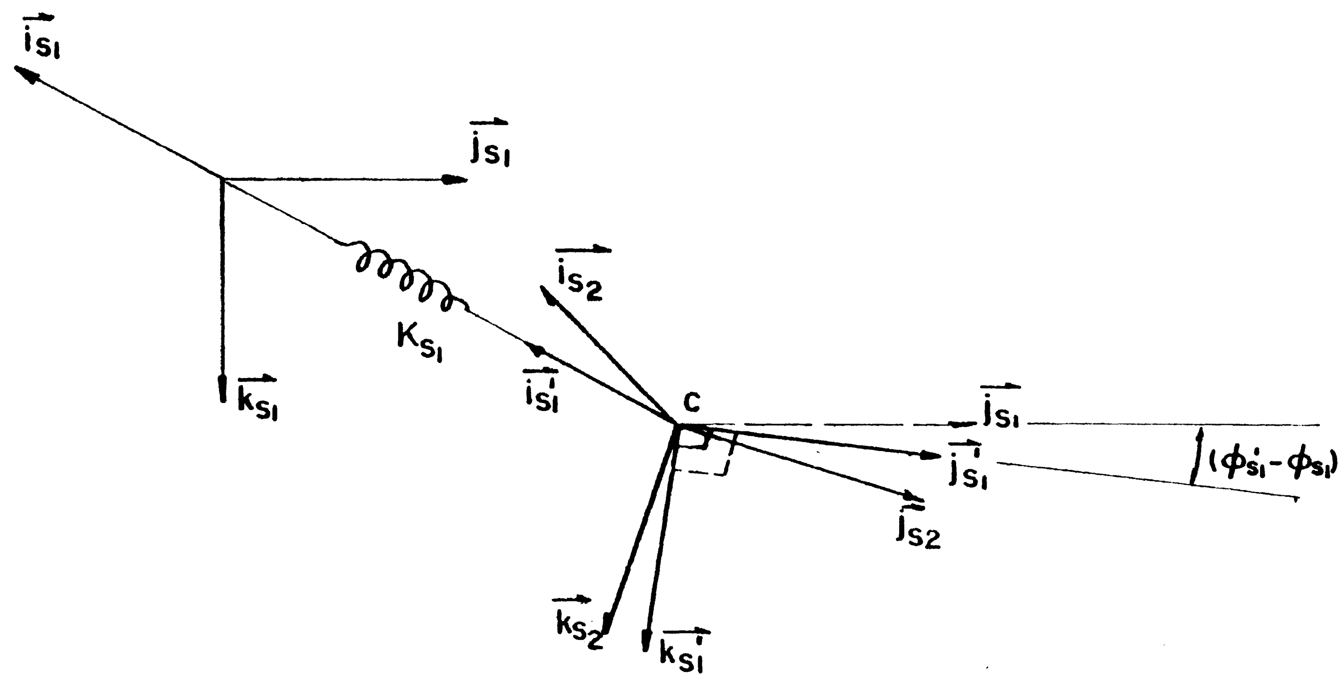


Figure C.14. Representation of the conventional fifth wheel arrangement in the yaw/roll model.

$$\vec{j}\,'_{s_1} \cdot \vec{k}_{s_2} = 0 \tag{60}$$

Both $\vec{j}\,'_{s_1}$ and $\vec{k}_{s_2}$ can be expressed in terms of the inertial unit vector ($\vec{i}_n$, $\vec{j}_n$, $\vec{k}_n$) using the transform Equation (9). Upon doing so, Equation (60) can be written as:

$$\left\{\begin{matrix} (-\sin\psi'_{s_1}\cos\phi'_{s_1} + \cos\psi'_{s_1}\sin\phi'_{s_1}\theta'_{s_1})\ \vec{i}_n \\ (\cos\psi'_{s_1}\cos\phi'_{s_1} + \sin\psi'_{s_1}\sin\phi'_{s_1}\theta'_{s_1})\ \vec{j}_n \\ \sin\phi'_{s_1}\ \vec{k}_n \end{matrix}\right\} \bullet$$

$$\left\{\begin{matrix} (\sin\psi_{s_2}\sin\phi_{s_2} + \cos\psi_{s_2}\cos\phi_{s_2}\theta_{s_2})\ \vec{i}_n \\ (-\cos\psi_{s_2}\sin\phi_{s_2} + \sin\psi_{s_2}\cos\phi_{s_2}\theta_{s_2})\ \vec{j}_n \\ \cos\phi_{s_2}\ \vec{k}_n \end{matrix}\right\} = 0 \tag{61}$$

Upon carrying out the dot product and solving for $\phi'_{s_1}$, we get

$$\phi'_{s_1} = \tan^{-1}\left[\frac{\sin\phi_{s_2}\cos(\psi_{s_2}-\psi'_{s_1}) - \theta_{s_2}\cos\phi_{s_2}\sin(\psi_{s_2}-\psi'_{s_1})}{\theta'_{s_1}\sin\phi_{s_2}\sin(\psi_{s_2}-\psi'_{s_1}) + \cos\phi_{s_2}}\right] \tag{62}$$

Since $\psi'_{s_1} = \psi_{s_1}$ and $\theta'_{s_1} = \theta_{s_1}$, we get

$$\phi'_{s_1} = \tan^{-1}\left[\frac{\sin\phi_{s_2}\cdot\cos(\psi_{s_2}-\psi_{s_1}) - \theta_{s_2}\cos\phi_{s_2}\sin(\psi_{s_2}-\psi_{s_1})}{\theta_{s_1}\sin\phi_{s_2}\sin(\psi_{s_2}-\psi_{s_1}) + \cos\phi_{s_2}}\right] \tag{63}$$

The roll moment $M_{x_1} = K_{s_1}\cdot(-\phi_{s_1} + \phi'_{s_1})$

$$M_{x_1} = K_{s_1}\left\{-\phi_{s_1} + \tan^{-1}\left[\frac{\sin\phi_{s_2}\cos(\psi_{s_2}-\psi_{s_1}) - \theta_{s_2}\cos\phi_{s_2}\sin(\psi_{s_2}-\psi_{s_1})}{\theta_{s_1}\sin\phi_{s_2}\sin(\psi_{s_2}-\psi_{s_1}) + \cos\phi_{s_2}}\right]\right\} \tag{64}$$

The constraining moments acting on the trailing unit are

$$M_{x_2} = - M_{x_1} T_{11} \tag{65}$$

and

$$M_{y_2} = - M_{x_1} T_{21} \tag{66}$$

where $T_{11}$ and $T_{21}$ are defined in Equation (56).

C.5.3 Roll and Pitch Moments for an Inverted Fifth Wheel Arrangement. The inverted fifth wheel is an arrangement in which the lower and upper halves of a conventional fifth wheel coupling are reversed. The inverted fifth wheel arrangement is shown in Figure C.15.

The coupler permits free rotational motion of the trailing unit along the pitch axis, $\vec{j}_{s_2}$, of the trailing unit and the yaw axis, $\vec{k}_{s_1}$, of the lead unit. Unlike the conventional fifth wheel arrangement, the pitch axis of the inverted coupler is always lined up with the pitch axis of the trailer for all values of articulation angles. The inverted fifth wheel coupling can therefore transmit a roll-resisting moment from the lead unit to the trailing unit for all values of the relative yaw angle between the lead and the trailing units. In the case of the inverted fifth wheel, the structural compliance in roll is modeled by a torsional spring of stiffness $K_{s_2}$, along the $\vec{i}_{s_2}$ axis of the trailing unit. Upon carrying out the derivation, we get:

$$M_{x_2} = K_{s_2} \left\{ \tan^{-1} \left[ \frac{\sin \phi_{s_1} \cos(\psi_{s_1} - \psi_{s_2}) - \theta_{s_1} \cos \phi_{s_1} \sin(\psi_{s_1} - \psi_{s_2})}{\theta_{s_2} \sin \phi_{s_1} \sin(\psi_{s_1} - \psi_{s_2}) + \cos \phi_{s_1}} \right] - \phi_{s_2} \right\} \tag{67}$$

The roll and pitch moment acting on the lead unit are given by

$$M_{x_1} = - M_{x_2} T_{11} \tag{68}$$

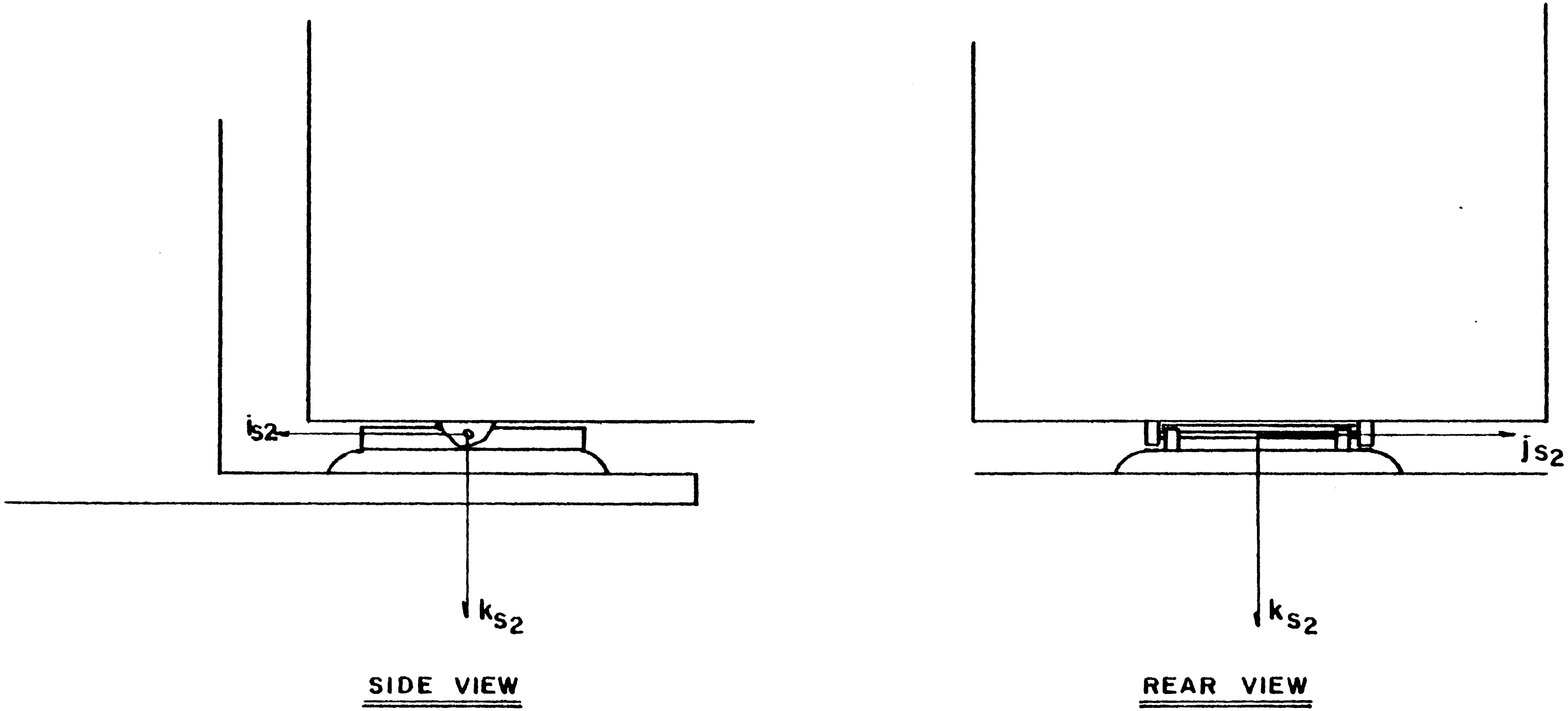


Figure C.15. The inverted fifth wheel arrangement.

$$M_{y_1} = - M_{x_2} T_{12} \qquad (69)$$

where $T_{11}$ and $T_{12}$ are once again defined in Equation (56).

C.5.4 Roll and Pitch Moments for a Kingpin-Type Connection. In a kingpin-type arrangement, only yaw motion is permitted between the lead and the trailing units. Hence, constraint moments act in both the pitch and yaw directions. The structural compliance is therefore represented by torsional springs, $K_{x_1}$ and $K_{y_1}$, along the pitch and roll axes. Shown in Figure C.16 is an axis system ($\vec{i}'_{s_1}$, $\vec{j}'_{s_1}$, $\vec{k}'_{s_1}$) which has the same yaw angle, $\psi_{s_1}$, as the lead unit, but different roll and pitch angles $\phi'_{s_1}$ and $\theta'_{s_1}$, respectively. The axis system is so oriented that the $k'_{s_1}$ axis is parallel to the $\vec{k}_{s_2}$ axis of the trailing unit. Therefore, the vector equations

$$\vec{i}'_{s_1} \cdot \vec{k}_{s_2} = 0 \qquad (70)$$

and

$$\vec{j}'_{s_1} \cdot \vec{k}_{s_2} = 0 \qquad (71)$$

have to be satisfied. Equation (70) yields the pitch angle

$$\theta'_{s_1} = \theta_{s_2} \cos(\psi_{s_2} - \psi'_{s_1}) + \tan \phi_{s_2} \sin(\psi_{s_2} - \psi'_{s_1}) \qquad (72)$$

Since $\psi'_{s_1} = \psi_{s_1}$, Equation (72) can be rewritten as

$$\theta'_{s_1} = \theta_{s_2} \cos(\psi_{s_2} - \psi_{s_1}) + \tan \phi_{s_2} \sin(\psi_{s_2} - \psi_{s_1}) \qquad (73)$$

Therefore

$$M_{y_1} = K_{y_1} (\theta'_{s_1} - \theta_{s_1})$$

$$= K_{y_1} [\theta_{s_2} \cos(\psi_{s_2} - \psi_{s_1}) + \tan \phi_{s_2} \sin(\psi_{s_2} - \psi_{s_1}) - \theta_{s_1}] \qquad (74)$$

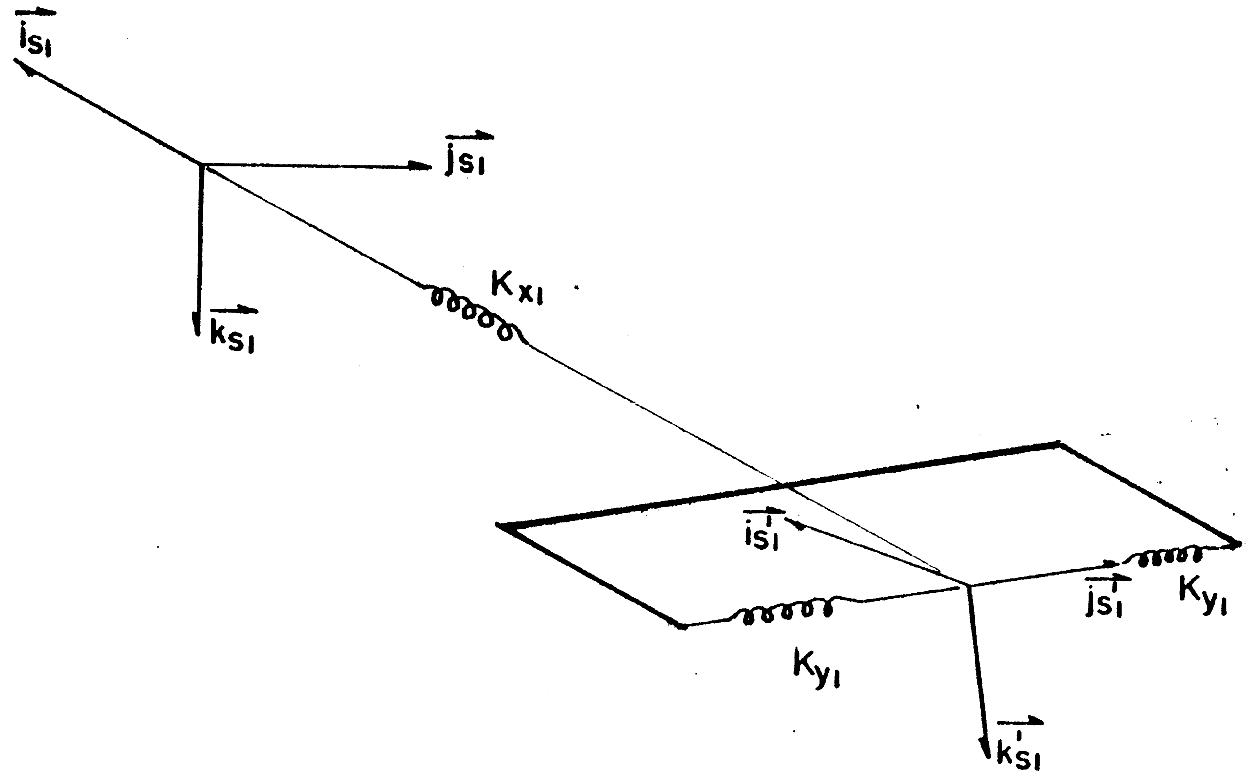


Figure C.16. Representation of the kingpin-type connection in the yaw/roll model.

Equation (71) yields a result which is identical to (62), therefore

$$M_{x_1} = K_{x_1} \left[ \tan^{-1} \left( \frac{\sin \phi_{s_2} \cos(\psi_{s_2} - \psi_{s_1}) - \theta_{s_2} \cos \phi_{s_2} \sin(\psi_{s_2} - \psi_{s_1})}{\theta'_{s_1} \sin \phi_{s_2} \sin(\psi_{s_2} - \psi_{s_1}) + \cos \phi_{s_2}} \right) - \phi_{s_1} \right] \tag{75}$$

The constraint moments, $M_{x_2}$, $M_{y_2}$, acting on the trailing unit are now given by

$$M_{x_2} = - M_{x_1} T_{11} - M_{y_1} T_{12} \tag{76}$$

and

$$M_{y_2} = - M_{x_1} T_{21} - M_{y_1} T_{22} \tag{77}$$

where $T_{11}$, $T_{12}$, $T_{21}$, and $T_{22}$ are once again defined in Equation (56).

## C.6 Forces and Moments at the Tire-Road Interface

The simulation utilizes measured tire data for computing the lateral forces and aligning moments generated at the tire-road interface. If the sideslip angle and the vertical load acting on a tire are known, the lateral force and aligning moment can be computed by a linear interpolation of the tabulated tire data. Expressions for the sideslip angle and the vertical load at the tire-road interface will now be derived in terms of the velocities and displacements of the sprung and unsprung masses.

C.6.1 Sideslip Angles. Let us first express the sideslip angle at the tire-road interface in terms of the body-fixed velocities of the sprung mass and the axle. The sideslip angle at the $j^{th}$ tire on axle i is given by the expression:

$$\alpha_{ji} = \tan^{-1} (v_{axle_i} / u_{tire_{ji}}) - \text{STEER} \tag{78}$$

where the lateral velocity, $v_{axle_i}$, at the axle is:

$$v_{axle_i} = [v_s - z_{R_i} p_s]\cos\phi_s + x_{u_i} r_s/\cos\phi_s - p_{u_i} HR_i \cos\phi_{u_i} \tag{79}$$

The longitudinal velocity $u_{tire_{ji}}$ is different at each of the four tires on an axle. The longitudinal velocities at the tires are:

$$u_{tire_{1i}} = u_s + (T_i + GY_i)r_s \tag{80}$$

$$u_{tire_{2i}} = u_s + T_i r_s \tag{81}$$

$$u_{tire_{3i}} = u_s - T_i r_s \tag{82}$$

$$u_{tire_{4i}} = u_s - (T_i + GY_i)r_s \tag{83}$$

The term "STEER" in Equation (78) represents the angle made by the wheel plane with respect to the longitudinal axis of the sprung mass coordinate system.

C.6.2 Vertical Loads. The vertical compliance in the tires is modeled by linear springs, $K_{T_{ji}}$. Therefore, if the vertical deflection, $\delta_{ji}$, at the tire is known, the vertical tire load, $F_{z_{ji}}$, can be calculated from the expression:

$$F_{z_{ji}} = KT_{ji}\delta_{ji} \tag{84}$$

The vertical deflection at the tires can be expressed in terms of the deflection of the sprung and unsprung masses. The deflection of the outer left tire on axle i is given by the equation:

$$\begin{aligned}\delta_{1i} = \delta_{0i} + \Delta z_s - z_{R_i}(1 - \cos\phi_s) + z_{u_i}\cos\phi_{u_i} - z_{u_{0i}} \\ - (T_i + GY_i)\sin\phi_{u_i} - x_{u_i}\theta_s\end{aligned} \tag{85}$$

where

$\Delta z_s$ is the vertical deflection of the sprung mass c.g. along the inertial axis $\vec{k}_n$.

$$\Delta z_s = 0.0 \text{ at time } t = 0.0$$

$z_{u_{0i}}$ is the vertical distance between the roll center, $R_i$, and the axle c.g. at time t = 0.0

$\delta_{0i}$ is the static deflection of the tires at time t = 0.0.

The deflection of the other three tires on axle i are:

$$\delta_{2i} = \delta_{1i} + GY_i \sin \phi u_i \tag{86}$$

$$\delta_{3i} = \delta_{2i} + 2T_i \sin \phi u_i \tag{87}$$

$$\delta_{4i} = \delta_{3i} + GY_i \sin \phi u_i \tag{88}$$

# APPENDIX D

## YAW/ROLL MODEL PARAMETERS

Parameters needed to describe the candidate tractor-semitrailers and tractor-semitrailer-semitrailer combinations are presented in this appendix. Figure D.1 illustrates the parameters needed to define the layout of an 11-axle tractor-semitrailer-semitrailer combination. The symbols are defined in Table D.1. Parameter values are listed in Tables D.2 and D.3 for all of the 17 configurations which were analyzed.

The following tire distribution was assumed:

| | |
|---|---|
| Tractor front axle: | 15x22.5 rib |
| Tractor rear axle: | 10x20 rib |
| Trailer axles which are loaded to 13,000 lb: | 9x20 rib |
| Trailer axles which are loaded to 18,000 lb: | 10x20 rib |

The cornering force and aligning torque data for these tires are from References D.1 through D.3.

The suspension spring characteristics which were assumed are illustrated in Figure D.2.

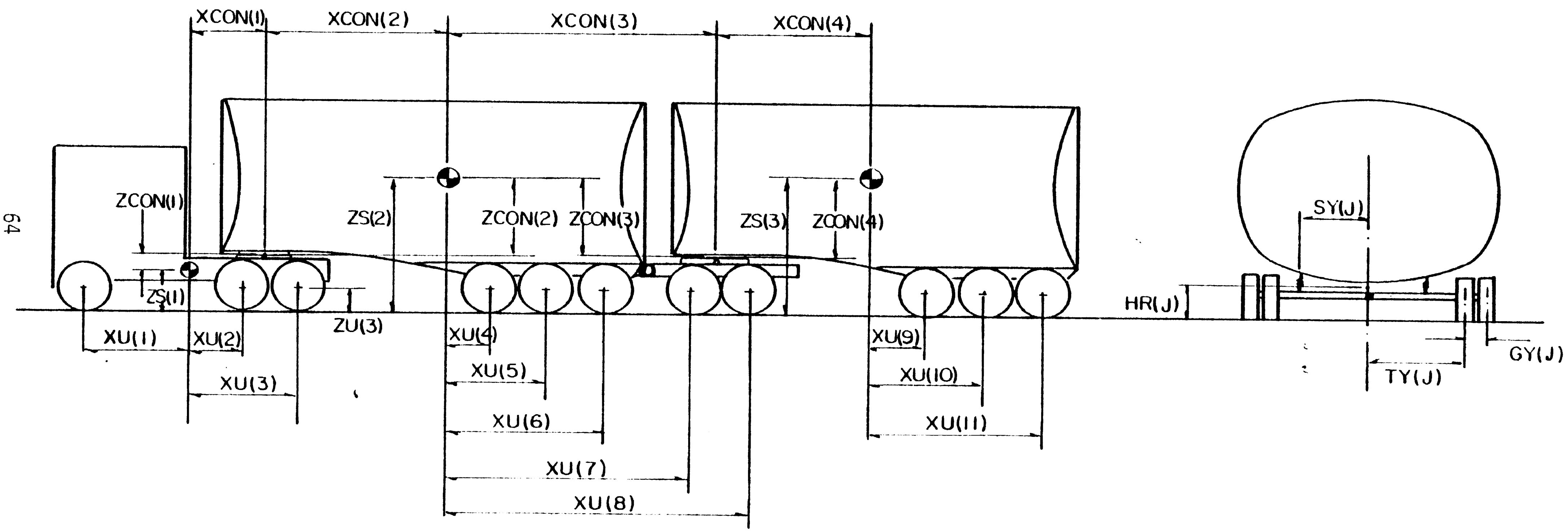


Figure D.1. Parameters needed to define the layout of a tractor-semitrailer-semitrailer combination.
Note: In the case of the TSS combinations, the shelf projecting from the rear of the front semitrailer is treated as an integral part of the front semitrailer.

TABLE D.1 LIST OF SYMBOLS

| | |
|---|---|
| WS(I) | Weight of $i^{th}$ sprung mass (lb) |
| WU(J) | Height of $j^{th}$ axle (lb) |
| WINIT(J) | Vertical load carried by axle J (lb) |
| XU(J) | Longitudinal distance from the $j^{th}$ axle to the c.g. of the sprung mass on which it is mounted. XU(J) is positive if axle is mounted ahead of the sprung mass c.g. (in) |
| ZS(I) | Height of sprung mass c.g. above ground (in) |
| ZU(J) | Height of axle c.g. above ground (in) |
| XCON(K) | Longitudinal distance from the sprung mass c.g. to an articulation point. (See Figure D.1). XCON(K) is positive when the articulation point is ahead of the sprung mass c.g. (in) |
| ZCON(K) | Vertical distance from the sprung mass c.g. to the articulation point. (See Figure D.1). ZCON(K) is positive when the articulation point is below the sprung mass c.g. (in) |
| KCONX(K) | Roll stiffness at the articulation point (in.lb./deg.) |
| GY(J) | Lateral distance between dual tires on axle J. GY(J) is zero for single tires (in) |
| KT(J) | Vertical stiffness of each tire mounted on axle J (lb/in) |
| CF(J) | Coulomb friction in each of the suspension springs on axle J (lb) |
| IXXS(I) | Roll moment of inertia of the $i^{th}$ sprung mass (lb.in.sec$^2$) |
| IZZS(I) | Yaw moment of inertia of the $i^{th}$ sprung mass (lb.in.sec$^2$) |
| IXXU(J) | Roll moment of inertia of axle J. (The yaw moment of inertia of the axle is assumed to be equal to the roll moment of inertia). (lb.in.sec $^2$) |
| HR(J) | Height of roll axis above ground (in) |
| TY(J) | Half the lateral distance between the inner tires (inner of the dual pair) on axle J (in) |
| TIRE(J) | Table # for the tire data used on axle J. See cornering force and aligning torque tables at the end of this appendix. |
| SY(J) | Half the lateral distance between the suspension springs on axle J. (in) |

TABLE D.2 PARAMETERS FOR CANDIDATE TRACTOR-SEMITRAILER CONFIGURATIONS

| | 1 | 2a | 2b | 3a | 3b | 4a | 4b | 5a |
|---|---|---|---|---|---|---|---|---|
| # of axles on Tractor | 3 | 3 | 3 | 3 | 3 | 3 | 3 | 3 |
| # of axles on Trailer | 2 | 3 | 3 | 4 | 4 | 5 | 5 | 6 |
| WS(1) | 9300 | 9300 | 9300 | 9300 | 9300 | 9300 | 9300 | 9300 |
| WS(2) | 60000 | 65500 | 80500 | 77000 | 82000 | 88500 | 93500 | 100000 |
| WU(1) | 1200 | 1200 | 1200 | 1200 | 1200 | 1200 | 1200 | 1200 |
| WU(2) | 2340 | 2340 | 2340 | 2340 | 2340 | 2340 | 2340 | 2340 |
| WU(3) | 2160 | 2160 | 2160 | 2160 | 2160 | 2160 | 2160 | 2160 |
| WU(4) | 1500 | 1500 | 1500 | 1500 | 1500 | 1500 | 1500 | 1500 |
| WU(5) | 1500 | 1500 | 1500 | 1500 | 1500 | 1500 | 1500 | 1500 |
| WU(6) | - | 1500 | 1500 | 1500 | 1500 | 1500 | 1500 | 1500 |
| WU(7) | - | - | - | 1500 | 1500 | 1500 | 1500 | 1500 |
| WU(8) | - | - | - | - | - | 1500 | 1500 | 1500 |
| WU(9) | - | - | - | - | - | - | - | 1500 |
| WINIT(1) | 14000 | 14000 | 14000 | 14000 | 14000 | 14000 | 14000 | 14000 |
| WINIT(2) | 16000 | 16000 | 16000 | 16000 | 16000 | 16000 | 16000 | 16000 |
| WINIT(3) | 16000 | 16000 | 16000 | 16000 | 16000 | 16000 | 16000 | 16000 |
| WINIT(4) | 16000 | 13000 | 18000 | 13000 | 18000 | 13000 | 18000 | 13000 |
| WINIT(5) | 16000 | 13000 | 18000 | 13000 | 13000 | 13000 | 13000 | 13000 |
| WINIT(6) | - | 13000 | 18000 | 13000 | 13000 | 13000 | 13000 | 13000 |
| WINIT(7) | - | - | - | 13000 | 13000 | 13000 | 13000 | 13000 |
| WINIT(8) | - | - | - | - | - | 13000 | 13000 | 13000 |
| WINIT(9) | - | - | - | - | - | - | - | 13000 |
| XU(1) | 40 | 40 | 40 | 40 | 40 | 40 | 40 | 40 |
| XU(2) | -71.5 | -71.5 | -71.5 | -71.5 | -71.5 | -71.5 | -71.5 | -71.5 |
| XU(3) | -121.5 | -121.5 | -121.5 | -121.5 | -121.5 | -121.5 | -121.5 | -121.5 |
| XU(4) | -189.6 | -137.7 | -26.1 | -88.2 | -31.2 | -45.6 | 14.50 | -5.16 |
| XU(5) | -231.6 | -181.7 | -135.1 | -132.2 | -140.2 | -89.6 | -94.5 | -49.16 |
| XU(6) | - | -225.7 | -244.1 | -176.2 | -184.2 | -133.6 | -138.5 | -93.16 |
| XU(7) | - | - | - | -220.2 | -228.2 | -177.6 | -182.5 | -137.16 |
| XU(8) | - | - | - | - | - | -221.6 | -226.5 | -181.16 |
| XU(9) | - | - | - | - | - | - | - | -225.16 |

Table D.2, continued

| | 1 | 2a | 2b | 3a | 3b | 4a | 4b | 5a |
|---|---|---|---|---|---|---|---|---|
| ZS(1) | 40 | 40 | 40 | 40 | 40 | 40 | 40 | 40 |
| ZS(2) | 75.7 | 76.5 | 80.1 | 77.8 | 79.4 | 80.7 | 82.6 | 84.0 |
| ZU(1) | 22.5 | 22.5 | 22.5 | 22.5 | 22.5 | 22.5 | 22.5 | 22.5 |
| ZU(2) | 22.5 | 22.5 | 22.5 | 22.5 | 22.5 | 22.5 | 22.5 | 22.5 |
| ZU(3) | 22.5 | 22.5 | 22.5 | 22.5 | 22.5 | 22.5 | 22.5 | 22.5 |
| ZU(4) | 20.0 | 20.0 | 20.0 | 20.0 | 20.0 | 20.0 | 20.0 | 20.0 |
| ZU(5) | 20.0 | 20.0 | 20.0 | 20.0 | 20.0 | 20.0 | 20.0 | 20.0 |
| ZU(6) | - | 20.0 | 20.0 | 20.0 | 20.0 | 20.0 | 20.0 | 20.0 |
| ZU(7) | - | - | - | 20.0 | 20.0 | 20.0 | 20.0 | 20.0 |
| ZU(8) | - | - | - | - | - | 20.0 | 20.0 | 20.0 |
| ZU(9) | - | - | - | - | - | - | - | 20.0 |
| XCON(1) | -69.2 | -69.20 | -69.20 | -69.2 | -69.2 | -69.2 | -69.2 | -69.2 |
| XCON(2) | 197.0 | 202.3 | 215.7 | 228.8 | 221.5 | 247.8 | 230.4 | 256.3 |
| ZCON(1) | -10.0 | -10.0 | -10.0 | -10.0 | -10.0 | -10.0 | -10.0 | -10.0 |
| ZCON(2) | 25.7 | 26.5 | 30.1 | 27.8 | 29.4 | 30.7 | 32.6 | 34.0 |
| KCONX(1) | 500,000 | 500,000 | 500,000 | 500,000 | 500,000 | 500,000 | 500,000 | 500,000 |
| *GY(J) | 13.0 | 13.0 | 13.0 | 13.0 | 13.0 | 13.0 | 13.0 | 13.0 |
| **KT(J) | 5000 | 5000 | 5000 | 5000 | 5000 | 5000 | 5000 | 5000 |
| CF(1) | 250 | 250 | 250 | 250 | 250 | 250 | 250 | 250 |
| CF(2) | 500 | 500 | 500 | 500 | 500 | 500 | 500 | 500 |
| CF(3) | 500 | 500 | 500 | 500 | 500 | 500 | 500 | 500 |
| CF(4) | 500 | 500 | 500 | 500 | 500 | 500 | 500 | 500 |
| CF(5) | 500 | 500 | 500 | 500 | 500 | 500 | 500 | 500 |
| CF(6) | - | 500 | 500 | 500 | 500 | 500 | 500 | 500 |
| CF(7) | - | - | - | 500 | 500 | 500 | 500 | 500 |
| CF(8) | - | - | - | - | - | 500 | 500 | 500 |
| CF(9) | - | - | - | - | - | - | - | 500 |
| IXXS(1) | 18200 | 18200 | 18200 | 18200 | 18200 | 18200 | 18200 | 18200 |
| IXXS(2) | 34570 | 41000 | 56800 | 54200 | 61000 | 70700 | 78000 | 92000 |

*Tractor front axle has single tires, all the rest have duals.

**Same value used for all tires.

Table D.2, continued

| | 1 | 2a | 2b | 3a | 3b | 4a | 4b | 5a |
|---|---|---|---|---|---|---|---|---|
| IZZS(1) | 65000 | 65000 | 65000 | 65000 | 65000 | 65000 | 65000 | 65000 |
| IZZS(2) | 2,763,000 | 3,360,000 | 4,216,000 | 4,450,800 | 4,510,000 | 5,200,000 | 5,545,000 | 5,800,000 |
| IXXU(1) | 3700 | 3700 | 3700 | 3700 | 3700 | 3700 | 3700 | 3700 |
| IXXU(2) | 4500 | 4500 | 4500 | 4500 | 4500 | 4500 | 4500 | 4500 |
| IXXU(3) | 4500 | 4500 | 4500 | 4500 | 4500 | 4500 | 4500 | 4500 |
| IXXU(4) | 4100 | 4100 | 4100 | 4100 | 4100 | 4100 | 4100 | 4100 |
| IXXU(5) | 4100 | 4100 | 4100 | 4100 | 4100 | 4100 | 4100 | 4100 |
| IXXU(6) | - | 4100 | 4100 | 4100 | 4100 | 4100 | 4100 | 4100 |
| IXXU(7) | - | - | - | 4100 | 4100 | 4100 | 4100 | 4100 |
| IXXU(8) | - | - | - | - | - | 4100 | 4100 | 4100 |
| IXXU(9) | - | - | - | - | - | - | - | 4100 |
| HR(1) | 22 | 22 | 22 | 22 | 22 | 22 | 22 | 22 |
| HR(2) | 29 | 29 | 29 | 29 | 29 | 29 | 29 | 29 |
| HR(3) | 29 | 29 | 29 | 29 | 29 | 29 | 29 | 29 |
| HR(4) | 29 | 29 | 29 | 29 | 29 | 29 | 29 | 29 |
| HR(5) | 29 | 29 | 29 | 29 | 29 | 29 | 29 | 29 |
| HR(6) | - | 29 | 29 | 29 | 29 | 29 | 29 | 29 |
| HR(7) | - | - | - | 29 | 29 | 29 | 29 | 29 |
| HR(8) | - | - | - | - | - | 29 | 29 | 29 |
| HR(9) | - | - | - | - | - | - | - | 29 |
| TY(1) | 40.25 | 40.25 | 40.25 | 40.25 | 40.25 | 40.25 | 40.25 | 40.25 |
| TY(2) | 29.0 | 29.0 | 29.0 | 29.0 | 29.0 | 29.0 | 29.0 | 29.0 |
| TY(3) | 29.0 | 29.0 | 29.0 | 29.0 | 29.0 | 29.0 | 29.0 | 29.0 |
| TY(4) | 32.0 | 32.0 | 32.0 | 32.0 | 32.0 | 32.0 | 32.0 | 32.0 |
| TY(5) | 32.0 | 32.0 | 32.0 | 32.0 | 32.0 | 32.0 | 32.0 | 32.0 |
| TY(6) | - | 32.0 | 32.0 | 32.0 | 32.0 | 32.0 | 32.0 | 32.0 |
| TY(7) | - | - | - | 32.0 | 32.0 | 32.0 | 32.0 | 32.0 |
| TY(8) | - | - | - | - | - | 32.0 | 32.0 | 32.0 |
| TY(9) | - | - | - | - | - | - | - | 32.0 |

Table D.2, continued

| | 1 | 2a | 2b | 3a | 3b | 4a | 4b | 5a |
|---|---|---|---|---|---|---|---|---|
| TIRE (1) | 1 | 1 | 1 | 1 | 1 | 1 | 1 | 1 |
| TIRE (2) | 2 | 2 | 2 | 2 | 2 | 2 | 2 | 2 |
| TIRE (3) | 2 | 2 | 2 | 2 | 2 | 2 | 2 | 2 |
| TIRE (4) | 2 | 3 | 2 | 3 | 2 | 3 | 2 | 3 |
| TIRE (5) | 2 | 3 | 2 | 3 | 3 | 3 | 3 | 3 |
| TIRE (6) | - | 3 | 2 | 3 | 3 | 3 | 3 | 3 |
| TIRE (7) | - | - | - | 3 | 3 | 3 | 3 | 3 |
| TIRE (8) | - | - | - | - | - | 3 | 3 | 3 |
| TIRE (9) | - | - | - | - | - | - | - | 3 |
| Tractor front spring* | 1 | 1 | 1 | 1 | 1 | 1 | 1 | 1 |
| Tractor rear springs* | 2 | 2 | 2 | 2 | 2 | 2 | 2 | 2 |
| Trailer springs* | 3 | 3 | 3 | 3 | 3 | 3 | 3 | 3 |
| SY(1) | 16.3 | 16.3 | 16.3 | 16.3 | 16.3 | 16.3 | 16.3 | 16.3 |
| SY(2)-SY(3) | 19.0 | 19.0 | 19.0 | 19.0 | 19.0 | 19.0 | 19.0 | 19.0 |
| SY(4)-SY(9) | 22.0 | 22.0 | 22.0 | 22.0 | 22.0 | 22.0 | 22.0 | 22.0 |

*The numbers refer to the spring data shown in Figure D.2.

TABLE D.3 PARAMETERS FOR CANDIDATE TRACTOR/SEMITRACTOR/SEMITRAILER COMBINATIONS

| | I | IIa | IIb | III | IVa | IVb | V | VI | VII |
|---|---|---|---|---|---|---|---|---|---|
| # of axles on tractor | 3 | 3 | 3 | 3 | 3 | 3 | 3 | 3 | 3 |
| # of axles on semitrailer | 3 | 4 | 4 | 4 | 4 | 4 | 4 | 5 | 5 |
| # of axles on Pup trailer | 2 | 2 | 2 | 3 | 2 | 2 | 3 | 2 | 3 |
| WS(1) | 9300 | 9300 | 9300 | 9300 | 9300 | 9300 | 9300 | 9300 | 9300 |
| WS(2) | 48000 | 49000 | 66500 | 49000 | 49000 | 66500 | 49000 | 67500 | 67500 |
| WS(3) | 33500 | 44000 | 33500 | 55500 | 44000 | 33500 | 55500 | 44000 | 55500 |
| WU(1) | 1200 | 1200 | 1200 | 1200 | 1200 | 1200 | 1200 | 1200 | 1200 |
| WU(2) | 2340 | 2340 | 2340 | 2340 | 2340 | 2340 | 2340 | 2340 | 2340 |
| WU(3) | 2160 | 2160 | 2160 | 2160 | 2160 | 2160 | 2160 | 2160 | 2160 |
| WU(4) | 1500 | 1500 | 1500 | 1500 | 1500 | 1500 | 1500 | 1500 | 1500 |
| WU(5) | 1500 | 1500 | 1500 | 1500 | 1500 | 1500 | 1500 | 1500 | 1500 |
| WU(6) | 1500 | 1500 | 1500 | 1500 | 1500 | 1500 | 1500 | 1500 | 1500 |
| WU(7) | 1500 | 1500 | 1500 | 1500 | 1500 | 1500 | 1500 | 1500 | 1500 |
| WU(8) | 1500 | 1500 | 1500 | 1500 | 1500 | 1500 | 1500 | 1500 | 1500 |
| WU(9) | - | 1500 | 1500 | 1500 | 1500 | 1500 | 1500 | 1500 | 1500 |
| WU(10) | - | - | - | 1500 | - | - | 1500 | 1500 | 1500 |
| WU(11) | - | - | - | - | - | - | - | - | 1500 |
| WINIT(1) | 12000 | 12000 | 14000 | 12000 | 12000 | 14000 | 12000 | 14000 | 14000 |
| WINIT(2) | 13500 | 13500 | 16000 | 13500 | 13500 | 16000 | 13500 | 16000 | 16000 |
| WINIT(3) | 13500 | 13500 | 16000 | 13500 | 13500 | 16000 | 13500 | 16000 | 16000 |
| WINIT(4) | 13000 | 13000 | 13000 | 13000 | 13000 | 13000 | 13000 | 13000 | 13000 |
| WINIT(5) | 13000 | 13000 | 13000 | 13000 | 13000 | 13000 | 13000 | 13000 | 13000 |

TABLE D.3 PARAMETERS FOR CANDIDATE TRACTOR/SEMITRACTOR/SEMITRAILER COMBINATIONS (Cont.)

| | I | IIa | IIb | III | IVa | IVb | V | VI | VII |
|---|---|---|---|---|---|---|---|---|---|
| WINIT(6) | 13000 | 13000 | 13000 | 13000 | 13000 | 13000 | 13000 | 13000 | 13000 |
| WINIT(7) | 13000 | 13000 | 13000 | 13000 | 13000 | 13000 | 13000 | 13000 | 13000 |
| WINIT(8) | 13000 | 13000 | 13000 | 13000 | 13000 | 13000 | 13000 | 13000 | 13000 |
| WINIT(9) | - | 13000 | 13000 | 13000 | 13000 | 13000 | 13000 | 13000 | 13000 |
| WINIT(10) | - | - | - | 13000 | - | - | 13000 | 13000 | 13000 |
| WINIT(11) | - | - | - | - | - | - | - | - | 13000 |
| XU(1) | 40 | 40 | 40 | 40 | 40 | 40 | 40 | 40 | 40 |
| XU(2) | -71.5 | -71.5 | -71.5 | -71.5 | -71.5 | -71.5 | -71.5 | -71.5 | -71.5 |
| XU(3) | -121.5 | -121.5 | -121.5 | -121.5 | -121.5 | -121.5 | -121.5 | -121.5 | -121.5 |
| XU(4) | -101.1 | -73.1 | -80.7 | -58.9 | -92.7 | -105.3 | -77.3 | -77.7 | -64.2 |
| XU(5) | -145.1 | -117.1 | -124.7 | -102.9 | -136.2 | -149.3 | -121.3 | -121.7 | -108.2 |
| XU(6) | -202.5 | -185.1 | -168.7 | -157.3 | -200.8 | -193.3 | -172.3 | -165.7 | -152.2 |
| XU(7) | -27.8 | -229.1 | -225.7 | -201.3 | -244.8 | -249.7 | -216.3 | -226.7 | -202.5 |
| XU(8) | -71.8 | -71.9 | -17.6 | -37.5 | -88.6 | -23.7 | -50.3 | -270.7 | -246.5 |
| XU(9) | - | -115.9 | -61.6 | -81.5 | -132.6 | -67.7 | -94.3 | -64.8 | -31.2 |
| XU(10) | - | - | - | -125.5 | - | - | -138.3 | -108.8 | -75.2 |
| XU(11) | - | - | - | - | - | - | - | - | -119.2 |
| ZS(1) | 40 | 40 | 40 | 40 | 40 | 40 | 40 | 40 | 40 |
| ZS(2) | 77.6 | 80.4 | 83.0 | 83.5 | 77.4 | 79.5 | 79.8 | 82.1 | 84.8 |
| ZS(3) | 77.8 | 82.0 | 83.4 | 84.6 | 78.8 | 79.8 | 80.9 | 83.2 | 85.8 |
| ZU(1) | 22.5 | 22.5 | 22.5 | 22.5 | 22.5 | 22.5 | 22.5 | 22.5 | 22.5 |
| ZU(2) | 22.5 | 22.5 | 22.5 | 22.5 | 22.5 | 22.5 | 22.5 | 22.5 | 22.5 |
| ZU(3) | 22.5 | 22.5 | 22.5 | 22.5 | 22.5 | 22.5 | 22.5 | 22.5 | 22.5 |

TABLE D.3 PARAMETERS FOR CANDIDATE TRACTOR/SEMITRACTOR/SEMITRAILER COMBINATIONS (Cont.)

| | I | IIa | IIb | III | IVa | IVb | V | VI | VII |
|---|---|---|---|---|---|---|---|---|---|
| ZU(4) | 20.0 | 20.0 | 20.0 | 20.0 | 20.0 | 20.0 | 20.0 | 20.0 | 20.0 |
| ZU(5) | 20.0 | 20.0 | 20.0 | 20.0 | 20.0 | 20.0 | 20.0 | 20.0 | 20.0 |
| ZU(6) | 20.0 | 20.0 | 20.0 | 20.0 | 20.0 | 20.0 | 20.0 | 20.0 | 20.0 |
| ZU(7) | 20.0 | 20.0 | 20.0 | 20.0 | 20.0 | 20.0 | 20.0 | 20.0 | 20.0 |
| ZU(8) | 20.0 | 20.0 | 20.0 | 20.0 | 20.0 | 20.0 | 20.0 | 20.0 | 20.0 |
| ZU(9) | - | 20.0 | 20.0 | 20.0 | 20.0 | 20.0 | 20.0 | 20.0 | 20.0 |
| ZU(10) | - | - | - | 20.0 | - | - | 2.0. | 20.0 | 20.0 |
| ZU(11) | - | - | - | - | - | - | - | - | -20.0 |
| XCON(1) | -72.7 | -72.7 | -69.2 | -72.7 | -72.7 | -69.2 | -72.7 | -69.2 | -69.2 |
| XCON(2) | 126.4 | 108.4 | 145.7 | 92.5 | 128.4 | 174.2 | 111.4 | 150.8 | 134.9 |
| XCON(3) | -202.5 | -207.1 | -225.7 | -179.3 | -222.8 | -249.7 | -194.3 | -249.3 | -224.5 |
| XCON(4) | 109.2 | 102.8 | 86.8 | 133.9 | 121.2 | 100.0 | 154.9 | 95.1 | 123.5 |
| ZCON(1) | -10.0 | -10.0 | -10.0 | -10.0 | -10.0 | -10.0 | -10.0 | -10.0 | -10.0 |
| ZCON(2) | 27.6 | 30.4 | 33.0 | 33.5 | 27.4 | 29.5 | 29.8 | 32.1 | 34.8 |
| ZCON(3) | 23.6 | 26.4 | 29.0 | 29.5 | 23.4 | 25.5 | 25.8 | 28.1 | 30.8 |
| ZCON(4) | 23.8 | 28.0 | 29.4 | 30.6 | 24.8 | 25.8 | 26.9 | 29.2 | 31.8 |
| KCONX(1) | 500,000 | 500,000 | 500,000 | 500,000 | 500,000 | 500,000 | 500,000 | 500,000 | 500,000 |
| KCONX(2) | 750,000 | 750,000 | 750,000 | 750,000 | 750,000 | 750,000 | 750,000 | 750,000 | 750,000 |
| GY(J) | 13.0 | 13.0 | 13.0 | 13.0 | 13.0 | 13.0 | 13.0 | 13.0 | 13.0 |
| KT(J) | 5,000 | 5,000 | 5,000 | 5,000 | 5,000 | 5,000 | 5,000 | 5,000 | 5,000 |
| CF(1) | 250 | 250 | 250 | 250 | 250 | 250 | 250 | 250 | 250 |
| CF(2) | 500 | 500 | 500 | 500 | 500 | 500 | 500 | 500 | 500 |
| CF(3) | 500 | 500 | 500 | 500 | 500 | 500 | 500 | 500 | 500 |
| CF(4) | 500 | 500 | 500 | 500 | 500 | 500 | 500 | 500 | 500 |

TABLE D.3 PARAMETERS FOR CANDIDATE TRACTOR/SEMITRACTOR/SEMITRAILER COMBINATIONS (Cont.)

| | I | IIa | IIb | III | IVa | IVb | V | VI | VII |
|---|---|---|---|---|---|---|---|---|---|
| CF(5) | 500 | 500 | 500 | 500 | 500 | 500 | 500 | 500 | 500 |
| CF(6) | 500 | 500 | 500 | 500 | 500 | 500 | 500 | 500 | 500 |
| CF(8) | 500 | 500 | 500 | 500 | 500 | 500 | 500 | 500 | 500 |
| CF(9) | - | 500 | 500 | 500 | 500 | 500 | 500 | 500 | 500 |
| CF(10) | - | - | - | 500 | - | - | 500 | 500 | 500 |
| CF(11) | - | - | - | - | - | - | - | - | 500 |
| IXXS(1) | 18200 | 18200 | 18200 | 18200 | 18200 | 18200 | 18200 | 18200 | 18200 |
| IXXS(2) | 35260 | 41720 | 64000 | 46500 | 39400 | 56600 | 43600 | 62300 | 64500 |
| IXXS(3) | 28050 | 34500 | 30000 | 49000 | 33400 | 28800 | 47000 | 37700 | 47400 |
| IZZS(1) | 65000 | 65000 | 65000 | 65000 | 65000 | 65000 | 65000 | 65000 | 65000 |
| IZZS(2) | 1180600 | 1055500 | 2071500 | 777600 | 1206800 | 2562600 | 1004200 | 2206600 | 1898200 |
| IZZS(3) | 395500 | 750800 | 259800 | 1081800 | 897100 | 330200 | 1398000 | 624600 | 999800 |
| IXXU(1) | 3700 | 3700 | 3700 | 3700 | 3700 | 3700 | 3700 | 3700 | 3700 |
| IXXU(2) | 4500 | 4500 | 4500 | 4500 | 4500 | 4500 | 4500 | 4500 | 4500 |
| IXXU(3) | 4500 | 4500 | 4500 | 4500 | 4500 | 4500 | 4500 | 4500 | 4500 |
| IXXU(4) | 4100 | 4100 | 4100 | 4100 | 4100 | 4100 | 4100 | 4100 | 4100 |
| IXXU(5) | 4100 | 4100 | 4100 | 4100 | 4100 | 4100 | 4100 | 4100 | 4100 |
| IXXU(6) | 4100 | 4100 | 4100 | 4100 | 4100 | 4100 | 4100 | 4100 | 4100 |
| IXXU(7) | 4100 | 4100 | 4100 | 4100 | 4100 | 4100 | 4100 | 4100 | 4100 |
| IXXU(8) | 4100 | 4100 | 4100 | 4100 | 4100 | 4100 | 4100 | 4100 | 4100 |
| IXXU(9) | - | 4100 | 4100 | 4100 | 4100 | 4100 | 4100 | 4100 | 4100 |
| IXXU(10) | - | - | - | 4100 | - | - | 4100 | 4100 | 4100 |
| IXXU(11) | - | - | - | - | - | - | - | - | 4100 |

TABLE D.3 PARAMETERS FOR CANDIDATE TRACTOR/SEMITRACTOR/SEMITRAILER COMBINATIONS (Cont.)

| | I | IIa | IIb | III | IVa | IVb | V | VI | VII |
|---|---|---|---|---|---|---|---|---|---|
| HR(1) | 22.0 | 22.0 | 22.0 | 22.0 | 22.0 | 22.0 | 22.0 | 22.0 | 22.0 |
| HR(2) | 29.0 | 29.0 | 29.0 | 29.0 | 29.0 | 29.0 | 29.0 | 29.0 | 29.0 |
| HR(3) | 29.0 | 29.0 | 29.0 | 29.0 | 29.0 | 29.0 | 29.0 | 29.0 | 29.0 |
| HR(4) | 29.0 | 29.0 | 29.0 | 29.0 | 29.0 | 29.0 | 29.0 | 29.0 | 29.0 |
| HR(5) | 29.0 | 29.0 | 29.0 | 29.0 | 29.0 | 29.0 | 29.0 | 29.0 | 29.0 |
| HR(6) | 29.0 | 29.0 | 29.0 | 29.0 | 29.0 | 29.0 | 29.0 | 29.0 | 29.0 |
| HR(7) | 29.0 | 29.0 | 29.0 | 29.0 | 29.0 | 29.0 | 29.0 | 29.0 | 29.0 |
| HR(8) | 29.0 | 29.0 | 29.0 | 29.0 | 29.0 | 29.0 | 29.0 | 29.0 | 29.0 |
| HR(9) | - | 29.0 | 29.0 | 29.0 | 29.0 | 29.0 | 29.0 | 29.0 | 29.0 |
| HR(10) | - | - | - | 29.0 | - | - | 29.0 | 29.0 | 29.0 |
| HR(11) | - | - | - | - | - | - | - | - | 29.0 |
| TY(1) | 40.25 | 40.25 | 50.25 | 40.25 | 40.25 | 40.25 | 40.25 | 40.25 | 40.25 |
| TY(2) | 29.0 | 29.0 | 29.0 | 29.0 | 29.0 | 29.0 | 29.0 | 29.0 | 29.0 |
| TY(3) | 29.0 | 29.0 | 29.0 | 29.0 | 29.0 | 29.0 | 29.0 | 29.0 | 29.0 |
| TY(4) | 32.0 | 32.0 | 32.0 | 32.0 | 32.0 | 32.0 | 32.0 | 32.0 | 32.0 |
| TY(5) | 32.0 | 32.0 | 32.0 | 32.0 | 32.0 | 32.0 | 32.0 | 32.0 | 32.0 |
| TY(6) | 32.0 | 32.0 | 32.0 | 32.0 | 32.0 | 32.0 | 32.0 | 32.0 | 32.0 |
| TY(7) | 32.0 | 32.0 | 32.0 | 32.0 | 32.0 | 32.0 | 32.0 | 32.0 | 32.0 |
| TY(8) | 32.0 | 32.0 | 32.0 | 32.0 | 32.0 | 32.0 | 32.0 | 32.0 | 32.0 |
| TY(9) | - | 32.0 | 32.0 | 32.0 | 32.0 | 32.0 | 32.0 | 32.0 | 32.0 |
| TY(10) | - | - | - | 32.0 | - | - | 32.0 | 32.0 | 32.0 |
| TY(11) | - | - | - | - | - | - | - | - | 32.0 |

TABLE D.3 PARAMETERS FOR CANDIDATE TRACTOR/SEMITRACTOR/SEMITRAILER COMBINATIONS (Cont.)

| | I | IIa | IIb | III | IVa | IVb | V | VI | VII |
|---|---|---|---|---|---|---|---|---|---|
| TIRE(1) | 1 | 1 | 1 | 1 | 1 | 1 | 1 | 1 | 1 |
| TIRE(2) | 2 | 2 | 2 | 2 | 2 | 2 | 2 | 2 | 2 |
| TIRE(3) | 2 | 2 | 2 | 2 | 2 | 2 | 2 | 2 | 2 |
| TIRE(4) | 3 | 3 | 3 | 3 | 3 | 3 | 3 | 3 | 3 |
| TIRE(5) | 3 | 3 | 3 | 3 | 3 | 3 | 3 | 3 | 3 |
| TIRE(6) | 3 | 3 | 3 | 3 | 3 | 3 | 3 | 3 | 3 |
| TIRE(7) | 3 | 3 | 3 | 3 | 3 | 3 | 3 | 3 | 3 |
| TIRE(8) | 3 | 3 | 3 | 3 | 3 | 3 | 3 | 3 | 3 |
| TIRE(9) | - | 3 | 3 | 3 | 3 | 3 | 3 | 3 | 3 |
| TIRE(10) | - | - | - | 3 | - | - | 3 | 3 | 3 |
| TIRE(11) | - | - | - | - | - | - | - | - | 3 |
| Tractor front springs* | 1 | 1 | 1 | 1 | 1 | 1 | 1 | 1 | 1 |
| Tractor rear springs* | 2 | 2 | 2 | 2 | 2 | 2 | 2 | 2 | 2 |
| Trailer springs* | 3 | 3 | 3 | 3 | 3 | 3 | 3 | 3 | 3 |
| SY(1) | 16.3 | 16.3 | 16.3 | 16.3 | 16.3 | 16.3 | 16.3 | 16.3 | 16.3 |
| SY(2)-SY(3) | 19.0 | 19.0 | 19.0 | 19.0 | 19.0 | 19.0 | 19.0 | 19.0 | 19.0 |
| SY(3)-SY(11) | 22.0 | 22.0 | 22.0 | 22.0 | 22.0 | 22.0 | 22.0 | 22.0 | 22.0 |

*NOTE: The numbers refer to the spring data shown in Fig. D.2.

TABLE D.4 UNIROYAL FLEET-UNI-MASTER 15.00 x 22.5H [D.1]

CORNERING FORCE TABLE #1

LATERAL FORCE (LB.)

| Vertical Load / Slip Angle | 0.0 | 1.0 | 2.0 | 4.0 | 8.0 | 12.0 | 16.0 |
|---|---|---|---|---|---|---|---|
| | 2500.00 | 348.00 | 616.00 | 1036.00 | 1586.00 | 1859.00 | 1952.00 |
| | 5000.00 | 662.00 | 1195.00 | 2017.00 | 3121.00 | 3675.00 | 3812.00 |
| | 7500.00 | 945.00 | 1712.00 | 2944.00 | 4555.00 | 5221.00 | 5491.00 |
| | 10000.00 | 1139.00 | 2112.00 | 3715.00 | 5802.00 | 6618.00 | 6970.00 |

ALIGNING TORQUE TABLE #1

ALIGNING TORQUE (IN.LB.)

| Vertical Load / Slip Angle | 0.0 | 1.0 | 2.0 | 4.0 | 8.0 | 12.0 | 16.0 |
|---|---|---|---|---|---|---|---|
| | 2500.00 | 324.00 | 480.0 | 552.00 | 432.00 | 204.00 | 48.00 |
| | 5000.00 | 900.00 | 1392.00 | 1728.00 | 1524.00 | 780.00 | 168.00 |
| | 7500.00 | 1692.00 | 2700.00 | 3612.00 | 3108.00 | 1824.00 | 576.00 |
| | 10000.00 | 2496.00 | 5196.00 | 5796.00 | 5172.00 | 2868.00 | 1032.00 |

TABLE D.5. FIRESTONE 10.00 x 20 RIB [D.2]

## CORNERING FORCE TABLE #2

LATERAL FORCE (LB.)

Vertical Load

| Slip Angle | 0.0 | 1.0 | 3.0 | 4.0 | 5.0 | 7.0 | 10.0 |
|---|---|---|---|---|---|---|---|
| | 2000.00 | 356.00 | 824.00 | 1018.00 | 1221.00 | 1502.00 | 1767.00 |
| | 4000.00 | 580.00 | 1421.00 | 1770.00 | 2123.00 | 2612.00 | 3171.00 |
| | 6000.00 | 701.00 | 1808.00 | 2259.00 | 2711.00 | 3378.00 | 4182.00 |
| | 8000.00 | 767.00 | 2032.00 | 2583.00 | 3072.00 | 3849.00 | 4861.00 |
| | 9000.00 | 784.00 | 2104.00 | 2674.00 | 3182.00 | 4020.00 | 5056.00 |

## ALIGNING TORQUE TABLE #2

ALIGNING TORQUE (IN.LB.)

Vertical Load

| Slip Angle | 0.0 | 1.0 | 3.0 | 4.0 | 5.0 | 7.0 | 10.0 |
|---|---|---|---|---|---|---|---|
| | 2000.00 | 372.00 | 528.00 | 552.00 | 672.00 | 732.00 | 468.00 |
| | 4000.00 | 960.00 | 1716.00 | 1884.00 | 2268.00 | 2328.00 | 1896.00 |
| | 6000.00 | 1560.00 | 3132.00 | 3588.00 | 4248.00 | 4476.00 | 3948.00 |
| | 8000.00 | 2148.00 | 4644.00 | 5508.00 | 6384.00 | 6744.00 | 5676.00 |
| | 9000.00 | 2400.00 | 5424.00 | 6396.00 | 7488.00 | 7800.00 | 6780.00 |

TABLE D.6. HIGHWAY TREAD 9-20/F [D.3]

CORNERING FORCE TABLE #3

LATERAL FORCE (LB.)

Vertical Load

| Slip Angle | 0.0 | 1.0 | 2.0 | 4.0 | 8.0 | 12.0 | 16.0 |
|---|---|---|---|---|---|---|---|
| | 1400.00 | 238.00 | 440.00 | 718.00 | 1001.00 | 1263.00 | 1232.00 |
| | 2800.00 | 391.00 | 743.00 | 1286.00 | 1898.00 | 2500.00 | 2431.00 |
| | 4250.00 | 479.00 | 920.00 | 1631.00 | 2538.00 | 3082.00 | 3459.00 |
| | 5600.00 | 509.00 | 987.00 | 1805.00 | 2943.00 | 3690.00 | 4227.00 |
| | 6500.00 | 506.00 | 1005.00 | 1856.00 | 3115.00 | 3990.00 | 4628.00 |

ALIGNING TORQUE TABLE #3

ALIGNING TORQUE (IN.LB.)

Vertical Load

| Slip Angle | 0.0 | 1.0 | 2.0 | 4.0 | 8.0 | 12.0 | 16.0 |
|---|---|---|---|---|---|---|---|
| | 1400.00 | 240.00 | 396.00 | 456.00 | 240.00 | 72.00 | 0.0 |
| | 2800.00 | 624.00 | 1068.00 | 1416.00 | 1044.00 | 588.00 | 228.00 |
| | 4250.00 | 1008.00 | 1776.00 | 2556.00 | 2244.00 | 1416.00 | 888.00 |
| | 5600.00 | 1368.00 | 2424.00 | 3672.00 | 3540.00 | 2496.00 | 1668.00 |
| | 6500.00 | 1620.00 | 3000.00 | 4584.00 | 4620.00 | 3348.00 | 2292.00 |

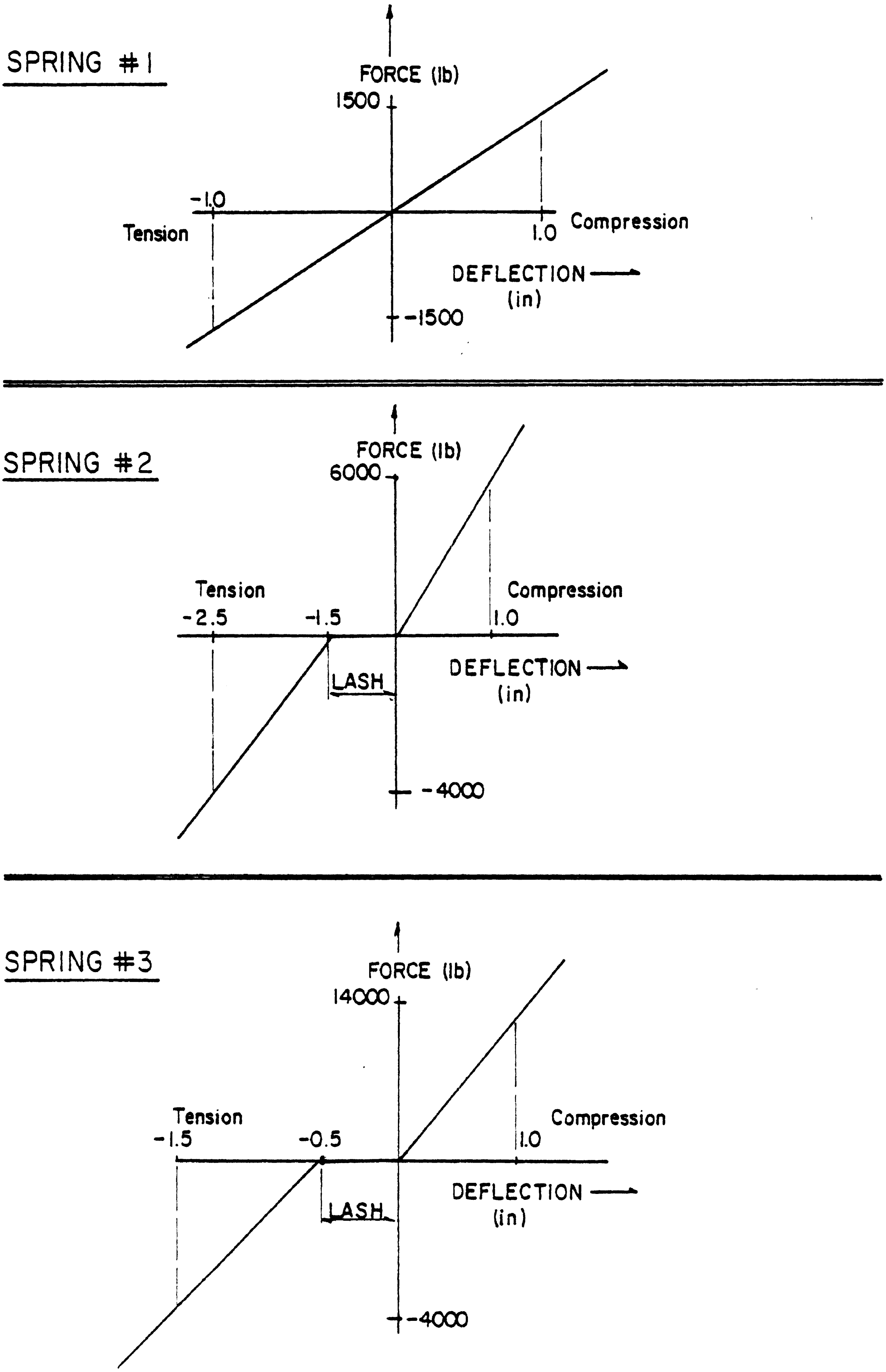


Figure D.2. Suspension spring characteristics

## REFERENCES

D.1 Ervin, R.D., et al. "Effects of Tire Properties on Truck and Bus Handling, Appendix C." Vol. II. Final Report, Contract DOT-HS-4-00943, December 1976.

D.2 Fancher, P.S., et al. "Simulation of the Directional Response Characteristics of Tractor-Semitrailer Vehicles." Final Report, MVMA Project #1.39.

D.3 Bernard, J.E., et al. "A Computer-Based Mathematical Method for Predicting the Directional Response of Trucks and Tractor-Trailers." Phase II Technical Report.

APPENDIX E

TANK SHELL GEOMETRY

Equations which are needed for computing the cross-sectional area and layout of the tank shells are developed in this appendix. A simple interactive computer program which is useful for computation of the payload capacity, shell height, and layout of the tank is also included in this appendix.

## Tank Cross-Sectional Area

As shown in Figure E.1, the tank cross-section geometry is defined in terms of the width, H1, height, H2, and the three curvatures: (1) the sidewall radius, $R_1$, (2) the top and bottom radius, $R_2$, and (3) the blend radius, $R_3$. The computation of the area enclosed by the shell is made easy by dividing the area into four segments. The four segments are illustrated in Figure E.2. In order to calculate the cross-sectional area, it is essential to determine the angles $\theta_1$ and $\theta_2$ (see Figure E.3) which are subtended by the arcs of radius $R_1$ and $R_2$, respectively. The areas of each of the four segments when expressed in terms of the shell radii and the angles $\theta_1$ and $\theta_2$ are:

$$A_1 = \frac{R_1^2\theta_1}{2} - \frac{R_1^2 \cos\theta_1 \sin\theta_1}{2} \tag{1}$$

$$A_2 = \frac{R_2^2\theta_2}{2} - \frac{R_2^2 \cos\theta_2 \sin\theta_2}{2} \tag{2}$$

$$A_3 = R_3^2\left(\frac{(\pi/2 - \theta_1 - \theta_2)}{2}\right) - R_3^2 \sin\left(\frac{\pi/2 - \theta_1 - \theta_2}{2}\right)\cos\left(\frac{\pi/2 - \theta_1 - \theta_2}{2}\right) \tag{3}$$

$$\begin{aligned} A_4 = {} & R_1 \sin\theta_1 \,(H_1/2 - R_1(1-\cos\theta_1)) + R_2 \sin\theta_2 (H_2/2 - R_2(1-\cos\theta_2)) \\ & + 1/2\,(H_1/2 - R_1(1-\cos\theta_1) - R_2 \sin\theta_2) \\ & \cdot (H_2/2 - R_2(1-\cos\theta_2) - R_1 \sin\theta_1) \end{aligned} \tag{4}$$

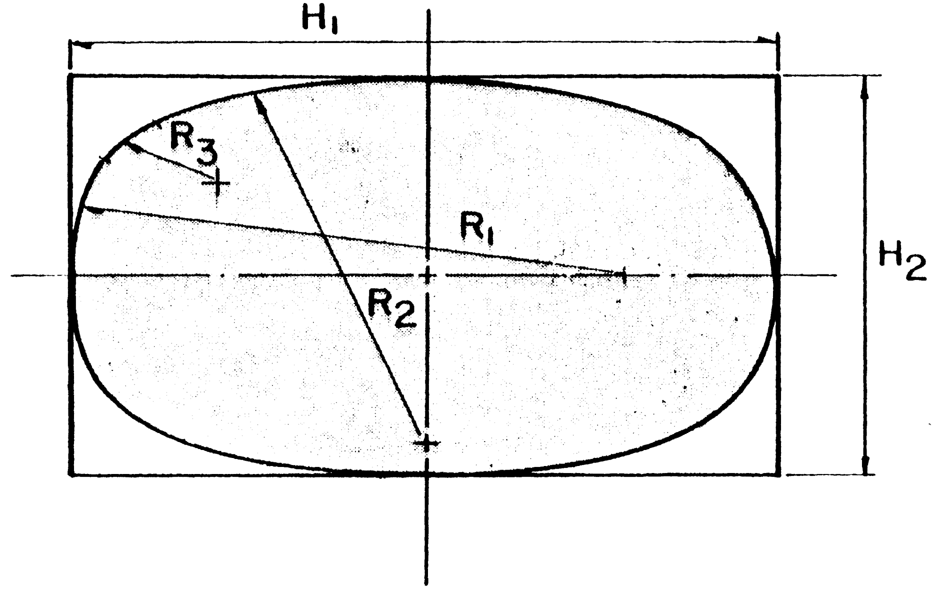


Figure E.1. Parameters needed to define tank cross-section geometry.

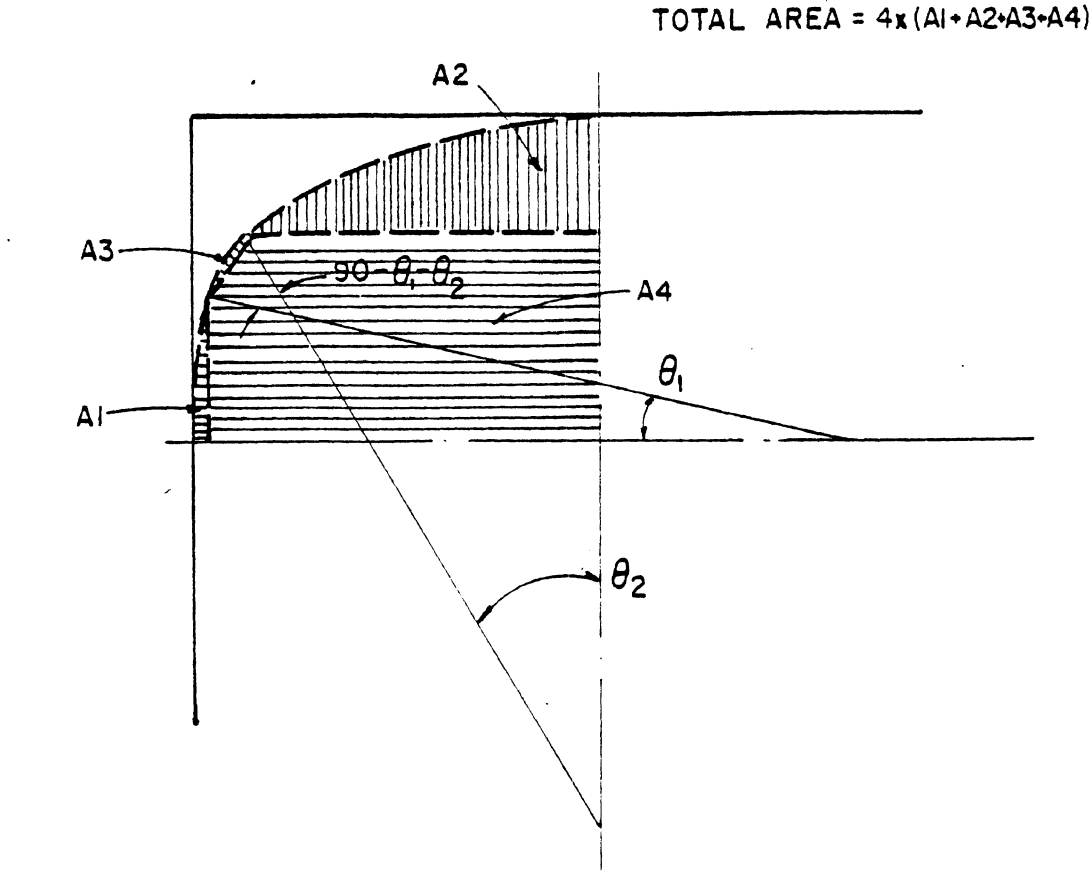


Figure E.2. Figure illustrating the division of the tank cross-sectional area into four segments - $A_1$, $A_2$, $A_3$, and $A_4$.

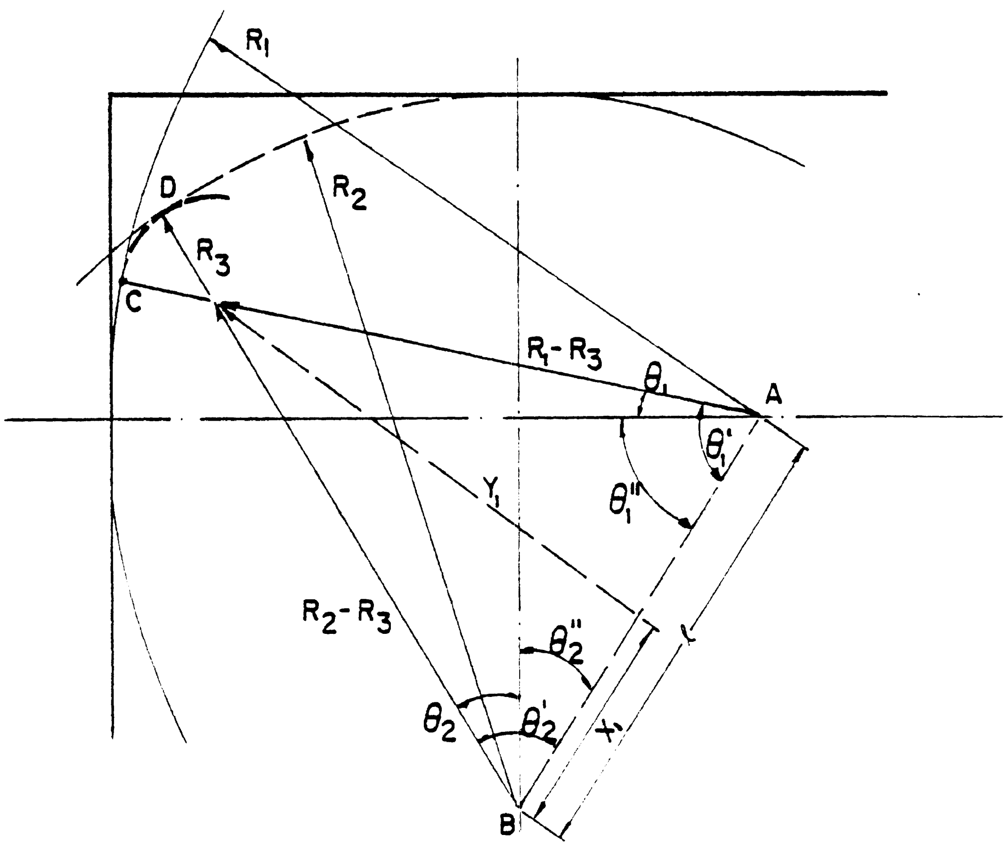


Figure E.3. Geometric construction needed for deriving the tank cross-sectional area equation.

The total cross-sectional area, A, of the tank is therefore given by the equation

$$A = (A_1 + A_2 + A_3 + A_4) \times 4 \tag{5}$$

The only unknown in Equations (1) through (4) are the angles $\theta_1$ and $\theta_2$. These two angles will now be expressed in terms of the shell radii and the height and width of the tank.

Referring to the geometric construction in Figure E.3, the lengths, $\ell$, $x_1$, and $y_1$, when defined in terms of the shell geometry parameters are:

$$\ell = \sqrt{(R_1-H_1/2)^2 + (R_2-H_2/2)^2} \tag{6}$$

$$x_1 = \frac{(R_2-R_3)^2 - (R_1-R_3)^2 + \ell^2}{2\ell} \tag{7}$$

$$y_1 = \sqrt{(R_2-R_3)^2 - x_1^2} \tag{8}$$

Hence $$\theta_2' = \tan^{-1} (y_1/x_1) \tag{9}$$

and $$\theta_2'' = \tan^{-1} \left(\frac{R_1-H_1/2}{R_2-H_2/2}\right) \tag{10}$$

$$\theta_2 = \theta_2' - \theta_2''$$

$$\theta_2 = \tan^{-1} (y_1/x_1) - \tan^{-1} \left(\frac{R_1-H_1/2}{R_2-H_2/2}\right) \tag{11}$$

The expression for the angle $\theta_1$, when derived along similar lines, is

$$\theta_1 = \tan^{-1}\left(\frac{y_1}{\ell - x_1}\right) + \tan^{-1}\left(\frac{R_1 - H_1/2}{R_2 - H_2/2}\right) - \pi/2 \qquad (12)$$

The cross-section area can therefore be computed by substituting Equations (11) and (12) into the area equations (1) through (4).

## Computer Program for Tank Layout Calculations

A simple computer program was developed for carrying out the calculations related to the geometry of drop-bottom tanks. The parameters needed for describing the geometry of a drop-bottom tank are shown in Figure E.4.

When the dimensions XL1, OVHANG, HEIT1, WIDTH, DROP, $R_1$, $R_2$, and $R_3$ and the front and rear loads, $W_1$ and $W_2$, are provided as input, the program computes the payload volume "PAYLD," the length of the tank "XL," and the wheelbase "WHBASE" of the tank. The calculation assumes no loss of volume due to the presence of dished ends at the front and rear ends of the tank. A length of 18 inches was therefore added to the total tank length (computed by the program) in order to account for the presence of dished ends.

The computer program which is written in Fortran IV is listed at the end of this appendix.

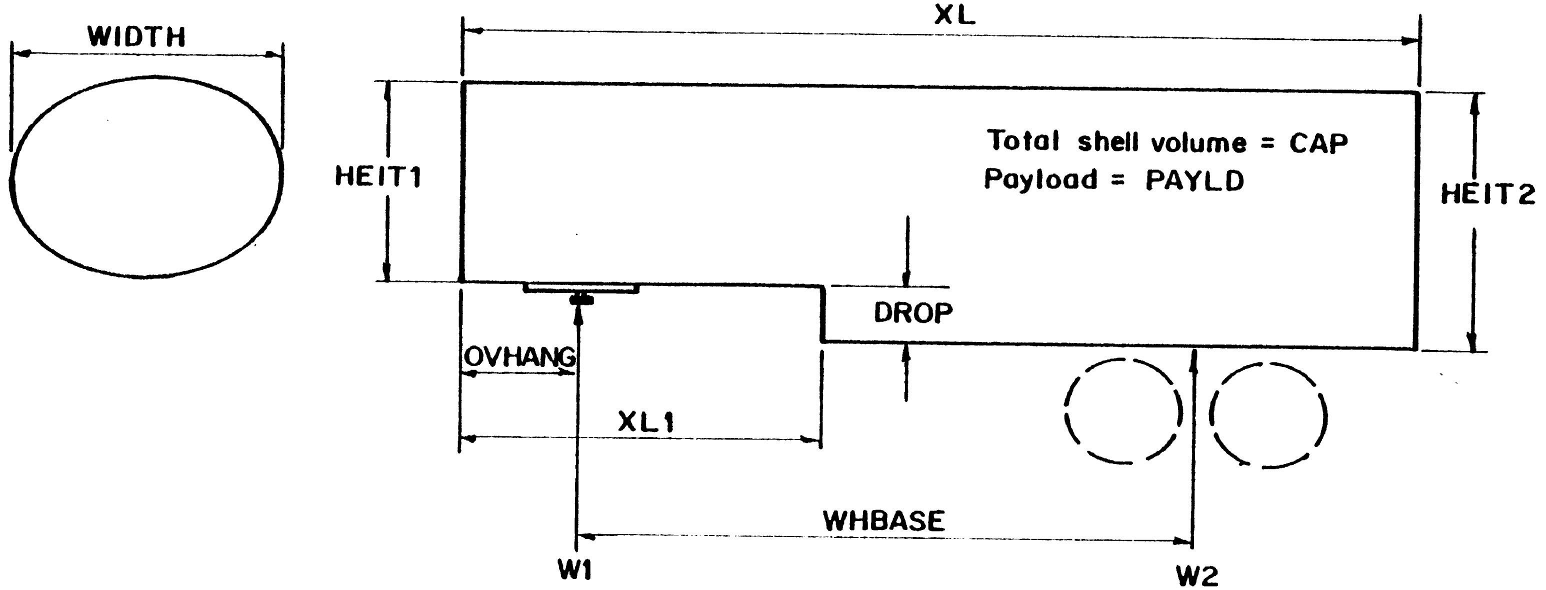


Figure E.4. Parameters needed to describe the geometry of a drop-bottom tank.

COMPUTER PROGRAM FOR COMPUTING THE LAYOUT OF A DROP-BOTTOM TANK

```
C
C  PROGRAM FOR COMPUTING THE LAYOUT  OF A DROP BOTTOM TANK
C  GIVEN - PATTERN, AXLE LAYOUT & OTHER DATA
C
C   R1=SIDE WALL RADIUS OF TANK SHELL
C   R2=TOP AND BOTTOM RADIUS OF TANK SHELL
C   R3=BLEND RADIUS
C   OVHANG=DISTANCE OF OVERHANG OF THE TANK FRONTEND BEYOND THE
C          KINGPIN
C   DROP= HEIGHT BY WHICH THE BELLY OF THE TANK IS DROPPED AT THE
C         REAR
C   XL1 = LENGTH OF THE FRONT END OF THE TANK OF A XSECTION HEIGHT
C         OF HEIT1
C   HEIT2= HEIT1+DROP
C   CAP  = TOTAL VOLUME OF THE TANK SHELL INCLUDING  OUTAGE
C   W1   = 5TH WHEEL LOAD-WEIGHT OF 5TH WHEEL ASSEMBLY
C   W2   = TRAILER AXLE LOAD - AXLE WEIGHT - CHASSIS WEIGHT
C   DENSE = PAYLOAD DENSITY (LB./GAL)
C   SHELL = SHELL WEIGHT IN (LB./GAL) OF SHELL VOLUME
C
C
C *****************************************************************
C
      COMMON R1, R2, R3, WIDTH
      WRITE (6,40)
      READ (5,70) R1, R2, R3
      WRITE (6,50)
      READ (5,70) WIDTH
      WRITE (6,110)
      READ (5,70) OUTAGE
      WRITE (6,120)
      READ (5,70) DENSE
      WRITE (6,130)
      READ (5,70) SHELL
      OUTAGE = OUTAGE / 100.0
      COMP = (DENSE/(1 + OUTAGE)) + SHELL
   10 WRITE (6,60)
      READ (5,70) XL1, OVHANG, W1, W2, DROP
      CAP = (W1 + W2) / COMP
      PAYLD = CAP / (1 + OUTAGE)
      WRITE (6,80)
      READ (5,70) HEIT1
   20 CALL AREA(HEIT1, A)
      HEIT2 = HEIT1 + DROP
      CALL AREA(HEIT2, B)
      XL = (CAP - XL1*A + XL1*B) / B
      WHBASE = (((XL1/2.0) - OVHANG)*XL1*A*COMP + (XL - XL1)*COMP*B*(((
     1XL + XL1)/2.0) - OVHANG)) / W2
      WRITE (6,100) A, B, XL, HEIT1, HEIT2, WHBASE, PAYLD
      WRITE (6,90)
      READ (5,70) HEIT1
      IF (HEIT1 .LT. 0.0) GO TO 10
      IF (HEIT1 .GT. 1000.0) GO TO 30
      GO TO 20
   30 CONTINUE
      STOP
   40 FORMAT (1H0, 'ENTER SIDE,TOP, & BLEND RADII OF PATTERN IN F FORMAT
     1')
   50 FORMAT (1H0, 'ENTER TANK WIDTH')
   60 FORMAT (1H0, 'ENTER  XL1,OVHANG,W1,W2,DROP')
   70 FORMAT (10F10.3)
   80 FORMAT (1H0, 'ENTER HEIGHT OF FRONT END')
   90 FORMAT (1H0, 'ENTER NEW ESTIMATE OF FRONT END HEIGHT')
  100 FORMAT (1H0, 'AREA1 = ', F10.3/'AREA2 = ', F10.3/'TANK LENGTH = ',
     1       F10.3/'HEIGHT1 = ', F10.3/'HEIGHT2 = ', F10.3/
     2       'WHEEL BASE = ', F10.3/'PAYLOAD VOL = ', F10.3)
  110 FORMAT (1H0, ' ENTER THE OUTAGE VOLUME IN % OF PAYLOAD VOLUME')
  120 FORMAT (1H0, ' ENTER DENSITY OF PAYLOAD (LB./GALLON)')
  130 FORMAT (1H0, ' ENTER DENSITY OF SHELL IN LB./GALLON OF SHELL VOL')
      END
```

```
C
C   SUBROUTINE FOR COMPUTING AREA OF TANK CROSS SECTION
C
      SUBROUTINE AREA(W2, AREA)
      COMMON R1, R2, R3, W1
   10 XL = SQRT((R1 - (W1/2.0))**2 + (R2 - (W2/2.0))**2)
      X1 = ((R2 - R3)**2 - (R1 - R3)**2 + XL**2) / (2.0*XL)
      Y1 = SQRT((R2 - R3)**2 - X1**2)
      TH21 = ATAN(Y1/X1)
      TH211 = ATAN((R1 - (W1/2.0))/(R2 - (W2/2.0)))
      THETA2 = TH21 - TH211
      TH11 = ATAN(Y1/(XL - X1))
      TH111 = 1.5708 - TH211
      THETA1 = TH11 - TH111
   20 IF (R1 .LT. (W1/2.0)) THETA1 = 1.5708 + TH11 + TH211
C
C
C  AREA
C
C
      SINTH1 = SIN(THETA1)
      COSTH1 = COS(THETA1)
      SINTH2 = SIN(THETA2)
      COSTH2 = COS(THETA2)
      AREA1 = (R1*R1*THETA1/2.0) - (R1*R1*COSTH1*SINTH1/2.0)
      AREA2 = (R2*R2*THETA2/2.0) - (R2*R2*COSTH2*SINTH2/2.0)
      AREA3 = (R3*R3*(1.5708 - THETA1 - THETA2)/2.0) - R3 * R3 * SIN((1.
     15708 - THETA1 - THETA2)/2.0) * COS((1.5708 - THETA1 - THETA2)/2.0)
      AREA4 = R1 * SINTH1 * ((W1/2.0) - (R1 - R1*COSTH1)) + R2 * SINTH2
     1* ((W2/2.0) - R2 + R2*COSTH2 - R1*SINTH1) + (((W1/2.0) - R1 + R1*
     2COSTH1 - R2*SINTH2)*((W2/2.0) - R2 + R2*COSTH2 - R1*SINTH1)/2.0)
      AREA = 4.0 * (AREA1 + AREA2 + AREA3 + AREA4) / 231.
      RETURN
      END
```

APPENDIX F

ROLL BEHAVIOR OF MULTI-AXLED VEHICLES

The material presented in this appendix is focused towards gaining a basic understanding of the roll behavior of multi-axled vehicles. Such an understanding is essential for: (1) interpreting the results obtained from computerized calculations of the roll behavior of such vehicles and (2) for providing an insight into the methods by which the rollover threshold of a vehicle can be improved.

A series of three roll plane models will be utilized for the purpose of understanding the physics of the rollover process. The models are progressively more complete in the treatment of the roll plane behavior of a vehicle. The models are not meant to provide an accurate method for computing the rollover threshold of a vehicle, but only to gain a qualitative understanding of the sensitivity of the rollover threshold of a vehicle to its roll properties.

## F.1 Rigid Block Model

Let us consider a roll plane representation in which the compliance of the suspension springs and tires are neglected. Such a representation is illustrated in Figure F.1. If the vehicle executes a steady turn of lateral acceleration $a_y$ (in the units of g's), the lateral force reacted at the tire-road interface is $W \cdot a_y$, and the overturning moment acting on the vehicle is $W \cdot a_y \cdot h$. This overturning moment is counterbalanced by two roll moments: (1) the roll-resisting moment produced by the side-to-side transfer of the vertical loads at the tires—$(F_2-F_1)T$, and (2) the overturning moment produced by the lateral shift in the c.g. of the vehicle—$W\,h\,\phi$. Therefore,

$$W\,h\,a_y = (F_2-F_1)T - W\,h\,\phi \qquad (1)$$

Each of the two terms on the right-hand side of (1) are plotted as a function of the roll angle in Figure F.2. The roll-resisting moment

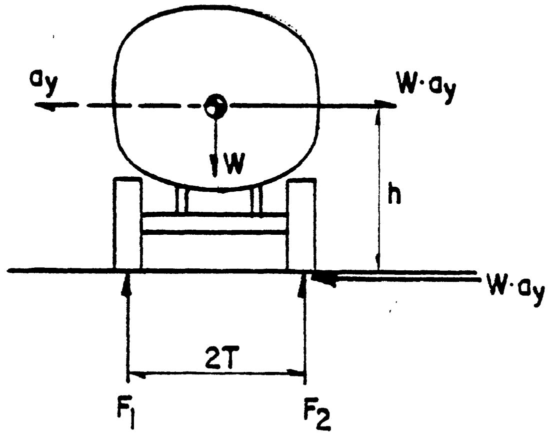


Figure F.1. Rigid block representation.

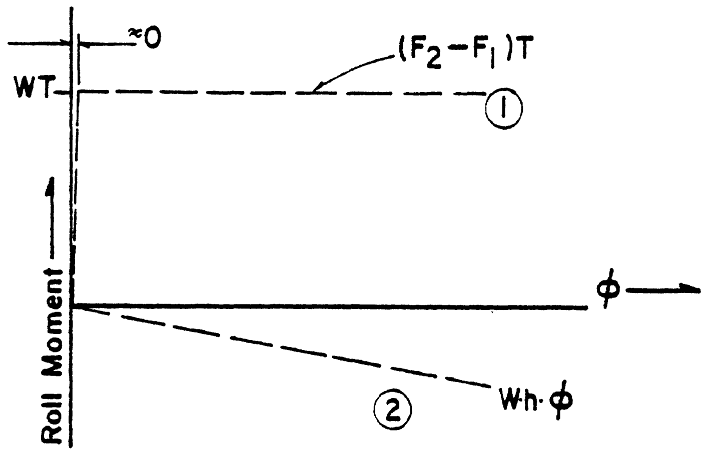


Figure F.2. Roll-resisting moment produced by side-to-side load transfer and the overturning moment produced by the lateral shift of c.g.

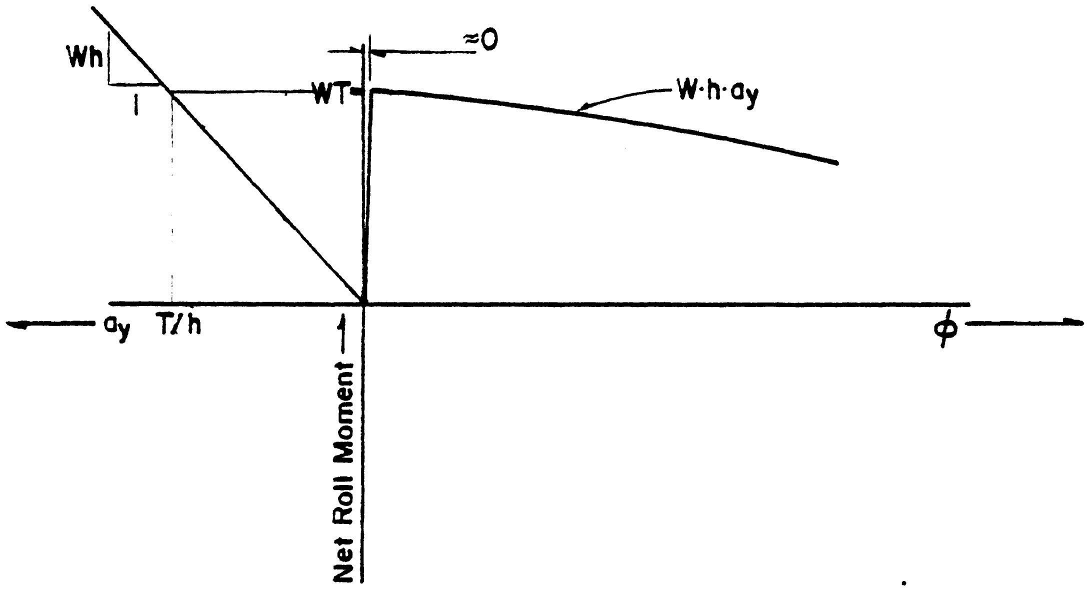


Figure F.3. Plot of net roll moment vs. roll angle.

which is produced by the side-to-side transfer of vertical load increases to the point where the tires on the left-hand side of the vehicle completely lift off the ground ($F_1 = 0.0$). At this point, the entire weight of the vehicle is carried by the tires on the right-hand side of the vehicle (i.e., $F_2 = W$), and the roll-resisting moment is W T. No additional roll-resisting moment is generated when the roll angle is increased beyond this point.

Upon combining the curves marked 1 and 2 in Figure F.2, we get the net roll-resisting moment produced by the vehicle. The net roll-resisting moment is plotted in Figure F.3. Since the net roll moment is directly proportional to the lateral acceleration, the left half of the abscissa in Figure F.3 is utilized for marking the lateral acceleration, $a_y$.

From Figure F.3 we note that the maximum net roll moment that can be reacted by the vehicle is W T and the corresponding lateral acceleration is T/h. At this lateral acceleration, the tires on one side of the vehicle lift off the ground plane. A stable equilibrium cannot be sustained beyond this point, since any further increase in the lateral acceleration would cause an uncontrolled increase of the roll angle until the vehicle completely rolls over.

The rollover threshold for the rigid block representation of the vehicle is therefore given by the simple expression

$$a_{y_c} = T/h \tag{2}$$

## F.2 Single-Axle Representation

The next level of complexity we shall consider is a model in which suspension and axle properties are considered, but are lumped together and represented by a single axle. Such a representation would be sufficiently accurate only if the tire and suspension spring rates of each axle were to be proportional to the static load carried by the axle, and if all of the axles had the same track width and roll center height.

The single-axle representation of the vehicle is shown in Figure F.4. The combined weight of the sprung and unsprung masses is represented by the weight, W, at a height, h, above the ground level. The roll angle is once again assumed to be small and the vehicle is assumed to roll about a point on the ground plane. The roll-resisting moment produced by the side-to-side transfer of the vertical tire loads and the overturning moment produced by the lateral shifting of the c.g. ($W\,h\,\phi$) are plotted as functions of the roll angle, $\phi$, in Figure F.5. The roll-resisting moment produced by side-to-side load transfer is shown in Figure F.5 for three levels of suspension roll stiffness. In drawing these curves, it was assumed that the suspensions and tires have linear properties.

It can be seen that the roll angles at which the tires lift off the ground depends upon the roll stiffness of the suspensions and tires. But the maximum roll-resisting moment produced by the side-to-side load transfer effect is unaffected by the roll stiffness of the vehicle and is given by the expression W T. By combining the curves marked 1 and 2 in Figure F.5, we get the net roll-resisting moment curves shown in Figure F.6. As the suspension and tires are made progressively stiffer in roll, the peak value for the net roll-resisting moment increases along the line marked AB in Figure F.6. For an infinitely stiff suspension, we revert to the rigid block model, and the maximum roll moment is therefore once again W T and the rollover threshold, $a_{y_{max}}$, is T/h.

If the roll angle at which the tires lift off the ground is $\phi_c$, the peak value for the net roll moment is given by the equation

$$\text{Max Roll-Resisting Moment} = W\,T - W\,h\,\phi_c \tag{3}$$

and the lateral acceleration threshold is given by the expression

$$a_{y_c} = T/h - \phi_c \tag{4}$$

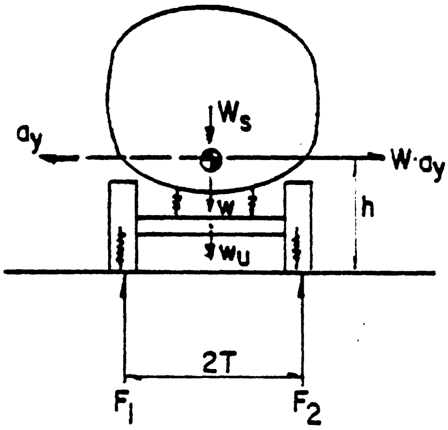

Figure F.4. Single-axle representation.

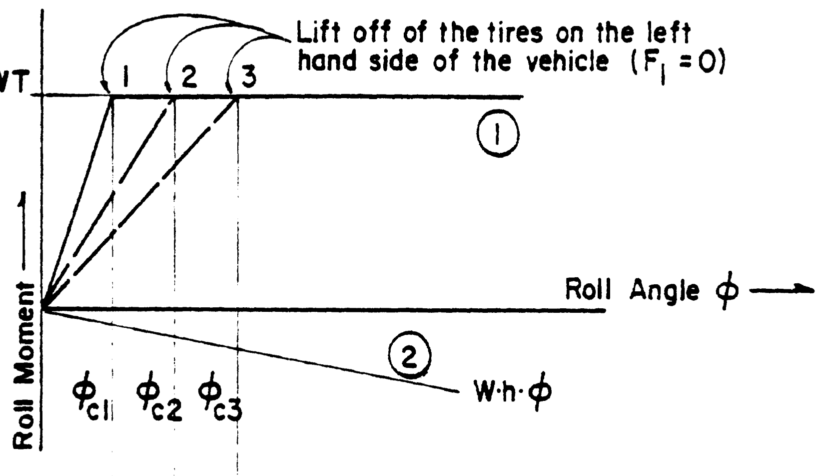

Figure F.5. Plot of roll moment vs. roll angle for three levels of roll stiffness.

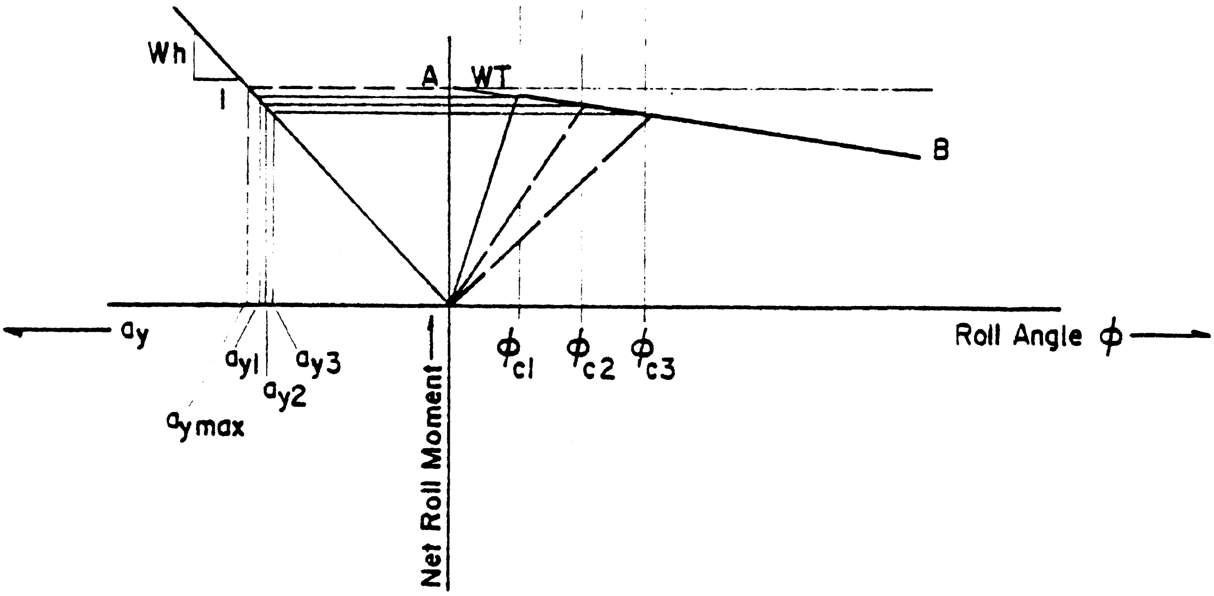

Figure F.6. Plot of net roll moment vs. roll angle.

This expression therefore indicates that the rollover threshold of a vehicle can be improved by increasing the roll stiffness of the suspensions on a vehicle.

The influence of suspension backlash on rollover threshold can be understood by using this simple roll plane model. The roll-resisting moment produced by the side-to-side transfer of vertical load and the overturning moment produced by the lateral shift in the c.g. are plotted in Figure F.7 for a vehicle which has a suspension backlash of $\delta$.

When the suspension on the left-hand side of the vehcle goes through the backlash, $\delta$, the sprung mass travels through an angle $\delta/2s$, where 2s is the lateral distance between the suspension springs. With reference to curve 1 in Figure F.7, the segment, XY, of the curve represents the travel of the sprung mass through the suspension backlash. After the backlash has been taken up, the suspension on the left-hand side goes into tension and produces an additional resisting moment until the tires on the left-hand side lose road contact. The loss of road contact by the tires on the left-hand side of the vehicle is represented by point Z in Figure F.7. Upon combining the roll-resisting moment produced by the side-to-side load transfer effect and the overturning moment produced by the lateral shift in the c.g. of the vehicle, we get the net roll-resisting moment curve OABCD which is shown in Figure F.8.

Tracing through the moment trajectory in Figure F.8, we see that when the lateral acceleration is increased, the plot of net roll moment versus roll angle, $\phi$, follows the line OA, whose slope represents the difference between the suspension/tire spring rate and the overturning moment slope, W h. When the lateral acceleration exceeds the level $a_{y_a}$, the sprung mass "jumps" through the lash, and falling along the slope, W h, to an "end of lash" roll angle which is represented by point B .

Further increases in the lateral acceleration result in an increase in the roll angle until the lateral acceleration level, $a_{y_c}$, is reached. The slope of segment BC is less than that of OA due to the fact that the

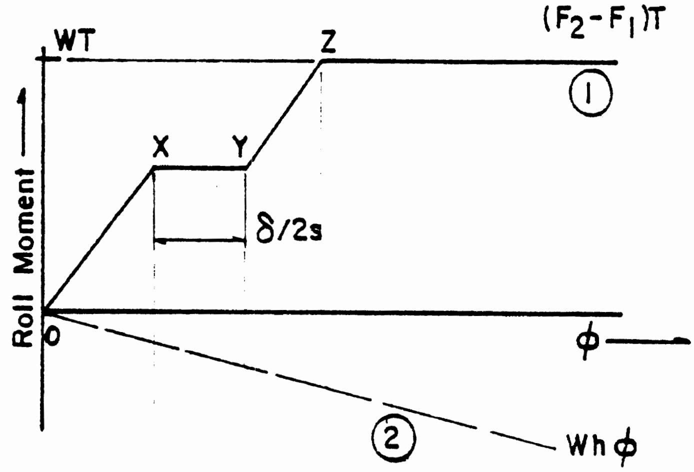


Figure F.7. Influence of suspension lash on the roll moment-roll angle relationship.

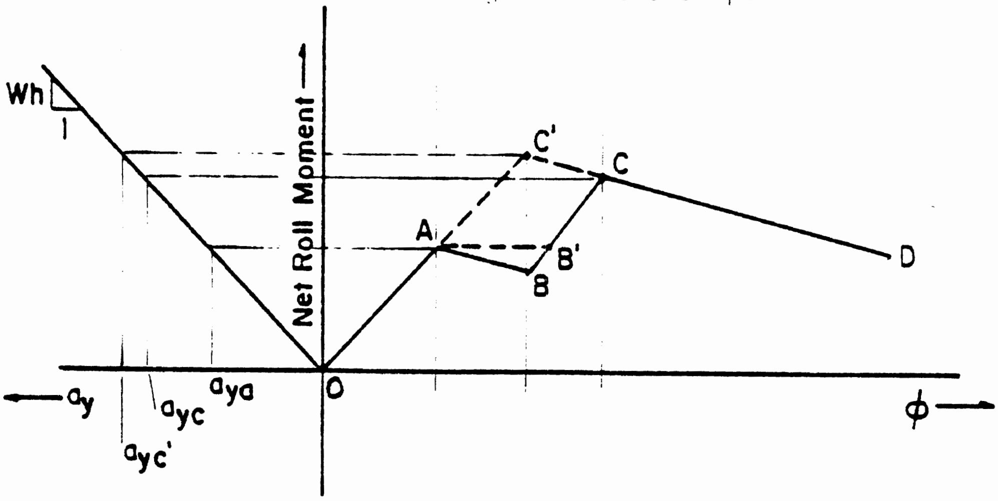


Figure F.8. Influence of suspension lash on net roll moment and rollover threshold.

suspension springs on one side are now being exercised in their low stiffness, tension direction. No stable equilibrium condition exists for lateral acceleration levels beyond $a_{y_c}$; therefore, the rollover threshold of the vehicle is equal to $a_{y_c}$.

If the backlash were to be eliminated, the plot of roll moment versus roll angle would follow the trajectory OAC' in Figure F.9, thereby attaining the higher rollover threshold level, $a_{y_{c'}}$. The improvement in rollover threshold that can be achieved by the elimination of suspension backlash is therefore evident from this figure.

## F.3 Three-Axle Representation

A single axle representation of the vehicle is not valid where the various axles of vehicles have roll stiffness levels which are not proportional to the static loads which are carried by the axles. In the case of typical tractor-semitrailer configurations, for example, the tractor front axle is equipped with a very soft suspension, while the suspension springs on the tractor rear axles are relatively stiff and carry a heavier load. The trailer suspensions are typically even stiffer than those on the tractor's rear axles. Accordingly, we find it appropriate to represent the tractor-semitrailer vehicle by a single sprung mass which is supported by three composite "axles"—(1) the tractor front axle, (2) a composite axle which represents the tractor rear axles and (3) a composite axle which represents all of the trailer axles.

If the loads carried by each of the three composite axles are $W_1$, $W_2$, and $W_3$, and their respective track widths are $2T_1$, $2T_2$, and $2T_3$, the maximum roll-resisting moment that can be produced by each axle is $W_1T_1$, $W_2T_2$, and $W_3T_3$, respectively. Depending upon the roll stiffness of each axle, the lift-off of the tires on one side of the axles takes place at different roll angles. The roll-resisting moment produced by each axle is plotted in Figure F.9 by the curves 1, 2, and 3, respectively. The curve that represents the overturning moment produced by the lateral shift of the c.g. of the vehicle is shown in this figure by the line marked 4.

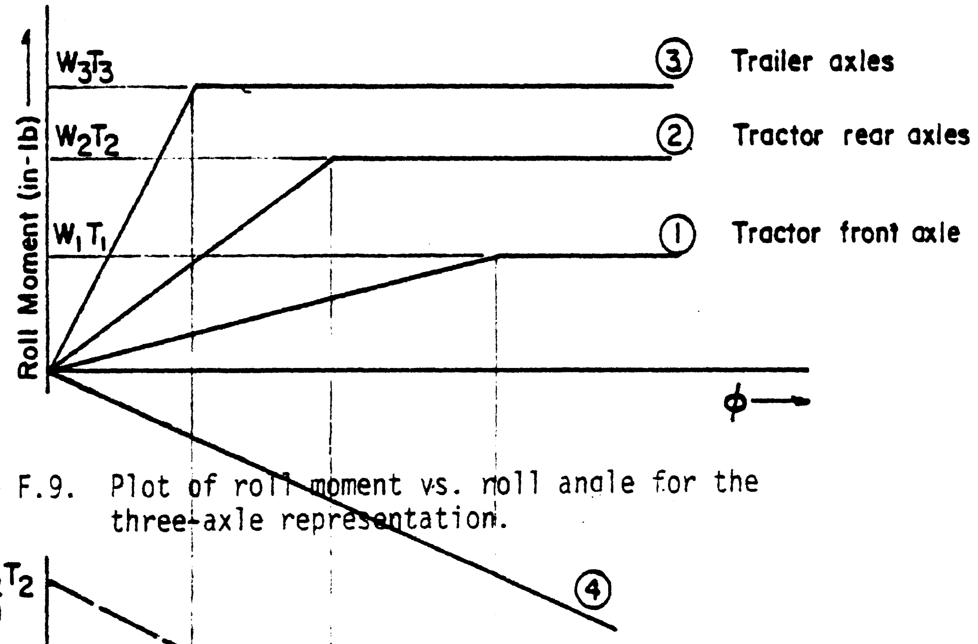


Figure F.9. Plot of roll moment vs. roll angle for the three-axle representation.

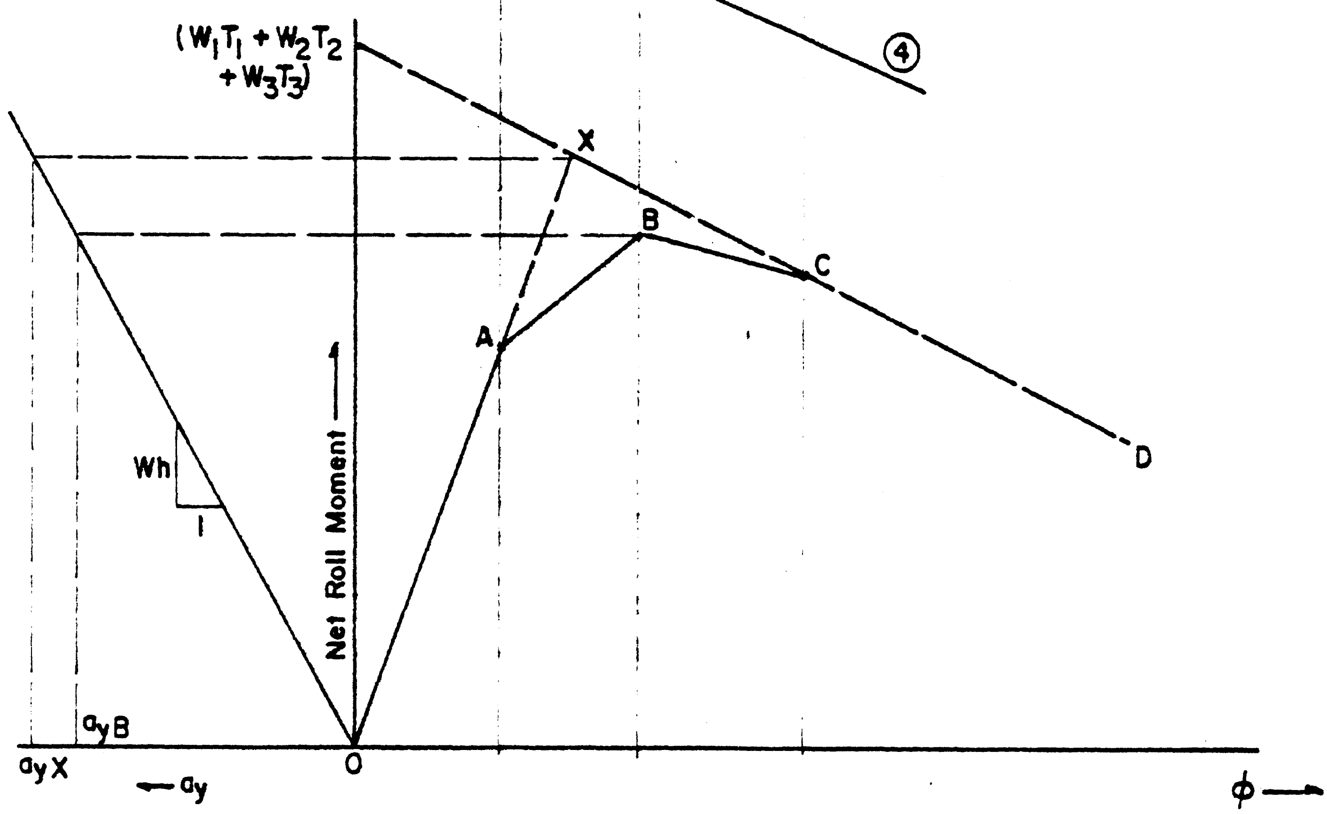


Figure F.10. Plot of net roll moment vs. roll angle for the three-axle representation.

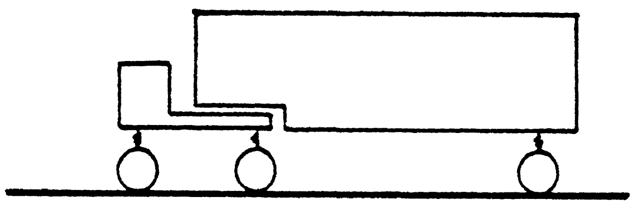

**3 Axle Representation**

If we combine (1) , (2) , (3) , and (4) in Figure F.9, we get a plot of the net roll-resisting moment versus the roll angle of the vehicle which is shown by the curve OABCD in Figure F.10. The points A, B, and C mark the lift off of the tires on the trailer axles, the tractor rear axles, and the tractor front axle, respectively. According to this figure, the maximum value for the net roll-resisting moment is reached when the tires on the tractor rear axle lift off the road surface. Beyond this point, no stable equilibrium points exist even though both the tires of the tractor front axle are still on the ground. The rollover threshold of the vehicle is therefore $a_{y_B}$.

If, instead of the three-axle representation, the roll properties of all the axles were to be lumped together and represented by a single axle, the net roll moment versus roll angle plot would follow the curve OXD which is superimposed on Figure F.10. The rollover threshold, $a_{y_X}$, which is indicated by the single-axle representation can be seen to be higher than the rollover threshold, $a_{y_B}$ which is predicted by the three-axle model. Hence, the lumping together of axles which have distinctly different roll properties can lead to significant errors in the prediction of rollover thresholds.

F.3.1 Influence of Suspension Stiffness. We shall now utilize the three-axle representation to investigate effects of varying the roll stiffness of each of the three composite axles, individually. The effects of stiffening the trailer axles, the tractor rear axles, and the tractor front axle on the net roll moment versus roll angle curve are illustrated in Figures F.11, F.12, and F.13, respectively.

Trailer suspension: With reference to Figure F.11, we note that in the baseline case, path OABCD, the trailer axles are stiffer than either the tractor rear axles or the tractor front axles such that the trailer axle tires lift off first, at point A. Any increase in the roll stiffness of the trailer suspension merely shifts the point of trailer tire lift off toward the left, as in path OA', thereby having no effect on the rollover threshold, $a_{y_B}$, of the vehicle. If the roll stiffness

F.3.2 Influence of Suspension Lash. Analysis performed using the single-axle model (in Section F.2) has shown that suspension lash degrades the rollover threshold of a vehicle. We shall now utilize the three-axle representation to clarify the mechanism by which lash in the trailer and tractor rear suspensions can degrade rollover threshold.

The influence of trailer suspension lash on roll response is illustrated in Figure F.14. For the case in which there is no lash in the trailer suspension, the net roll moment versus roll angle plot follows the trajectory OAC'DEF in Figure F.14. In this curve, point C' represents the lift off of the tires on one side of the trailer axles. The maximum roll-resisting moment is reached at point D. Beyond point D, the vehicle continues to roll without any increase in lateral acceleration level and ultimately overturns.

With the addition of a moderate amount of lash to the trailer suspension, the net roll moment versus roll angle curve becomes the solid line OABCDEF in Figure F.14. The segments AB and DE represent the rolling of the sprung mass through the lash in the trailer and tractor rear suspensions, respectively. It can be seen that the presence of this moderate amount of lash in the trailer suspension has no effect on the rollover threshold of the vehicle since the peak value D of the net roll moment remains unaffected.

With a further increase of the lash in the trailer suspension, the plot of net roll moment versus roll angle in Figure F.14 follows the trajectory OAB'D'EF. We note that the peak roll-resisting moment is now reduced to the level D', and hence results in a decrease of the rollover threshold of the vehicle. Further increases in the lash result in a decrease of the peak roll moment along the line DE.

The influence of tractor rear suspension lash on roll response is illustrated in Figure F.15. With zero lash in the tractor rear suspension, the curve of net roll moment versus roll angle follows the trajectory OABCD'F, and the peak value for the roll-resisting moment is reached at point D'. Considering increasing levels of lash in the tractor rear suspension, trajectories OABCDEF and OABCDE'F' indicate significant reductions in the rollover threshold.

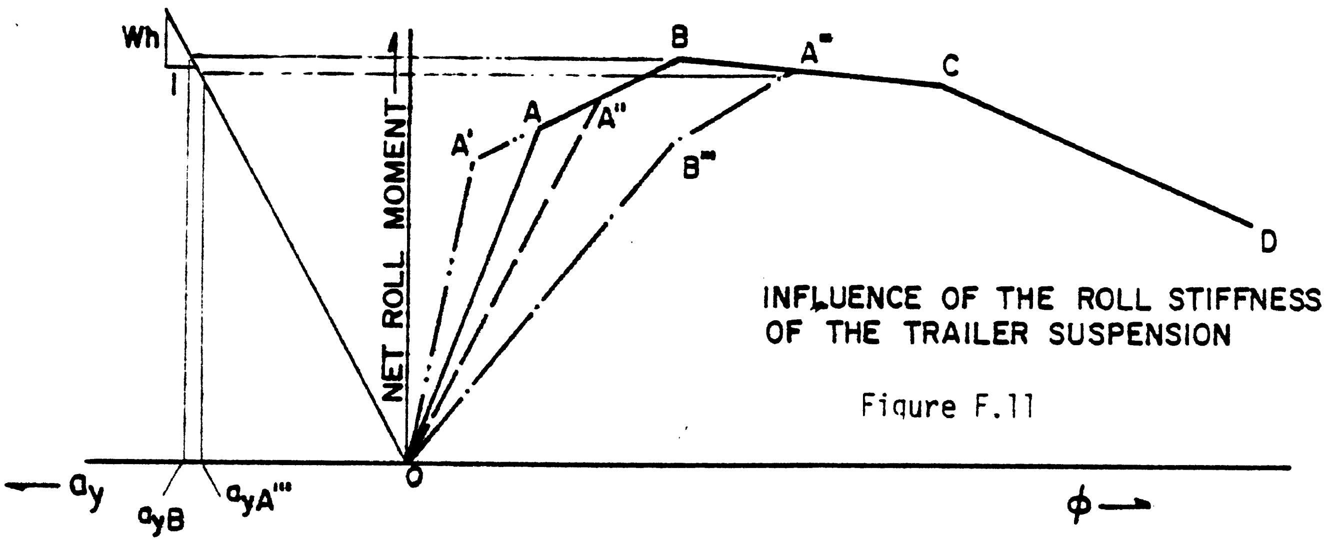


INFLUENCE OF THE ROLL STIFFNESS OF THE TRAILER SUSPENSION

Figure F.11

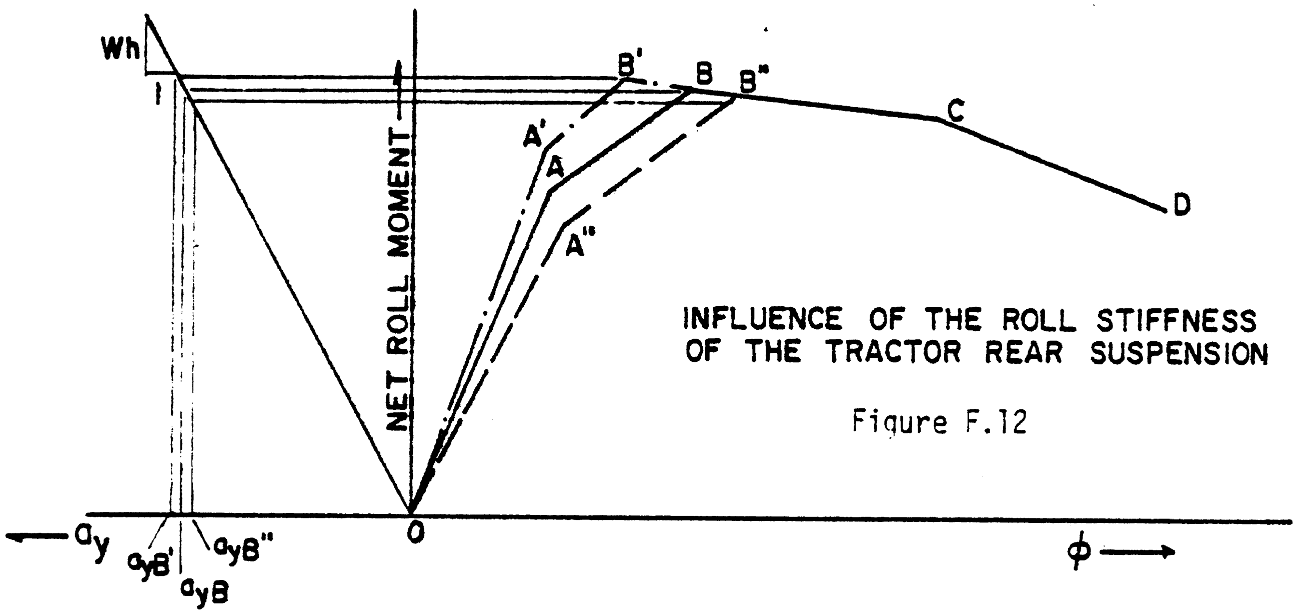


INFLUENCE OF THE ROLL STIFFNESS OF THE TRACTOR REAR SUSPENSION

Figure F.12

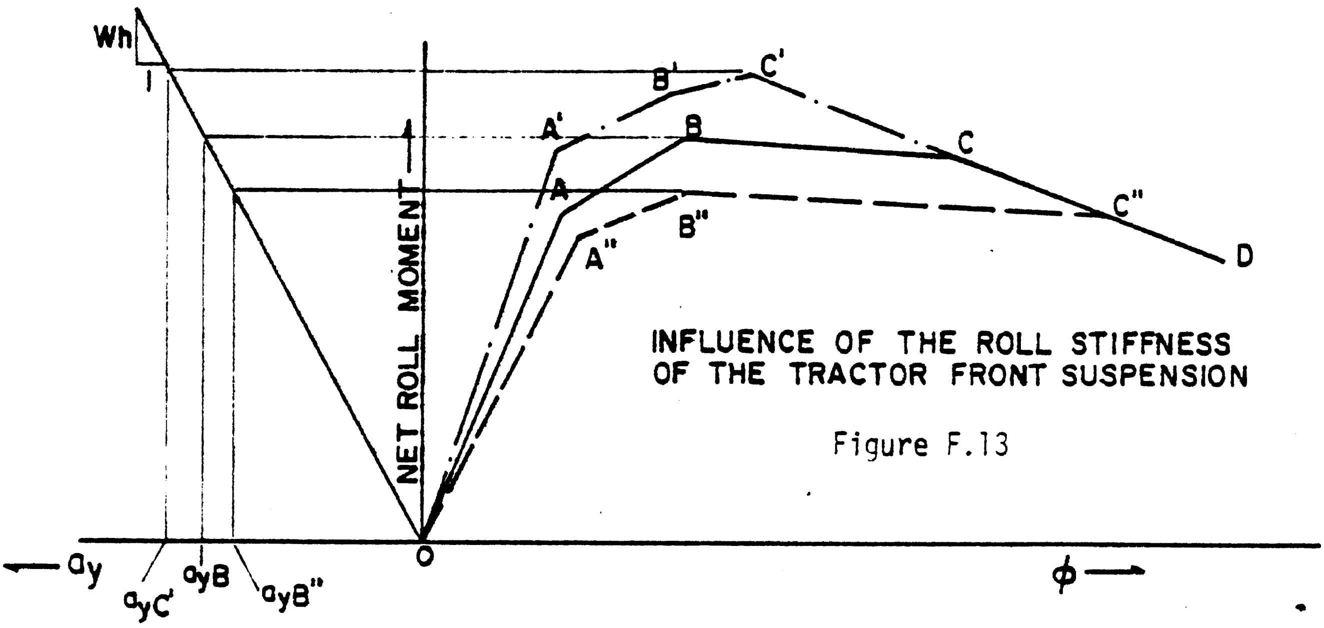


INFLUENCE OF THE ROLL STIFFNESS OF THE TRACTOR FRONT SUSPENSION

Figure F.13

of the trailer suspensions is reduced, the point, A, which marks the lift off of the trailer tires moves initially towards B, with no immediate influence on the rollover threshold, $a_{y_B}$. Indeed, we see that the rollover threshold of the overall vehicle is affected by changes in trailer suspension roll stiffness only if the roll stiffness is reduced to such a level that the trailer tires start to lift off at larger values of roll angles than that at which the tires on the tractor rear axle lift off. The path, OB''', A''', CD in Figure F.11, corresponds to such a situation. The rollover threshold is indicated in this case by point A'''. The rollover threshold, $a_{y_{A'''}}$, is below the value, $a_{y_B}$, which was attained in the baseline case. The rollover threshold will continue to decrease if the roll stiffness of the trailer suspension is reduced even further.

<u>Tractor rear axles</u>: Changes in the roll stiffness of the tractor rear axle have a direct effect on the rollover threshold of the vehicle. When the roll stiffness of the tractor rear axle is varied, the point, B, which signifies the tractor rear-axle lift off, shifts along the line, BC. As shown in Figure F.12, increasing the roll stiffness of the tractor rear axles, as indicated by a movement of point B toward the point B', leads to improvement in the rollover threshold of the vehicle. Similarly, reducing the roll stiffness of the rear axle, as indicated by movement of B toward B'', leads to a degradation of the rollover threshold of the vehicle.

<u>Tractor front axle</u>: The influence of the roll stiffness of the tractor front axle on the net roll moment versus roll angle curve is illustrated in Figure F.13. We note that the rollover threshold of the vehicle can be significantly improved by any degree of stiffening of the tractor front suspension. In the trajectory shown by points OA'B'C'D, for example, the tractor front suspension has been stiffened to such a degree that the rollover threshold is now determined by the lift off of the tractor front tire, at point C', rather than by the tractor rear axle lift off point, B, in the baseline case.

INFLUENCE OF TRAILER LASH

Figure F.14

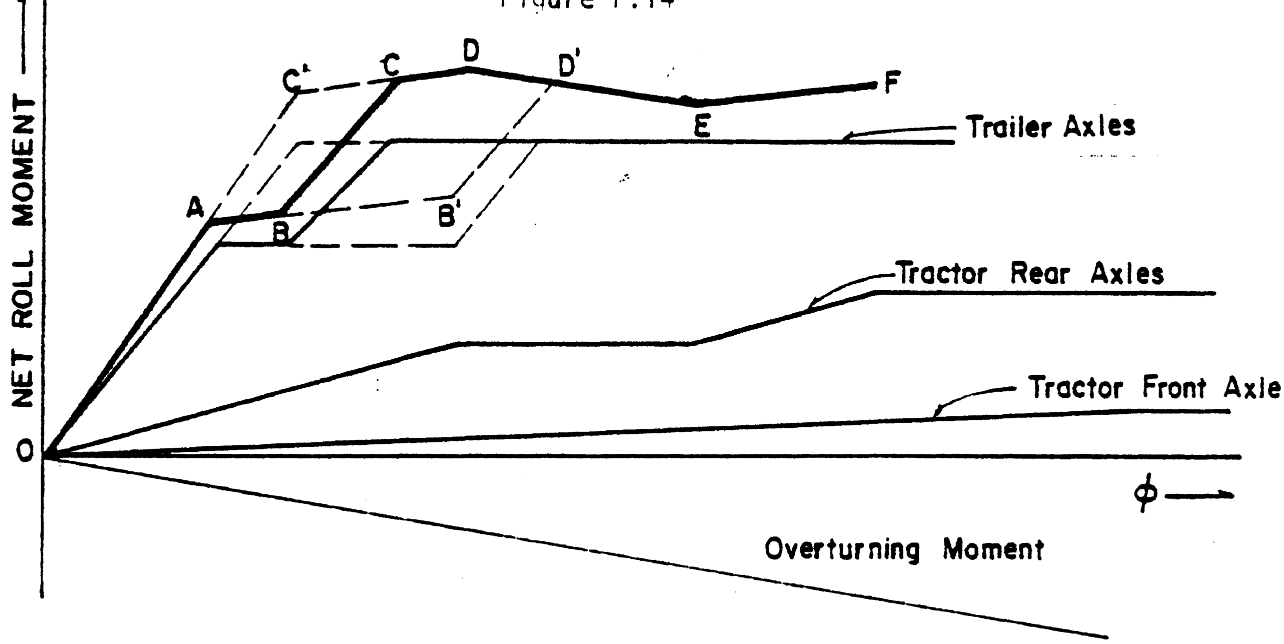


INFLUENCE OF TRACTOR LASH

Figure F.15

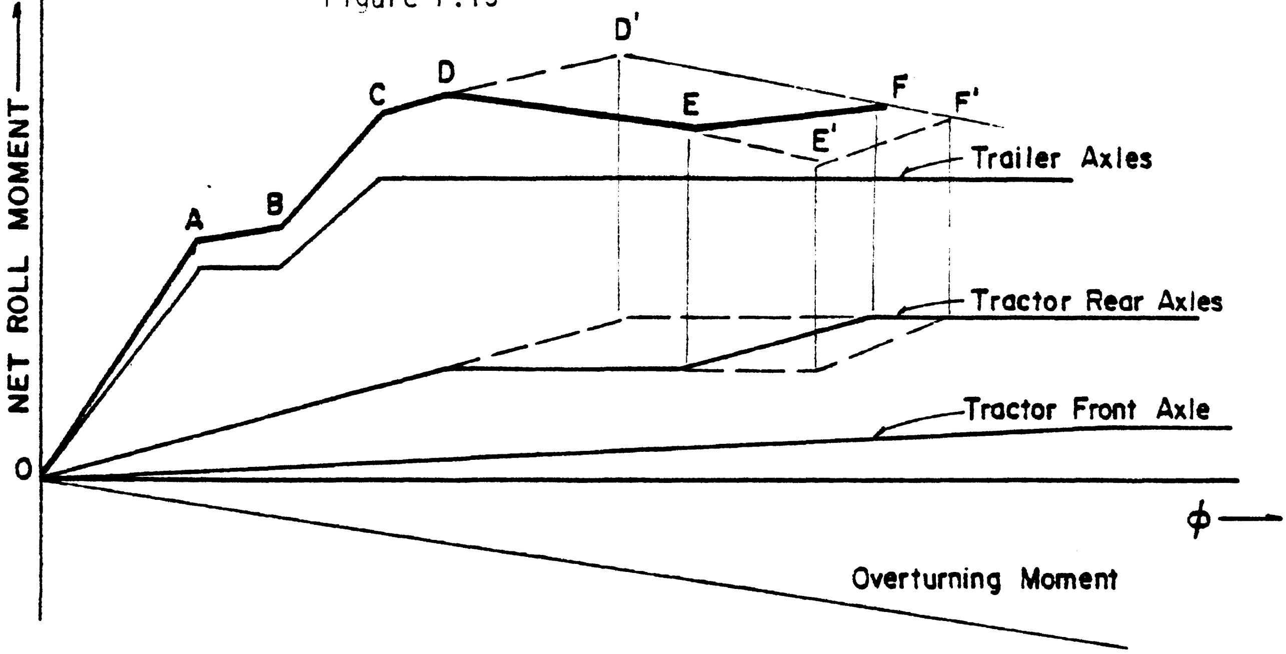

It should be noted that the observations made above are valid only for the particular combination of suspension parameters and axle loadings which were chosen for constructing Figures F.14 and F.15.

The above qualitative descriptions are supported, in Section 4.2.4 by numerical results from calculations performed using the static roll plane model (which is described in Appendix B) for various levels of tractor and trailer suspension stiffness.